

**Analysis of Driver and Cyclist Responses  
in Car-to-Cyclist Conflicts**

ZHAO Yuqing

## Abstract

Cycling is becoming popular because of environment and health demands. Cyclists have high traveling velocity and many cyclists are involved in traffic accidents. In Japan, the number of cyclist fatalities is 2,839 in 2020, which accounted for 14.8% of all traffic fatalities. Japanese police data shows that the largest percentage of cyclist's traffic accidents occurred at intersections (53.4%). The reduction of cyclist traffic accidents is one of the important issues to be addressed toward vision zero of traffic injuries. Hence, the objective of this dissertation is to identify the causes of car-to-cyclist collisions at perpendicular intersections through understanding driver responses and cyclist behavior from the drive recorder data.

The behaviors of cyclists and car drivers before collisions are difficult to be determined in police data and in-depth accident data. In this study, videos of drive recorders were collected. First, the car kinematics and driver responses interacting with cyclists in avoiding collisions were examined by comparing the near-miss incidents and the collisions of drive recorders. Second, the mechanism of cyclist avoided collisions was investigated by comparing near-misses avoided by the cyclists and the near-misses not avoided by the cyclist to understand the factors influencing the cyclist behavior in conflicts. In the analysis of driver and cyclist responses, statistical comparison and logistical regression analysis were applied. Driving simulator experiments were carried out to investigate driver responses in cyclist collisions. Finally, an autonomous emergency braking system (AEB) was applied in all collision reconstructions to estimate the effectiveness of AEB in avoiding car-to-cyclist collisions.

The collision occurred when the sum of the driver braking reaction time (BRT) and the car deceleration time is larger than the time-to-collision (TTC) when the cyclist is visible to drivers. In comparing between the near-misses and collisions in the videos, collisions occurred as the TTC was smaller and the BRT was longer. Two types of collisions were identified: one was small TTC with cyclist's sudden appearance and the other was long BRT with driver's inappropriate attention. From a physical point of view, collisions occurred when the required braking deceleration to stop before the cyclist path was beyond the braking limit ( $5.2 \text{ m/s}^2$ ). It was demonstrated in the video analysis that under the conflicts that exceeded the braking limit, the cyclist's behavior was effective to avoid the collisions. Cyclists were more likely to proactive collision avoidances as the TTC was smaller and the cyclist velocity was higher.

In the driving simulator experiments, participants showed various BRT which affected the

collision occurrence. Braking was effective to avoid collisions while swerving was not effective to avoid collisions. As the TTC was smaller, the driver responses changes from braking to swerving. The decision tree indicated that TTC provided the conflict environments, and BRT was the most important parameter to determine collision occurrences under the environment. Besides, the driver's BRT in the scenario from the far side was larger than from the near side, which was associated with drivers' gaze distributions. The driver's gaze angle between the cyclist and their looking position was larger at the time when the cyclist was visible from the far side than from the near side, therefore, it took time for drivers to move their eyes to notice the cyclists intruding from the far side.

All collisions in the drive recorder were reconstructed, and the collisions were reconstructed again when the AEB was installed. The effectiveness of AEB increased as the field of view (FOV) increased and the sensor delay time (DT) decreased. The AEB with 90° FOV and DT 0.5 s could avoid half of the car-to-cyclist collisions. The AEB was effective to avoid collisions caused by the driver's long BRT while not useful for the collisions with cyclist's sudden appearance behind obstacles even using an ideal AEB (360° FOV and DT 0 s). This result implies that collisions would continue to occur for autonomous cars even though an ideal AEB system is installed.

This study identified the driver and cyclist behaviors that cause car-to-cyclist collisions at perpendicular intersections. The effectiveness of AEB in protecting cyclists was determined. This study could contribute to developing advanced driver assistant systems in reducing the number of car-to-cyclist collisions, as well as to serve as basic data for considering measures against collisions for the future autonomous driving society.

## Nomenclature

$t_a$	Time when the cyclist is visible
$t_b$	Time when the driver starts braking
$t_n$	Time when the driver notices the cyclist
$t_r$	Time when the driver releases gas pedal
$t_s$	Time when the driver starts swerving
$t_e$	Time when the car enters intersections during turning
$a$	Car braking deceleration
$A_a$	Car acceleration at $t_a$
$D$	Distance from the car to the cyclist path
$V_a$	Car velocity at $t_a$
$V_b$	Car velocity at $t_b$
$v_a$	Cyclist velocity at $t_a$
$d_a$	Distance from the cyclist to the car path at $t_a$
$TTC_a$	Car time-to-collision at $t_a$
$TTC_b$	Car time-to-collision at $t_b$

# Contents

<b>Abstract</b> .....	i
<b>Nomenclature</b> .....	iii
<b>1. Introduction</b> .....	1
1.1. Accident analysis.....	1
1.1.1. Accident in Japan .....	1
1.1.2. Police data and in-depth data .....	2
1.1.3. Drive recorder data .....	3
1.2. Driver response in conflicts.....	5
1.2.1 Driver responses in intrusions of cars.....	6
1.2.2 Driver responses in intrusions of pedestrians .....	7
1.2.3 Driver responses in intrusions of cyclists .....	8
1.2.4 Driver’s gaze analysis .....	9
1.3. Cyclist behavior.....	11
1.3.1 Cyclist behavior in naturalistic cycling .....	11
1.3.2 Cyclist behavior in conflicts .....	12
1.4. Autonomous emergency braking system .....	14
1.4.1 AEB effectiveness in car-to-car collisions .....	14
1.4.2 AEB effectiveness in car-to-pedestrian collisions .....	15
1.4.3 AEB effectiveness in car-to-cyclist collisions .....	18
1.5. Scope and aims of this study.....	19
<b>2. Analysis of Causes of Collisions Using Drive Recorder</b> .....	22
2.1. Introduction.....	22
2.2. Methods.....	22
2.2.1. Drive recorder .....	22
2.2.2. Definition of parameters .....	23
2.2.3. Statistical analysis of parameters .....	26
2.3. Results .....	26

2.3.1. Driver behavior with TTC .....	26
2.3.2. Statistical analysis .....	27
2.3.3. Driver response before braking.....	29
2.3.4. Factors affecting collision occurrence .....	33
2.4. Discussion.....	36
2.5. Conclusions.....	38
<b>3. Cyclist Avoidance Behavior Interacting with Drivers.....</b>	<b>39</b>
3.1. Introduction.....	39
3.2. Method .....	39
3.2.1. Data of drive recorder .....	39
3.2.2. Definition of parameters .....	40
3.2.3. Calculation of cyclist velocity and distance .....	40
3.2.4. Identification of cyclist avoidable behavior.....	41
3.2.5. Statistical analysis.....	42
3.3. Results .....	44
3.3.1. The number of cyclist avoidance behavior .....	44
3.3.2. Descriptive parameters of car and driver .....	45
3.3.3. Cyclist avoidance behavior .....	46
3.3.4. Effects of right of way .....	50
3.3.5. Parameter determining taking avoidance behavior.....	50
3.4. Discussion.....	52
3.5. Conclusions.....	54
<b>4. Study of Driver Response in Avoiding Collisions Using Driving Simulator.....</b>	<b>56</b>
4.1. Introduction.....	56
4.2. Methods.....	56
4.2.1. Driving simulator and participants .....	56
4.2.2. Test procedure .....	57
4.2.3. Eye track .....	60
4.2.4. Participants.....	61
4.2.5. Statistical analysis.....	61

4.2.6. Threshold of collision occurrence.....	62
4.3. Results .....	62
4.3.1. Driver avoidable results .....	62
4.3.2. Descriptive statistics .....	64
4.4. Discussion.....	77
4.5. Conclusions.....	79
<b>5. Evaluation Effectiveness of AEB for Cyclist Protection Using Drive Recorder .....</b>	<b>81</b>
5.1. Introduction.....	81
5.2. Methods.....	81
5.2.1. Collision reconstruction .....	81
5.2.2. AEB algorithm .....	82
5.2.3. AEB parameter change .....	85
5.3. Results .....	85
5.3.1. Effectiveness of AEB in perpendicular collisions .....	85
5.3.2. Effectiveness of AEB in turning collisions .....	91
5.4. Discussion.....	94
5.5. Conclusions.....	96
<b>6. General Discussion and Conclusions.....</b>	<b>97</b>
6.1. General discussion .....	97
6.2. Conclusions.....	99
6.3. Future work.....	100
<b>References .....</b>	<b>101</b>
<b>Acknowledgements.....</b>	<b>112</b>

# Chapter 1

## Introduction

### 1.1. Accident analysis

#### 1.1.1. Accident in Japan

In Japan, many people sustain injuries in traffic accidents every year. Figure. 1.1 shows the number of fatalities and injuries involved in traffic accidents in the last decade, and there is a tendency that the number of fatalities and injuries is decreasing over time. The number of traffic fatalities decreases from 4,948 in 2010 to 2,839 in 2020, and the number of injuries also decreases from 896,297 in 2010 to 369,476 in 2020. Besides, the number of traffic accidents decreases from 725,924 in 2010 to 309,178 in 2020 (National Police Agency, 2021).

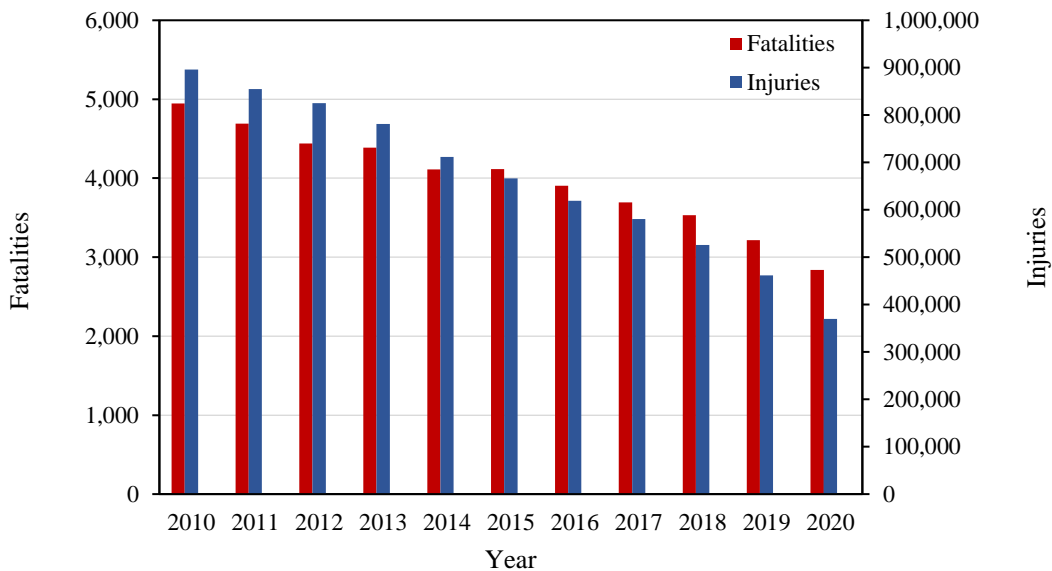


Fig. 1.1 The number of fatalities and injuries in traffic accidents in Japan.

Figure. 1.2 shows the percentage of traffic fatalities by road user of in Japan in 2020. The percentages of fatalities by vehicle occupants, motorcyclists, cyclist and pedestrians are 31.1%, 18.5%, 14.8% and 35.3%, respectively. Vulnerable road users (pedestrians, cyclists, and motorcyclists) account for 68.6% among all the fatalities. As environment and health concerns increase, cycling becomes popular, while cyclist accidents are gaining more attention. Blaizot et al. (2013) showed that the injury risk was 8 times higher for cyclists than for vehicle occupants. In Japan, the number of fatalities of cyclists (66,137) in accidents is larger than the



pedestrians (38,918) and motorcyclist (41,516), however, the fatality risk of cyclists is lower than that of pedestrians and motorcyclists (National Police Agency, 2021). Hence, prevention of cyclists has become an important issue in the field of traffic safety.

Most of cyclist accidents occurs between cyclists and vehicles (94%). Figure. 1.3 shows the configurations of vehicle-to-cyclist collisions in 2020. The percentages of configurations are large in the perpendicular collisions, rear-end collisions, left turn collisions, and right turn collisions, accounting for 56.8%, 11.5%, 10.1%, and 8.0%, respectively. Therefore, perpendicular vehicle-to-cyclist collisions need to be focused on to enhance the safety of cyclists.

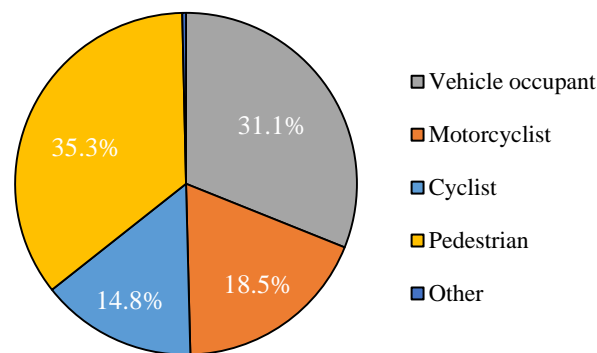


Fig. 1.2 Fatalities of various road users in traffic accidents in Japan in 2020.

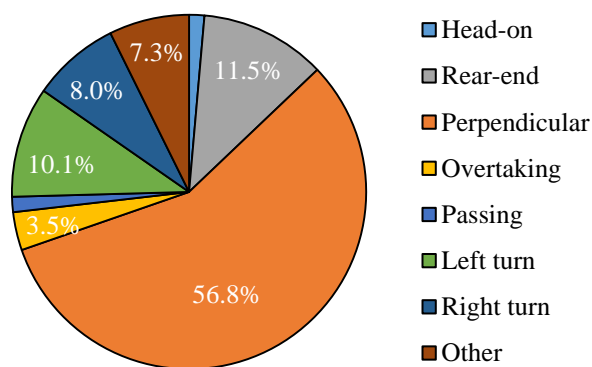


Fig. 1.3 Configurations of car-to-cyclist collisions in Japan in 2020.

### 1.1.2. Police data and in-depth data

Many people consider traffic safety issues as major barriers to cycling (Fruhen et al., 2019).

Risks while cycling are associated with sharing the road with motor vehicles, which can discourage people from riding bicycles (Fruhen and Flin, 2015; Thørrisen, 2013). Hence, it is important to reduce the risk of vehicle-to-cyclist accidents to encourage people cycling. First, it is necessary to figure out causes of car-to-cyclist collisions. Previous studies usually used in-depth accident data and police data to investigate factors of car-to-cyclist collisions. Bıl et al. (2010) conducted a multiple regression analysis of police accident data, and found that the critical factors affecting car-to-cyclist collisions were high vehicle velocity, head-on collisions, and nighttime. Kaplan et al. (2014) analyzed car-to-cyclist collisions to determine factors influencing the injury severity of cyclists. Their results show that car velocity limits above 70-80 km/h and slippery roads were factors that could lead to serious cyclist injuries. Räsänen and Summala (1998) found two common types of mechanisms of collision occurrences based on car-to-cyclist in-depth collision data: one was inappropriate allocation of attention causing the other not noticed, and the other had unjustified expectation of others' behaviors.

Most studies use police data and in-depth data to investigate accidents. It should be noted most single-cyclist crashes are not registered in the police accident database. Therefore, the number of single cyclist collisions and that of cyclist minor injuries are probably underestimated (Billot-Grasset et al. 2016; Isaksson-Hellman, 2012). In-depth accident data are usually collected in a limited area with a limited number of cases and for specific collision configurations, thereby results obtained by in-depth accident data are difficult to apply to the entire country (Larsen, 2004; Aust, 2010; Habibovic et al. 2013). The drawback of car-to-cyclist collisions using in-depth accident data and police data is that they can include uncertain information of cyclist behavior (Loftus, 1979; Rosen, 2013). For example, the cyclist and driver behavior is generally based on the testimony of persons involved in accidents and witnesses. In addition, the vehicle velocity is determined based on tire skid marks and the cyclist's throw distance. Therefore, the in-depth accident data and the police data have difficulties to investigate the time process that led to accident occurrences.

### *1.1.3. Drive recorder data*

With the development of technology, drive recorders (dashboard cameras) are widely used as a tool to record events during the driving process. The drive recorders are installed on the windshield and can record kinematics of vehicles and behaviors of people involved in the traffic before and after an event (Arai et al. 2001; Ito et al. 2018; Lin et al. 2008; Stange et al. 2017).

Naturalistic driving data recorded by car drive recorders can provide important information before conflicts for analyzing the factors that contribute to crashes, especially risks of human errors (Cheng et al., 2011; Shino et al., 2010; Klauer et al., 2006; Uchida et al., 2010; Habibovic et al., 2013).

Some previous researches explored factors influencing the occurrence of car-to-pedestrian conflicts using the videos of drive recorders. Habibovic et al. (2013) used a modified reliability and error analysis to understand causes of incidents using 90 cases of car-to-pedestrian incidents collected in Japan. Their results shows that the incidents occur because the drivers' attention was not properly allocated, causing them to fail to timely recognize the pedestrians at intersections. Matsui et al. (2011, 2013) analyzed 103 car-to-pedestrian near-miss incidents collected in Japan, and they showed that the time-to-collision (TTC) in the incidents where the pedestrian was walking on roads with crosswalks was smaller than that without crosswalks. Moreover, the average TTC was smaller in the cases where pedestrians emerging from obstacles than in the cases where the driver's sight was unobstructed.

It is generally considered that conflicts involved cyclists are different from pedestrians. Lin et al. (2011) compared car-to-pedestrian and car-to-cyclist conflicts using videos of taxi drive recorder data collected in Beijing. They concluded that most of car-to-cyclist conflicts occurred at intersections and T-junctions, and the largest proportion of car-to-pedestrian conflicts occurred at intersections. Compared to car-to-pedestrian collisions, car-to-cyclist collisions usually occur at lower impact speeds, and injuries to cyclists are less frequent and less severe than those to pedestrian (Maki et al., 2003; Peng et al., 2012). Consequently, a separate study of car-to-cyclist conflicts is necessary.

Matsui et al. (2015, 2016) and Matsui and Oikawa (2015) compared near-misses database to the national car-to-cyclist collision database, and concluded that the near-miss was representative for collisions because the proportion of accident configurations between near-miss incidents and minor injuries were comparable. On the other hand, Ito et al. (2018) compared the perpendicular car-to-cyclist collisions and near-misses at intersections using the drive recorder data, and they found that there were two patterns of collisions: driver's braking delay with large TTC and cyclist's sudden appearance with small TTC. The percentage of small TTC cases was larger and that of large TTC cases was lower in collisions compared to near-miss incidents. They concluded that the proportion of response types (i.e. braking or swerving) were different depending on the emergency situations (TTC) in near-miss incidents and

accidents although the near-miss database included all patterns of driver responses in incidents. Thus, the near-miss incidents will not be enough to examine driver responses in extreme emergency situations, and it is necessary to use collision data to investigate driver responses before/during/after collisions.

## **1.2. Driver response in conflicts**

Drivers show various responses in emergency situations. Many researches have used test tracks and driving simulator experiments to understand driver's responses in many traffic situations (Markkula et al., 2019; Bella and Silvestri, 2018; Wu et al., 2018; Calvi and D'amico, 2013). The test track (proving ground) is a useful tool to obtain behaviors of driver in a realistic environment in various experimental scenarios. Previous studies have used the test track to investigate driver responses to intrusions of cars, pedestrians, and cyclists. Test tracks could provide drivers with similar experiences to that of a real car during testing, however, it has limitations in terms of repeatability, data collection and experimental costs (Boda et al., 2018). In addition, there are limitations on the scenarios for ethics related reasons in test tracks such as tests in emergency collisions. As the cost of driving simulator experiments decreases and the fidelity increases, driving simulators became commonplace (McGehee et al., 2002). Driving simulators simulates the real-world driving environments, and driver behaviors can be investigated effectively and safely (Boda et al., 2018; Underwood et al., 2011).

Hamdar et al. (2016) used a driving simulator to study the drivers' behaviors in various weather and road configurations. Their results show that in addition to dealing with different weather conditions, drivers need to spend more efforts to address road challenges such as other road users. Chang et al. (2019) recruited participants to drive in 3 weather conditions: clear zone, transition zone and fog zone. They found that a warning system was useful in assisting a driver to slow down before entering a foggy area. Papantoniou et al. (2019) examined the drivers' performance with various types of distractions (no distractions, talking to passengers and using smartphones) in the rural and urban roads, and they found that characteristics of drivers and the road configurations were the only important factors influencing drivers' behaviors instead of talking to passengers and using smartphones. Malaterre et al. (1988) used test tracks to study the driver's reaction to the obstacles (plastic cones) appeared on the race track, and they found that drivers tended to use intuition to make decisions rather than sophisticated perceptual judgments in emergency situations. However, the intersections of roads

are locations where accidents occur frequently (Wei and Lovegrove, 2013; Poch and Mannering, 1996; Simon et al., 2009; Kumara et al., 2003). Thus, it is important to investigate drivers' reactions at the intersections.

### *1.2.1 Driver responses in intrusions of cars*

Previous researches examined the drivers' response in the car-to-car conflicts at intersections (Lechner and Malaterre, 1991; Hankey et al., 1991; McGehee et al., 1999; Markkula et al., 2012; Li et al., 2019). Lechner and Malaterre (1991) used a driving simulator to study the driver reactions of 49 participants facing an unexpected emergency at an intersection. Most of the drivers in their study applied braking to avoid collisions. They indicated that drivers would be more successful in avoiding collisions if drivers could properly use lateral swerving at the right time. Muttart (2005) showed that braking was the most primary response in avoiding collisions, and driver also combined with swerving to avoid collisions in scenarios where there was small time-to-collision (TTC) due to lateral intrusions. Li et al. (2019) used a driving simulator to analyze reactions of 45 drivers in three scenarios: perpendicular collision, head-on collision, and pedestrian collision. They found that applied braking alone was the most common reaction, and that long braking reaction time and wrong turn directions were the main causes of collisions. In the scenarios with small TTC, drivers have to use the fastest initial reaction time to avoid a collision, thereby, more drivers used steering as an initial reaction in extremely dangerous situations (Hankey et al., 1996).

McGehee et al. (2002) used a test track to analyze the behavior of 192 participants in response to cars approaching laterally at an intersection. According to their study, the average time of releasing gas pedal after the mock-up car appeared was 1.28 s, and that the driver reaction after releasing gas pedal had a more important effect on collision avoidance than the time of releasing gas pedal. Morita et al. (2013) recruited 56 participants to conduct experiments on collision avoidance maneuvers in a scenario that a mock-up car suddenly appeared from the left side of the road (near side in Japan). They found that drivers avoided collisions by braking although they also used steering when the mock-up car suddenly appeared from the side. In their study, the average brake reaction time (BRT) of the drivers was 0.45 s and the average braking deceleration was 7 m/s<sup>2</sup>.

### 1.2.2 Driver responses in intrusions of pedestrians

In the driver responses to pedestrian intrusions, Fu et al. (2018) proposed a driver model to make a decision based on the car speed and the distance to the pedestrian path in the situation where pedestrians were crossing the road. In their study, drivers have three phase in decision: driver cannot yield to pedestrian (Phase I), drivers uncertainly yield (Phase II), and drivers can yield to pedestrians (Phase III) (Fig. 1.4). In the Phase I, the drivers judge that the car cannot stop before arriving at the pedestrian path, and they would decide to pass the pedestrian path. In the Phase III, the driver judge that the car can safely stop and they would yield to the pedestrian since the car speed is low and the distance to pedestrian path is large. Phase II is dangerous for drivers because the driver is not sure if the car can safely stop before arriving the pedestrian path.

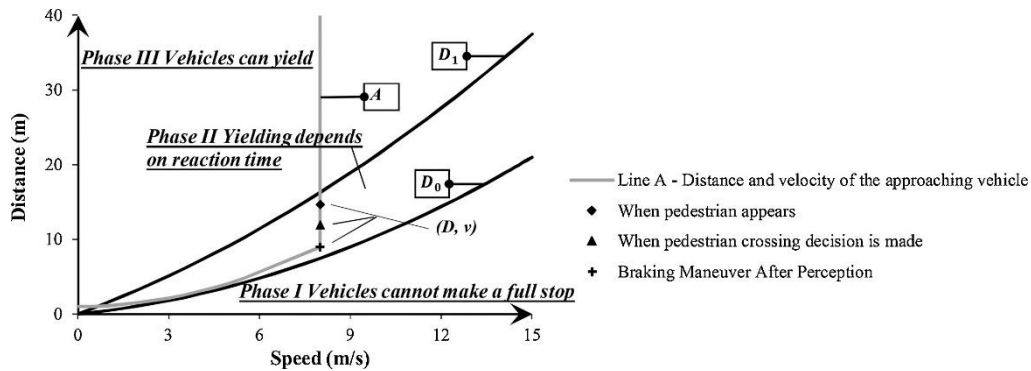


Fig. 1.4 Driver decision making in pedestrians crossing roads based on the relationship of car speed and distance to pedestrian path (Fu et al., 2018).

Lubbe and Rosén (2014) conducted a test track to quantify the driver comfort boundaries in pedestrians' crossing roads, and this could be used as a guide for warning systems appropriately working in the driver's comfort zone. They found that the average time-to-collision (TTC) at the driver started braking was independent of driving velocity. In addition, the order of the trials in scenarios had no effects on TTC at driver's braking start time.

In the emergency situation of pedestrians intruding laterally, Jurecki et al. (2014) conducted two scenario trials with pedestrians intruding from the left and the right side on the track. They found that the driver braking reaction time (BRT) for pedestrians intruding from the left side (far side) was longer than that from the right side (near side). Moreover, they also found that the braking reaction time was linearly related to TTC at the time when the pedestrian intruded into the road.

### *1.2.3 Driver responses in intrusions of cyclists*

Some researchers investigated driver responses in lateral intrusions of cyclists at intersections though the number of these studies are limited (Toxopeus et al., 2018; Boda et al., 2018; Petzoldt et al., 2017). Petzoldt et al. (2017) recruited 42 participants and instructed them to sit in a car to respond against cyclists approaching at different speeds. Participants was instructed to express their willingness to cross the intersection by depressing the pedal, which was quantified by an accept gap (gap from the car position to entry of the intersection). They found that as a cyclist speed increased, the accept gap to cross intersections became shorter. Toxopeus et al. (2018) conducted a simulated experiment on 13 male and 13 female university students in a scenario where the cyclist appeared from the right side. They concluded that the average time-to-impact was 3.26 s from the time when the cyclist appeared at the stop sign, and that there was no differences in driver response time between male and female. Moreover, in emergency scenarios when the cyclist suddenly appears, braking rather than steering was a primary response used to avoid collisions.

Some researchers have also used test tracks to study the driver responses to car-to-cyclist conflicts. Boda et al. (2018) examined driver responses to cyclists approaching laterally at a non-signalized intersection using a test track and a driving simulator. They shows that the configuration of the intersection affects the driver's strategy approaching the intersection although it does not directly affect the driver braking response, and the time-to-arrival (TTA) of cyclist presence has the greatest effect on driver responses of braking. From braking reaction processes of participants, the relationship between the TTC at the time of braking onset ( $TTA_{BO}$ ) and TTA (Fig. 1.5): TTA of cyclist visibility and  $TTA_{BO}$  is close to linear when the TTA is small, and  $TTA_{BO}$  tends to be constant when TTA is large. Thus, the driver starts immediately when the cyclist intrudes suddenly with small TTC whereas they do not start braking immediately if the driver has enough time to avoid collisions with cyclists.

Most studies of driver responses in car-to-cyclist collisions have focused on near-side cyclist's intrusions using drive simulators. However, accident data show that the number of car-to-cyclist collisions at intersections are comparable for cyclists' crossing at intersections from the near-side and the far-side of the car (Den Camp et al. 2017). Besides, there are no research on driver behavior in car-to-cyclist conflicts based on real-world accidents.

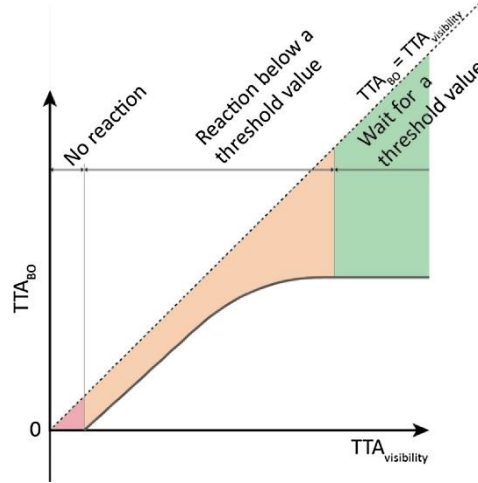


Fig. 1.5 Relationship of TTA at cyclist visible and TTA at braking onset (Boda et al., 2018).

#### 1.2.4 Driver's gaze analysis

The gaze of drivers reflects intension of driving behavior. Hence, analyzing driver gaze and eye movements is useful to understand driver behavior in driving and collision avoidance. Lee (1976) proposed an optical time-to-time, indicating the time to reach a target ahead was the inverse of the image expansion rate of the target on the driver's retina. The time to the object  $T_c$  in the vehicle following scenario was calculated as follows:

$$T_c = \frac{\theta_1}{(\theta_2 - \theta_1)/(t_2 - t_1)} \quad (1.1)$$

where  $\theta_1$  and  $\theta_2$  were the angular separations of the image point at times  $t_1$  and  $t_2$ , and  $(\theta_2 - \theta_1)/(t_2 - t_1)$  represents the image expansion rate from  $t_1$  to  $t_2$ . McLeod and Ross (1983) recruited 24 volunteers to conduct an experiment showing film clips, and found that the observers estimated the information of objects based on the changes of optical array rather than the observers' viewing time.

Later, many researchers used inverse tau (inverse of  $T_c$ ) to quantify kinematic metrics in vehicle-to-vehicle rear-end conflicts. Wada et al. (2006) included the change of area of the preceding car on the retina of driver's eyes as a parameter for braking in their driver model for approaching a preceding car in longitudinal direction. Markkula et al. (2016) performed a time series recording analysis of 116 collisions and 241 near-crashes using collected naturalistic driving rear-end conflict data. They proposed a model of the driver's braking response in the car following scenario (Figure 1.6). In their study, the driver's reaction is depended on the visual



looming cues such as inverse tau, the driver's perception of the urgency of the leading vehicle gradually increased as the visual looming increased. The driver usually starts braking in less than 1 s when the urgency reaches a threshold (i.e.,  $0.2 \text{ s}^{-1}$ ), and the braking deceleration also depends on the urgent level. According to Eiríksdóttir (2016), the driver's last glance off the ahead road before events is related to visual looming cues. Short glance durations are usually accompanied by rapid changes of situations, while longer glance duration could lead to collisions. Kovaceva et al. (2010) used an expansion rate and the inverse tau to analyze the driver's reaction in overtaking a leading bicycle. They combined the experimental data from driving simulators and test tracks, and concluded that a model based on inverse tau was more appropriate to analyze driver behaviors than using the expansion rate.

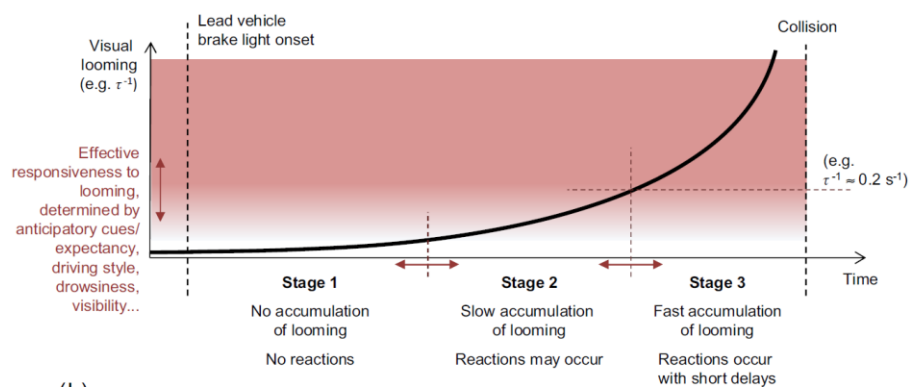


Fig 1.6 Driver's reactions to leading vehicle in rear-end conflicts quantifying with visual looming cues (Makkula et al., 2016).

In addition, drivers' eye movements have been examined during reactions against interacting with hazards (Lamble et al., 1999; Klauer et al., 2006; Pomarjanschi et al., 2012; Sarkar et al., 2021). Lamble (1999) used the eccentricity of sight to quantify the effects of driving tasks on drivers' responses in a car following scenario, showing that TTC was inversely proportional to the eccentricity of the task to the normal sight. Pomarjanschi et al. (2012) concluded that driver's eye movements guided by gaze were highly correlated with the tasks in the driving. In Klauer's research (2006), the driver's eyes off the ahead road for more than 2 s could increase the risk of collisions and near-miss incidents by two times. Crundall et al. (1998) shows that the driver's detection rate is significantly greater in the near eccentricity than in the far eccentricity in both high-demand and low-demand tasks. This may be because the fact that intrusion at a distance would use the driver's peripheral retina and the detection rate was slower in far intrusions (Green, 2000).

Previous researches on the driver's gaze and eye movements have examined the driver reactions to the tasks in a forward or longitudinal direction, while a few studies were carried out for the driver's eye movement of traffic intrusions from lateral direction.

### **1.3. Cyclist behavior**

#### *1.3.1 Cyclist behavior in naturalistic cycling*

In car-to-cyclist collisions, not only driver behavior but also cyclist behavior is critical for avoiding accident occurrences. Studying the cyclist behavior in naturalistic condition is instructive to the research of the cyclist behavior under conflicts and collisions. The cyclist behavior in naturalistic cycling has been investigated in many studies from real time cycling data collected using instruments with global position system (GPS) and accelerometers.

Blanc and Figliozzi (2016) used an application with GPS to collect naturalistic cycling data. They used ordinal logistic regression to establish a function with cyclist comfort as the dependent variable and bicycle facility types, trip stress and trip characteristics as the independent variables. They found that bicycle boulevards and separated paths increased cyclist comfort. Strauss et al. (2013) shows that the building environment such as subway entrances and schools near intersections has a significant influence on cycling activity, and the number of cyclists significantly increased near that buildings. In addition, the traffic volume of bicycles and motor vehicles are the main factors influencing the injury risk for cyclists. For every 1% increase of bicycle volume, the number of injuries of cyclists increased by 0.87%.

Another method of collecting cycling data is using cameras to record traffic participants at specific locations at a certain time, and the cyclist associated data is then filtered from all recorded data. This method is usually applied at intersections to obtain effects of traffic flow on the cyclist behavior. Ling and Wu (2004) used a video camera to collect data of 561 cyclists at a wide and complex signalized intersection. They concluded that the crosswalks and the pedestrians on the road affected the cyclist behavior, and they obeyed traffic rules less often.

The cyclist speed is an important parameter in the analysis of cyclist behavior. Obtaining the cyclist speed is important for traffic control, accident safety analysis, and sight distance analysis (Kassim et al., 2020). Thompson et al. (1997) measured the speeds of 152 cyclists by using a radar gun and a stopwatch on roads without motor vehicles, showing the average cycling speed was 14.8 km/h. Dill and Gliebe (2008) investigated the cyclist behavior using GPS data, and their study shows that the route choice of cyclists is affected by cycling purposes (commuting

or leisure), cycling distance, availability of bicycle lanes, and traffic signals. In their study, the average total speed of cyclists was 17.4 km/h, and the average speed after removing time of zero speed (i.e., time of waiting traffic lights) was 17.9 km/h.

The cycling speed usually changes when cyclists approach intersections. Pein (1997) collected data from 16 intersections for 442 cyclists using camera videos, and they calculated the average speed of cyclists crossing the intersection was 12.7 km/h. In Ling and Wu’s study, the average crossing speed at the signalized intersection was 11.44 km/h. Kassim et al. (2020) used meta analysis and summarized the average cyclist speeds at the road sections and the signalized intersections in many studies. The frequency distribution of average cyclist speed is shown in Fig. 1.7. The average speed distributes from 15 km/h to 25 km/h at the road sections, and the average velocity distributes closer to the low speed at intersections and the maximum frequency distribution was between 10 km/h and 15 km/h.

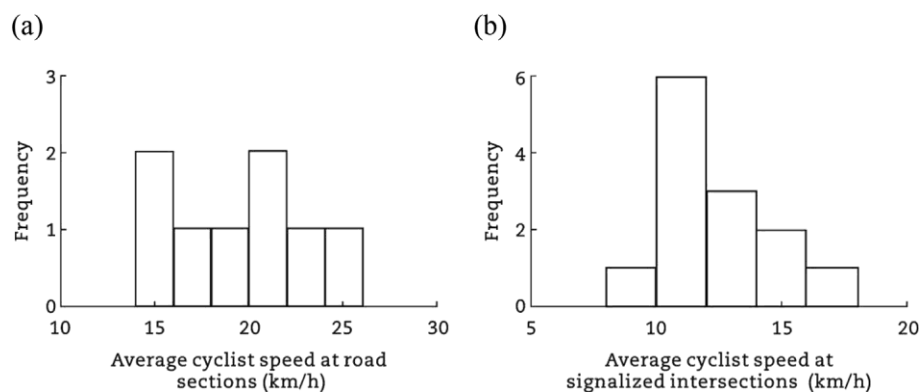


Fig. 1.7 Frequency distribution of average cyclist velocity at the road sections (a) and the signalized intersections (b) (Kassim et al., 2020).

### 1.3.2 Cyclist behavior in conflicts

The cyclist behavior in conflicts has also been studied using in-depth accident data, self-reports of cyclists, naturalistic cycling and cycling simulators. Using in-depth accident data, Räsänen (1998) examined the avoidance behavior of drivers and cyclists in car-to-cyclist collisions. The collision occurrence depends on the perception of driver or cyclist each other, and misunderstanding of cyclists for driver’s yielding behavior when a cyclist is traveling on the priority road. De Camp et al. (2017) investigated the cyclist behavior before collisions to make scenarios of car-cyclist autonomous braking tests in EuroNCAP. The road crossing of cyclists occupies the largest percentage, followed by right and left turn of the car. The cyclist velocity of 50 percentile was 12 to 15 km/h, and the 90 percentile was 20 to 25 km/h.

The self-report of participants is also an effective method to know the cyclist behavior in critical events. Kováčsová et al. (2019) showed participants video clips that the car intruded into the path of cyclists (participants). The participants answered to slow down their bicycle when anticipating the car did not stop, especially when the car was accelerating. Their study shows that the cyclist's behavior depends on the driver's behavior, deciding to go or stop based on whether the driver perceives them and yields the path for the cyclist. Lehtonen et al. (2015) showed participants video clips of the cyclist in critical events, asking them to indicate their caution level by using a slider. They showed the caution level was high for high-velocity cyclists and for cyclist's traveling on sidewalks than on bicycle paths.

Naturalistic cycling of participants is a useful method to investigate the cyclist behavior (Johnson et al., 2010; Dozza and Werneke 2014; Werneke et al., 2015). The data including critical events are collected from the cycling of participants who rides a bicycle with video. In Johnson's study (2010), cyclists avoided collisions by braking (75.9%) and steering (7.4%), and no reactions were 11.1%. The participants reported subjectively in interviews that the reaction time was smaller when they traveled at a high velocity. In a study by Werneke (2015), critical events between cars and cyclists occurred around intersections (86%), and half of the participants reported that they traveled at high velocity.

Cyclist avoidance behavior with braking and steering maneuvers against stationary obstacles was investigated in experiments of participants (Lee et al. 2020). The participants applied braking with constant deceleration. As the cyclist velocity increased, they started to brake earlier, maintaining constant time-to-collision. The higher the cyclist speed, the steering maneuver tended to delay compared to the braking. In Lee's study, the participants already knew the presence of the obstacle in advance, and an instructor directed to apply braking or steering to avoid the obstacle, which may be different from their behavior in a collision.

To avoid collisions, the cyclist's behavior might be more effective than the driver's because the bicycle can stop with a short distance. Though many studies investigated drivers' avoidance behavior in critical events in car-to-cyclist conflicts, limited information is available on cyclist's avoidance behavior in such emergency situations. Besides, the fundamental relationship between cyclist behavior and crash avoidance has not been understood yet (Billot-Grasset et al., 2016; Werneke et al., 2015).

#### 1.4. Autonomous emergency braking system

Autonomous emergency braking system is an active safety technology designed to avoid collisions with other cars and other road users in the driving. AEB uses a sensor system to detect potential hazards, and AEB calculates the distance to the front cars or the time-to-collision (TTC) at different intervals to evaluate the hazardous level (Fig. 1.8). AEB applies braking if drivers did not take actions in time to avoid collisions. Current AEB sensing systems contain cameras, radar and LiDAR, and car manufacturers may have various combinations of these systems.

There are various types of AEB, which are commonly classified into two types for high speed driving and low speed driving. The sensing system of AEB for low speed driving generally combines a camera and a LiDAR. In the AEB for high speed driving, a combination of a radar and a camera is usually applied in cars in order to detect hazards at longer distances (Euro NCAP, 2014).

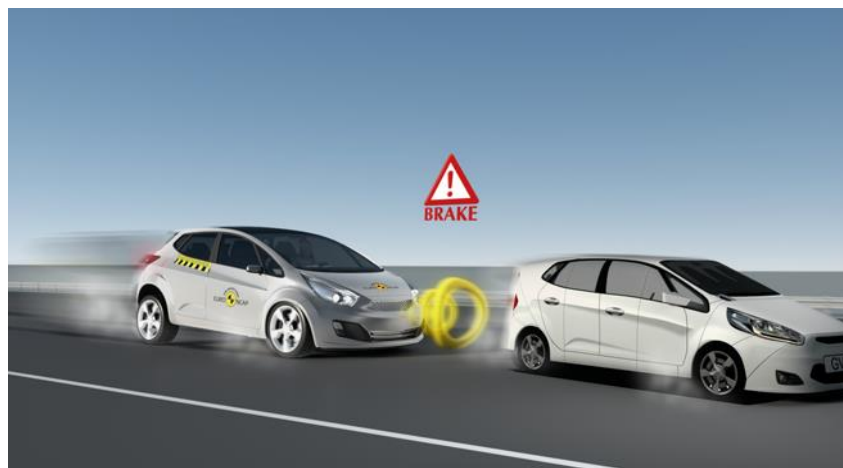


Fig. 1.8 AEB system installed in the car; adapted from Euro NCAP

##### 1.4.1 AEB effectiveness in car-to-car collisions

Rear-end collisions account for a large portion of accidents involving passenger cars, and this collision type usually occurs when driving at low speeds in cities (Isaksson-Hellman and Lindman, 2012; Euro NCAP, 2014). Thus, AEB is first applied in cars in rear-end collisions. The effectiveness of AEB in rear-end collisions is usually studied using the database from police reported data of injured accidents and insurance accident data.

Isaksson-Hellman and Lindman (2012) used insurance claims data of 2009-2011 to compare the difference in claim rates between the AEB-equipped Volvo XC60 model (also named as City Safety in this model) and other Volvo models that were not equipped with AEB. Their

study found that the XC60 model with AEB systems had 23% lower collision claim rates than other models without AEB. They then went on to use insurance claims data from 2010 to 2015 to compare the collision rates between Volvo V70 model with AEB and V70 model without AEB (Volvo V70 model with AEB was introduced as standard from 2012). Their result indicates that cars equipped with low-speed AEB had lower rear-end frontal collision rates by 27% and lower severity collision rates by 37% than the cars without low-speed AEB (Isaksson-Hellman and Lindman, 2016).

Rizzi et al. (2014) used police reported injury accidents data in Sweden from 2010 to 2014 to compare cars with and without AEB from the same manufacturer as well as cars without AEB from other manufacturers to assess the overall effectiveness of AEB in Sweden. Their study shows that AEB could reduce 54%-57% rear-end collisions at the car speed lower than 50 km/h and reduce 35%-41% rear-end collisions for all speed conditions. Cicchino (2014) used police reported accident data in 2010-2014 from 22 states in the US to compare the collision rates of AEB equipped vehicles of the same model without AEB, and he reported that AEB equipped cars were able to reduce rear-end accidents by 43%.

Fildes et al. (2015) used a meta-analysis to combine data collected from government, organizations and researchers from various countries. They compared the number of vehicle collisions in the vehicles with and without AEB, and they concluded that AEB equipped vehicles could reduce 38% rear-end collisions overall. AEB can greatly reduce the rear-end collisions at low speed and thus, it is probable that more accidents can be avoided if AEB system can work at wider speed (Cicchino, 2014; Den Camp et al., 2017).

#### *1.4.2 AEB effectiveness in car-to-pedestrian collisions*

As the effectiveness of AEB in reducing rear-end collision in car-to-car scenarios was confirmed in accident data, AEB was expected to be applied in more scenarios (Coelingh et al., 2010). AEB protection for pedestrians has been tested by Euro NCAP since 2016 (Euro NCAP, 2016). A vehicle impact velocity is a key factor in evaluating the injury outcomes when vulnerable road users (VRU) collide with vehicles. Thus, AEB protection for VRU should be reflected in collision avoidances or reduction of vehicle velocity at the time impacting with VRU.

Coelingh's study (2010) was the first to test the effectiveness of AEB for pedestrian protection. They conducted experiment using Volvo third generation AEB (named collision

warning with full auto brake and pedestrian detection (CWAB-PD)) with a long range radar and a wide angle camera. The field of view (FOV) of the camera and the radar was  $48^\circ$  and  $60^\circ$ , and the deceleration with full automatic braking was  $10 \text{ m/s}^2$ . Their result shows that the CWAB-PD system could avoid collisions with car velocity up to 35 km/h. Gruber et al. (2019) installed a virtual AEB system on the car to simulate in-depth accident data from CEDATU (Austria), GIDAS (Germany) and P-VAD (Sweden). The detection distance of the virtual AEB was 80 m, and three FOV of  $60^\circ$ ,  $90^\circ$  and  $120^\circ$  were used. Two braking deceleration jerk of  $24.5 \text{ m/s}^3$  and  $35 \text{ m/s}^3$  and two decelerations of 0.8 g and 1.1 g could be combined for the AEB system, and AEB was triggered to activate when the TTC of the car was less than 1 s. According to their results, the effectiveness of AEB for pedestrians depends on the parameters of AEB and selected accident databases. Their result shows that the AEB with  $\pm 60^\circ$  FOV and an advanced braking system (1.1 g and  $35 \text{ m/s}^3$  deceleration jerk) could avoid 42% of CEDATU accidents. Besides, the lower the car average velocity in collisions, the more effective AEB was for collision avoidance.

Hamdane et al. (2015) investigated the effectiveness of AEB in car-to-pedestrian conflicts by reconstructing 100 real world accidents from CASR (Australia) and IFSTTAR-LMA (France). The simulated AEB has a specification of detection distance of 40 m and FOV of  $20^\circ$ - $40^\circ$ , and the maximum braking deceleration of  $8 \text{ m/s}^2$ . In their study, the position of pedestrians distributed relative to the car with different TTC was a critical factor affecting the effectiveness of AEB. Before TTC of 1.5 s, pedestrians are scattered relative to the front of the car, and TTC between 1.5 s and 0.5 s is the critical time for AEB activating, as pedestrians gather in front of the car (Fig. 1.9). Thus, the trigger time of AEB should be set during TTC of 1.5-0.5 s for pedestrians, and the FOV should include as many pedestrians as possible. In addition, they indicated that the effectiveness of AEB decreased as reaction time of sensor increased. 70% of collisions could be avoided despite using  $20^\circ$  FOV, and the effectiveness of AEB rapidly declined when the reaction time of the AEB system was larger than 1 s.

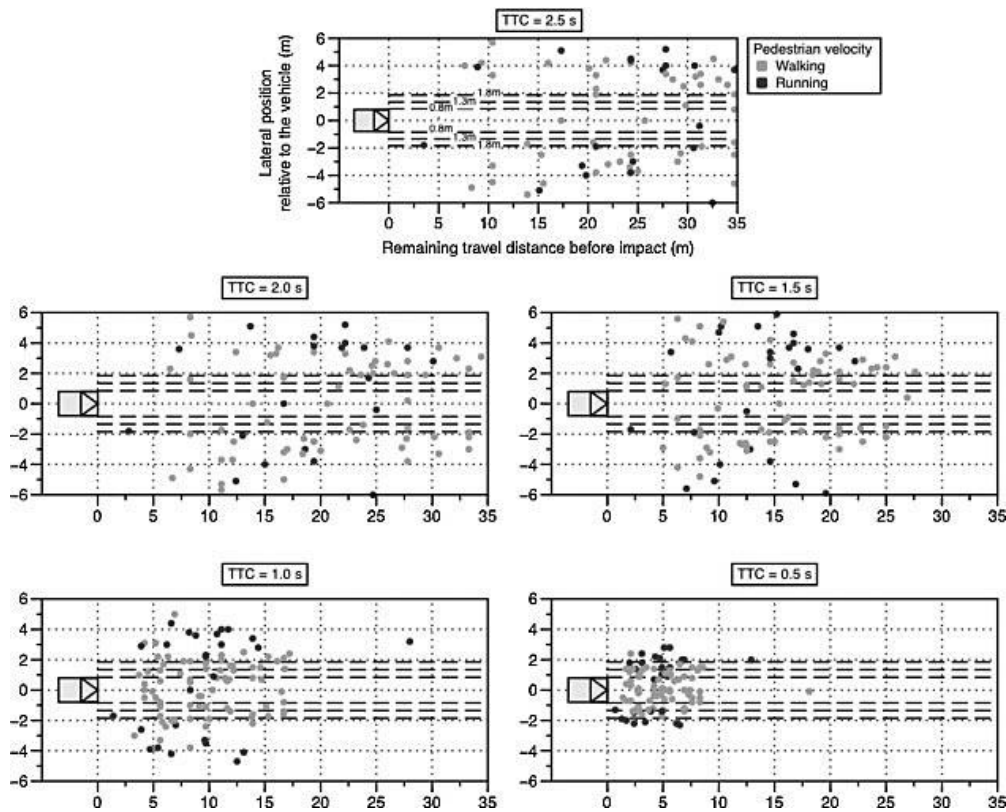


Fig. 1.9 Position of pedestrians relative to the car with different TTCs (Hamdane et al., 2015).

Some researchers used different methods to evaluate the benefit of AEB in car-to-pedestrians collisions by calculating the injury risks and nominal benefits (Edwards et al., 2014; Haus et al., 2019; Jeppsson et al., 2018; Lubbe and Kullgren, 2015). Jeppsson et al. (2018) used an AEB system with vacuum emergency brake (VEB) to estimate the injury risk of pedestrians in 526 accidents (GIDAS). The maximum braking deceleration with 1.3 g, 1.5 g and 1.8 g was applied in AEB. They shows the relationship of TTC and the car speed at the pedestrian was visible in Fig. 1.10, and more pedestrians could be avoided as the braking deceleration increased. In their study, the AEB with VEB could reduce 8-22% pedestrian casualties compared to AEB without VEB. Haus et al. (2018) concluded that the AEB with TTC 1.5 s and delay time 0 s could reduce the fatality risk by 84-87%, and MAIS3+ injury risk by 83-87%. Lubbe and Kullgren (2015) estimated that the AEB could reduce 25% of casualty costs in the pedestrian collisions. Edwards et al. (2018) used UK and German accident database and calculated the change in speed distribution in pedestrian collisions by AEB, and the application of AEB brought nominal benefits of £119-385 million and €63-216 million in the UK and Germany per year, respectively.



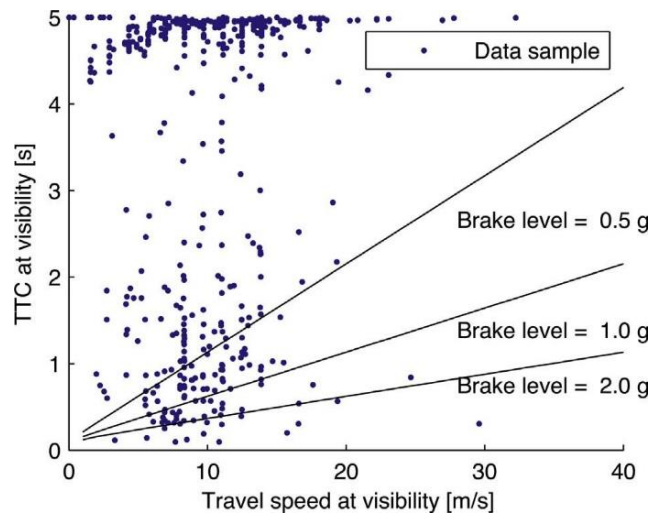


Fig. 1.10 Relationship of TTC and the car speed at the time when the pedestrian was visible. Three brake levels of AEB was shown (Jeppsson et al., 2018).

#### 1.4.3 AEB effectiveness in car-to-cyclist collisions

Cyclists have higher travelling velocity compared to pedestrians, thus AEB for pedestrian protection may not be enough for cyclist protection. Lenard et al. (2018) analyzed the position of pedestrians and cyclists relative to the cars at different TTCs using 175 car-to-pedestrian accidents and 127 car-to-cyclist accidents in UK. Their study shows that the positions of cyclists distributes in a wider area relative to cars than those of pedestrians: 90% of the pedestrians locates in the  $\pm 20^\circ$  FOV of the cars whereas 90% of the cyclists locates in the  $\pm 80^\circ$  FOV (Fig. 1.11). Therefore, the AEB designed for pedestrians is not appropriate for cyclists. Besides, the test of the effectiveness of AEB for cyclists was implemented by Euro NCAP since 2018 (Euro NCAP, 2018).

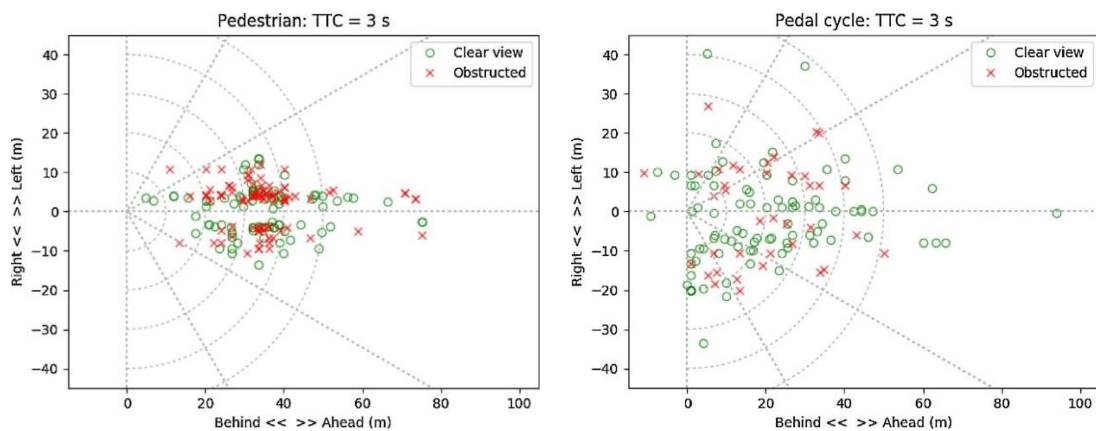


Fig. 1.11 Position of pedestrians and cyclist relative to the car at TTC 3 s (Lenard et al., 2018).

Previous analyses of the effectiveness of AEB for cyclists usually used in-depth data or police-reported accident data (Den Camp et al., 2017; Fredriksson et al., 2015; Chajmowicz et al., 2019; Jeppsson and Lubbe, 2020). Fredriksson et al. (2015) used 34 car-to-cyclist accidents from GIDAS to evaluate the effectiveness of the passive safety, the active safety and the integrated safety system in protecting cyclists from collisions. The FOV of the three simulated AEB was 40°, 40° and 60°, and the AEB trigger width (width beside the car path) was 1 m and 3 m, respectively. Their study showed that the AEB with 60° FOV and trigger width 3 m had the highest protection effectiveness of 48% on cyclists. Den Camp et al. (2017) simulated the AEB effectiveness for velocity reduction in the three most common car-to-cyclist scenarios (cyclist crossing from the near side, cyclist crossing from the near side with obstructions, and cyclist crossing from the far side). Their result shows that the AEB with  $\pm 24^\circ$  FOV and DT 0 s for pedestrians was insufficient for cyclist, and the performance of AEB for cyclist protection depends on the FOV of the sensor at low vehicle velocities (under 60 km/h). Besides, the AEB in reducing car velocity was not effective in the car velocity of 10-20 km/h because the cyclist and the car have comparable velocity and the direction of the cyclist relative to the car unchanged, thereby the cyclist was difficult to be detected by the AEB sensor.

Some researchers evaluated AEB benefits in preventing cyclist collisions with injury severity and combination post-crashes (Rosen, 2013; Leo et al., 2020). Rosen (2013) used 8 fatal and 43 injury car-to-cyclist collision from GIDAS-PCM to calculate the AEB effectiveness in reducing fatalities and serious injuries (AIS3+F). He concluded that AEB protection for cyclists was close to 50% under ideal conditions (weather and light), but the effectiveness of AEB in protecting against fatal injuries was greatly reduced in dark and high-speed conditions. Leo et al. (2020) analyzed 112 car-to-cyclist collisions from CEDATU database using the simulated AEB with 60° FOV and DT 0.2 s. Their study shows that the car speed of collisions against cyclist would be reduced by 1/3 with after installing AEB, and the position, angle and velocity of impact of the cyclist head against cars were all greatly reduced.

### **1.5. Scope and aims of this study**

The cyclist safety is more and more important because a bicycle is positioned as an important role as a commuter and a travelling. Perpendicular car-to-cyclist intersection collisions needs to be focused because they occupy more than 50% among all cyclist collisions. To reduce the number of cyclist accidents, it is necessary to understand driver and cyclist responses in

emergency situations. Many previous studies examined the factors influencing collision occurrences and evaluated the effectiveness of AEB to prevent vulnerable road users from collisions using various approaches. However, there were still some limitations and problems that were not solved:

- Previous researches studied the driver response in emergency situations based on in-depth accident data and police data, which have limitations and uncertainty to understand driver behavior before collisions.
- Previous studies examined the cyclist behavior usually used the naturalistic traveling data, and some studies used questionnaires and some information of cyclists recorded in the in-depth data to obtain the cyclist behavior in emergencies, which had subjectivities and uncertainty. The mechanism of cyclist avoidance in collisions at intersections was not clear.
- Some studies investigated the relationship of TTC and BRT in the scenarios with lateral intrusions, however the relationship of TTC and BRT in the emergency situation involving cyclists at intersections was not clear.
- The driver's braking reaction time against the lateral intrusions in the far side was larger than in the near side, however the reason of BRT differences in the far side and the near side was not investigated.
- The AEB effectiveness for pedestrians in the collisions was evaluated based on the in-depth data or police data in the previous studies, however the AEB effectiveness for cyclists was not evaluated.

In this study, the drive recorder data in collisions are newly collected in corporation with Aichi and Nagoya taxi association, and the driver and cyclist behavior are investigated based on video observations. The purpose of this study is to understand driver responses in emergency in car-to-cyclist perpendicular conflicts, which resulted in near-miss or collision. First, videos from drive recorders are analyzed for perpendicular car-to-cyclist near-misses and collisions to identify the boundary or the threshold to separate collisions and near-misses and the causes of collisions. Also, the factors affecting collision avoidance by cyclists is examined by comparing the near-misses avoided by cyclists and not avoided by cyclists in the videos of drive recorders. Next, three typical collisions (large TTC near side, small TTC near side and far side) are extracted from the drive recorder and reconstructed in the driving simulator to explore causes of collision occurrences through understanding of driver and cyclist responses in emergency

situations. Finally, all collisions are reconstructed with autonomous emergency braking (AEB) to examine the collision prevention effectiveness of AEB for cyclists to reduce the number of cyclist victims in the traffic conflicts.

This dissertation consists of the following 6 chapters. Chapter 1 introduces the background of traffic collisions worldwide and in Japan and the collected data of drive recorders. Chapter 2 analyzes the driver's responses in the collisions and the near-misses using the videos of drive recorders. Chapter 3 analyzes the cyclist's behavior in avoiding collision using the videos of drive recorders. Chapter 4 examines the driver's responses in scenarios from the drive recorder video using the driving simulator experiments. In Chapter 5, the effectiveness of autonomous emergency braking (AEB) for preventing the cyclist involved in the car-to-cyclist collisions is evaluated. Finally, Chapter 6 summarizes the general discussion and conclusions.

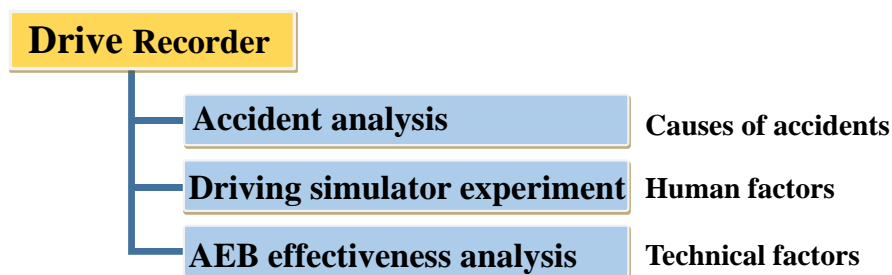


Fig. 1.12 Dissertation structure.

## Chapter 2

### Analysis of Causes of Collisions Using Drive Recorder

#### 2.1. Introduction

Previous studies usually analyzed accidents based on police data and in-depth data. This data were recorded referring to the testimonies of people involved in the collisions and witnesses, as well as judging the velocities of the vehicles and the cyclist behavior before crash through the vehicle skid marks of the vehicles and the cyclist fall distance. Hence, this data contains uncertain information (Loftus, 1979; Rosen, 2013). Another drawback of using police recorded data and in-depth data is that this data usually focused on fatal accidents and serious injury accidents and thus, the single-bicycle collisions and the cyclist victims of minor injuries are underestimated (Billot-Grasset et al. 2016).

In this chapter, the videos from drive recorder are used to analyze the collision occurrences, which clearly provides the drivers' responses and the cyclist behaviors before crash. The car kinematics and the drivers' responses leading to collision occurrences for the cyclists crossing perpendicular intersections are compared in the near-miss incidents and the collisions. Also, the boundary separates collisions and near-misses is obtained using the data from taxi drive recorders.

#### 2.2. Methods

##### 2.2.1. Drive recorder

Figure. 2.1 shows the image of the video of the drive recorder used in this study. The drive recorder can record time, global position system (GPS) information, acceleration, velocity, indicator and brake lamp on/off, and the front video. An event before 10 s and after 5 s is automatically saved and upload when the lateral or longitudinal car acceleration exceeds 0.45  $g$ .



Fig. 2.1 Image of video of drive recorder.

### 2.2.2. Definition of parameters

Figure. 2.2 shows the car velocity over time sequence in avoiding collisions from the time before cyclist is visible to the time when the car stops. The time when the cyclist is visible to drivers (the cyclist appears from) behind the obstacles such as buildings or stopping cars is defined as  $t_a$ . The driver starts to brake is defined as  $t_b$  after the driver notices the cyclist at  $t_n$ .  $t_r$  is time when the driver's foot releases the gas pedal before  $t_b$ .  $t_s$  is defined as time of swerving onset (note that  $t_s$  in the Fig. 2.2 is schematic, and the driver may apply swerving before or after  $t_b$ ).

The time interval of  $t_a$  and  $t_b$  is define as the driver's braking reaction time ( $BRT = t_b - t_a$ ), and the time interval of  $t_a$  and  $t_s$  is defined as swerving reaction time ( $SRT = t_s - t_a$ ). Moreover, the time interval of  $t_a$  and  $t_r$  is defined as gas releasing time ( $GRT = t_r - t_a$ ). The car velocity at  $t_a$  and  $t_b$  is given as  $V_a$  and  $V_b$ , respectively.

The car acceleration at the time when the cyclist is visible ( $t_a$ ) is defined as  $A_a$ , which is calculated by the average acceleration during 1.0 s before and after  $t_a$  in this study. Unlike braking deceleration  $a$ , the car acceleration  $A_a$  might be used to examine the driver's behavior to anticipate hazards at  $t_a$  in intersections and to judge whether drivers are proactive.

The relative position and distance between the driver and the cyclist in the perpendicular configuration is shown in Fig. 2.3. Since the vehicle is driven in the left side of roads in Japan, the cyclist appears from the left side of the car is near side with respect to the car, and the right side is far side.

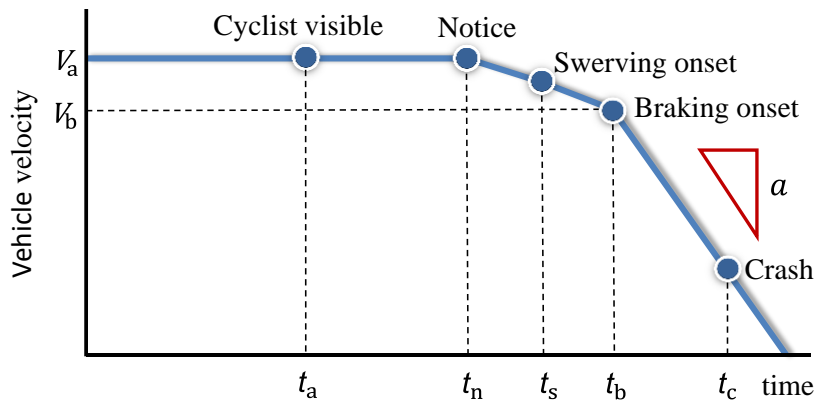


Fig. 2.2 Car velocity over time sequence in avoiding collisions.

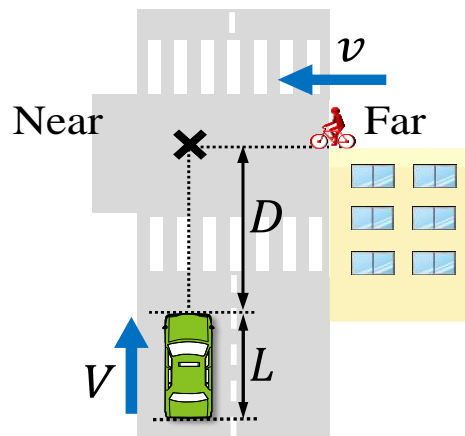


Fig. 2.3 Relative position and distance of the car and the cyclist in perpendicular configuration (cyclist intruding from the left corresponds to near side and the right corresponds to far side in Japan).

The time-to-collision (TTC) is the remaining time before crash, which can be calculated by the braking distance  $D$  between the car and the bicycle and the car velocity  $V$  as following:

$$TTC = \frac{D}{V} \quad (2.1)$$

The TTC at  $t_a$  (cyclist is visible) and  $t_b$  (start braking) is denoted as  $TTC_a$  and  $TTC_b$ , respectively.

Assume that the driver applies braking at constant deceleration  $a$  until the car makes

contact with the cyclist. At the time of braking ( $t_b$ ), the collision occurs if the distance between the car and the cyclist is small than that calculated by the car velocity  $V_b$  and the car braking deceleration ( $a$ ) as follows:

$$D_b \leq \frac{V_b^2}{2a} \quad (2.2)$$

Substitute Eq. (2.2) into Eq. (2.1) and eliminate the braking distance  $D$ , the braking deceleration limit is determined as:

$$a = \frac{V_b}{2 \cdot TTC_b} \quad (2.3)$$

The car cannot avoid a crash when the car deceleration required to stop is higher than the braking deceleration limit. The braking deceleration limit depends on the friction coefficient between the car's tires and the road surface, and varies depending on the road conditions such as dry, wet, and snow. The speed at which the driver presses the brake pedal also affects the braking deceleration limit.

Collisions occur when the distance between the cyclist and the car is smaller than the sum of braking distance and the car travel distance during braking reaction time.

$$D_a \leq BRT \cdot V_a + \frac{V_b^2}{2a} \quad (2.4)$$

Assuming that the driver does not react and the car velocity remains constant from  $t_a$  to  $t_b$  ( $V_a = V_b$ ), the following equation is obtained with dividing both side by  $V_a$  in Eq. (2.5) as:

$$TTC_a \leq BRT + \frac{V_b}{2a} = BRT + TTC_b \quad (2.5)$$

Using Eqs. (2.2) (2.4) and (2.5), the available time and distance before collisions can be examined from the driver's braking reaction time ( $BRT$ ) and the braking acceleration ( $a$ ).



### 2.2.3. Statistical analysis of parameters

The parameters affecting the collision occurrences is examined in the drive recorders. The mean of car velocity,  $TTC$ , driver  $BRT$ , and car acceleration  $A_a$  at the  $t_a$  when the cyclist is visible are compared between the near-misses group and the collision group. Moreover, the mean of the parameters is also compared in the near side and the far side to investigate effects of cyclist's appearing sides.

To examine the significance of means, first, the parameters in near-misses and in collision are tested for equality of variance for the data using F-test. Based on the results of F-test, the Student's t-test for the data of heterogeneity and Welch t-test for the data of homogeneity of variance is employed to examine significances of the two groups. In all tests, p-value of 0.05 is taken to say that the differences of the mean of the two groups are statistically significant.

The driver responses can affect collision occurrences in emergency situations. A logistic regression analysis is used to analyze the independent parameters  $TTC_a$ ,  $BRT$ , and  $A_a$  affecting collision occurrences. The logistic regression of collision occurrences can be expressed as follows:

$$\ln \frac{P}{1-P} = \beta_0 + \beta_1 x_1 + \dots + \beta_n x_n \quad (2.6)$$

where  $P$  is the probability of collision occurrences (0 is near-misses and 1 is collisions).  $x_i$  ( $i = 1, 2, 3$ ) is explanatory variables, and  $\beta_i$  is their coefficients.  $TTC_a$ ,  $BRT$ , and  $A_a$  are applied in the logistic regression as explanatory variables to investigate the factors influencing collision occurrences. All the significant level of statistical analysis is set to 0.05 in this study.

Generally, drivers slow down at low velocities at intersections because the drivers yield for the right of way, and this decelerations are not the responses for the cyclist appearance. Therefore, cases with car velocities below 20 km/h are removed in the analysis of drive recorders.

## 2.3. Results

### 2.3.1. Driver behavior with $TTC$

The driver behavior in emergency situation observed using drive recorder was compared. Figure. 2.4 shows the drivers' behavior classification in avoiding collisions in the near-miss and the collision with various  $TTC_a$ . Generally, the drivers are more likely to apply braking to avoid

collisions in the near-miss compared to the collisions group. In the near-miss group, three drivers apply braking with swerving with  $TTC_a$  greater than 2 s, and this is probably because the driver does not immediately notice the cyclists and does not take actions after the cyclists appear behind the obstacles until the cyclists gradually approach the car. In the collision group, most of drivers also apply braking to avoid collisions. However, more drivers apply braking with swerving and only swerving because the situation is more emergent in the collisions compared to near-miss. Another behavior of the driver is no reaction, which means that the drivers do not take any actions before the collision occurs because they do not notice the cyclists.

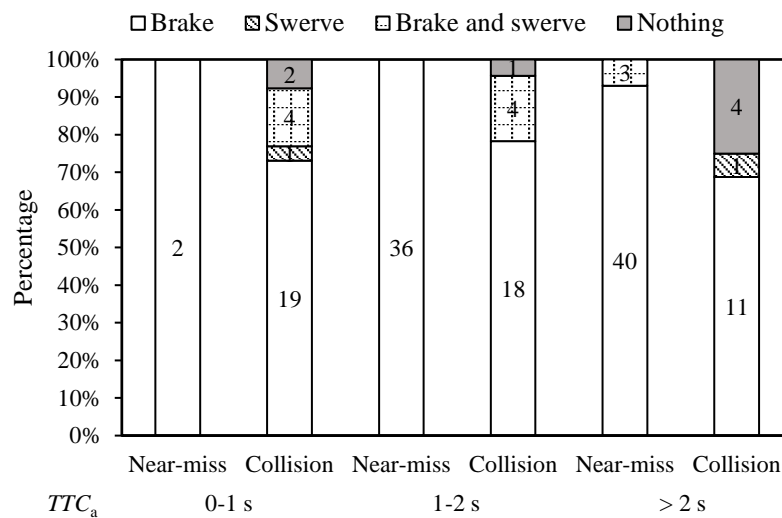


Fig. 2.4 Driver's response to avoid collisions in the near-miss and the collision with various  $TTC_a$ .

### 2.3.2. Statistical analysis

The parameters of driver responses are compared between the near-miss and the collision groups. Figure. 2.5 shows the mean of the parameter  $V_a$ ,  $TTC_a$ ,  $BRT$ , and  $A_a$  in the near-miss and the collision at  $t_a$  when the cyclist is visible.  $TTC_a$  is smaller, and  $BRT$  and  $A_a$  is larger in the collision group compared to the near-miss group. The mean of  $TTC_a$  in the near-miss is 2.15 s, which is significantly larger than  $TTC_a$  in the collisions 1.28 s ( $t(64) = 4.1, p < 0.001$ ). There is a significant difference in driver's  $BRT$  between the near-miss of 0.43 s and the collision of 0.88 s ( $t(41) = -3.11, p = 0.003$ ). Car velocity does not show significant differences in the near-miss and the collision ( $t(62) = -0.95, p = 0.34$ ). The mean value of car acceleration  $A_a$  in the near-miss is negative ( $-0.05 \text{ m/s}^2$ ) and in the collision is positive ( $0.33$

m/s<sup>2</sup>), showing a significant trend ( $t(86) = -1.81, p = 0.073$ ).

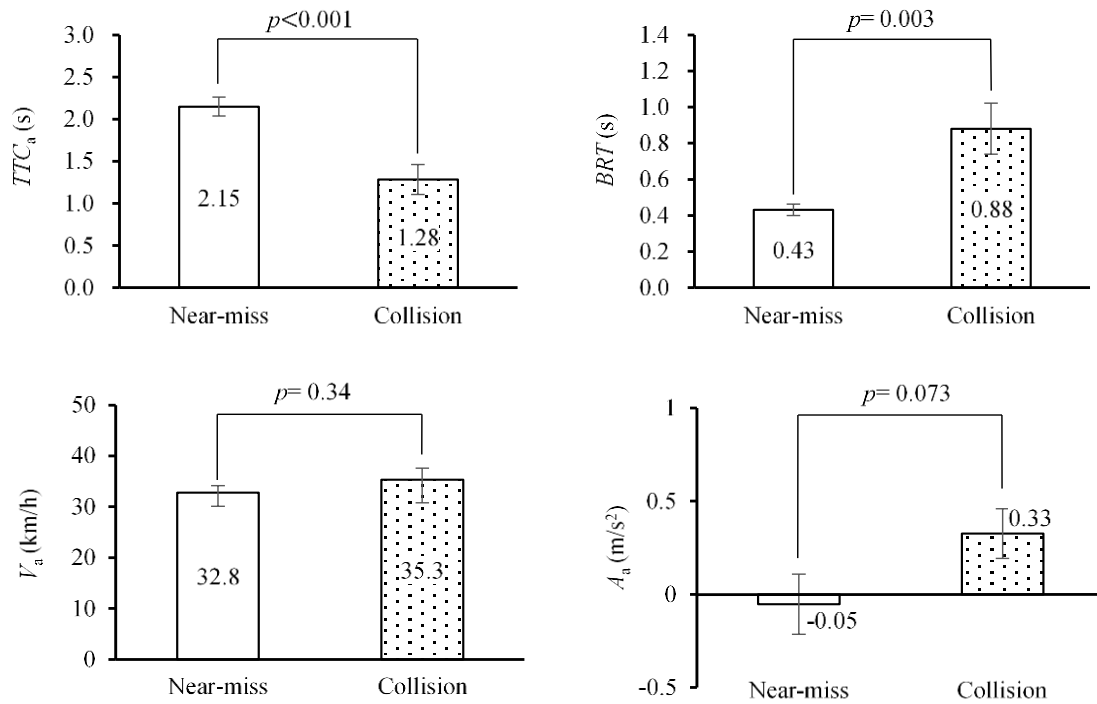


Fig. 2.5 Mean of  $V_a$ ,  $TTC_a$ ,  $BRT$ , and  $A_a$  at the cyclist visible time in the near-miss and the collision (the error bars represented standard errors).

The effects of cyclist appearance direction on driver responses were compared. The mean values of  $V_a$ ,  $TTC_a$ ,  $BRT$ ,  $A_a$  of the near side and the far side at the time  $t_a$  when the cyclist was visible are compared in Fig. 2.6. The mean value of  $V_a$  for the near side and the far side is 36.1 km/h and 31.5 km/h, respectively, showing a significant trend between these two groups ( $t(76) = 1.83, p = 0.07$ ). The average value of  $TTC_a$  is 1.76 s in the near side, and 1.87 s in the far side. The  $BRT$  of the near side and far side is 0.55 s and 0.71 s. The average of  $A_a$  of the near side and the far side is 0.06 m/s<sup>2</sup> and 0.17 m/s<sup>2</sup>, respectively. However, there are no significant differences in the variables of  $TTC_a$  ( $t(54) = -0.41, p = 0.69$ ),  $BRT$  ( $t(75) = -1.2, p = 0.24$ ) and  $A_a$  ( $t(64) = -0.49, p = 0.63$ ). In other words, the car velocity for the cyclist crossing from the far side was slightly lower than the near side, even though  $TTC_a$  was comparable between near side and far side.

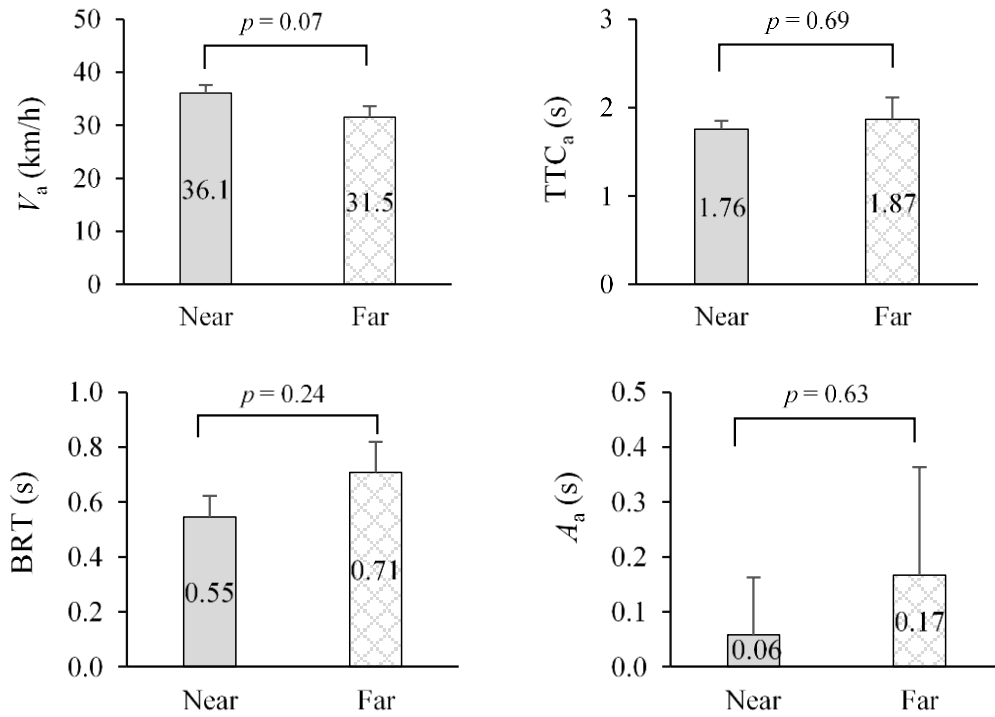


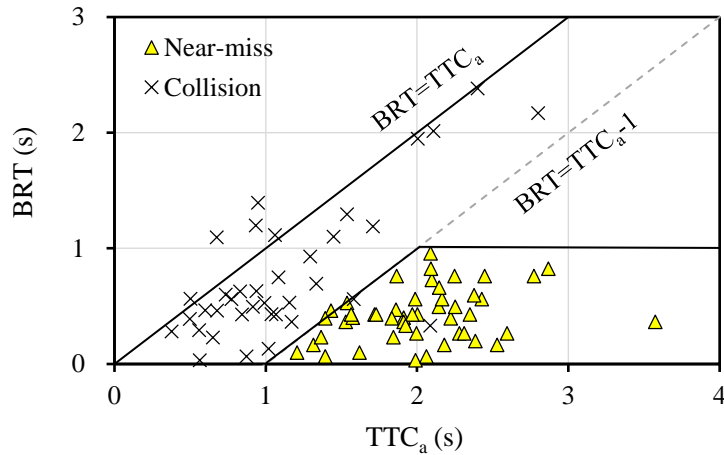
Fig. 2.6 Mean values in the near and far side incidents at  $t_a$  in drive recorder data.

### 2.3.3. Driver response before braking

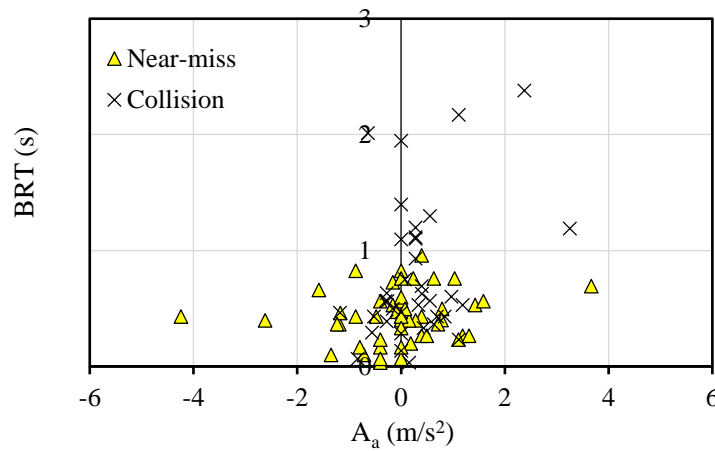
The driver braking reaction time is different between the near-miss and the collision group as well as far side and near side of cyclist appearance, which implies the braking reaction time is a key factor for collision occurrences. Figure. 2.7 shows the relationship of  $TTC_a$ ,  $BRT$  and  $A_a$  at the time  $t_a$  when the cyclist is visible. In Fig. 2.7(a), the area of the driver's  $BRT$  and the  $TTC_a$  can be divided into three areas for collision occurrence and near-miss by  $TTC_a$ . There are only collisions when  $TTC_a$  is less than 1 s regardless of  $BRT$ . In the area where  $TTC_a$  is greater than 1 s and less than 2 s (transition area from collision to near-miss), the collisions and the near-misses are separated by  $BRT = TTC_a - 1$ , and the collisions occurs when  $BRT$  is greater than  $TTC_a - 1$ . There were only near-misses in the area where  $TTC_a$  is greater than 2 s and the  $BRT$  is less than 1 s. In addition, the  $BRT$  of all the near-misses is less than 1 s. Figure. 2.7(a) implies that collisions and the near-miss incidents can be distinguished by  $TTC_a$  and  $BRT$ . Hence, it is confirmed that  $TTC_a$  and  $BRT$  are two variables that affect collision occurrences.

The relationship of  $BRT$  and car acceleration  $A_a$  when the cyclist is visible is shown in

Fig. 2.6(b). The near-misses are distributed in both  $A_a < 0$  and  $A_a > 0$ , while the collision are mostly distributed in the part of  $A_a > 0$ . The  $BRT$  increases gradually as  $A_a$  increased in the side of  $A_a > 0$ . It is probable that some drivers who did not pay attention in intersections accelerated to pass intersections and collided cyclists.



(a)  $BRT$  vs.  $TTC_a$



(b)  $BRT$  vs.  $A_a$

Fig. 2.7 The relationship between  $TTC_a$ ,  $BRT$  and  $A_a$  at  $t_a$  when the cyclist was visible.

The relationships between car velocity  $V_a$  and  $TTC$  at the time  $t_a$  when the cyclist is visible, and the time  $t_b$  of braking onset are plotted in Fig. 2.8(a) and (b), respectively. The cases with car velocity below 20 km/h are also included in the figures. From Fig. 2.8(a)(b), collision data distributes in the left upper area of the graph (high velocity and small  $TTC$ ).

The car braking deceleration was calculated from Eq. (2.3) using the car velocity and the

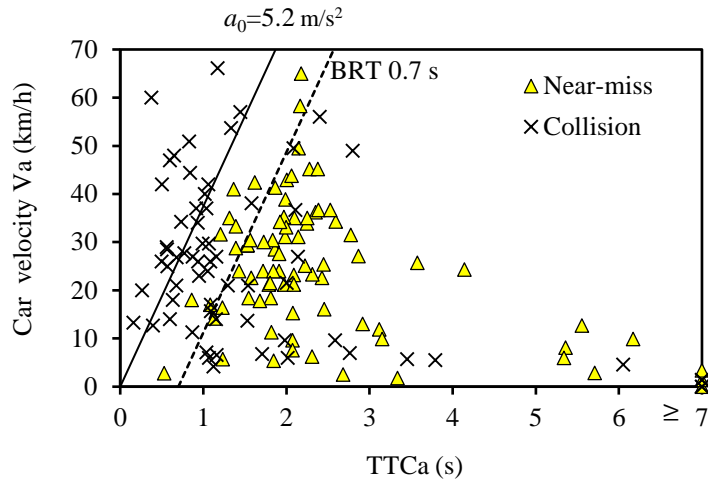
*TTC*. The car brake deceleration  $a$  and  $BRT$  in the near-misses and the collisions was respectively substituted into the logistic regression analysis as the only explanatory variable (0 corresponds to near-misses 1 corresponds to collisions). The following regressions is obtained:

$$P(a) = \frac{1}{1 + \exp(10.51 - 2.04a)} \quad (2.7)$$

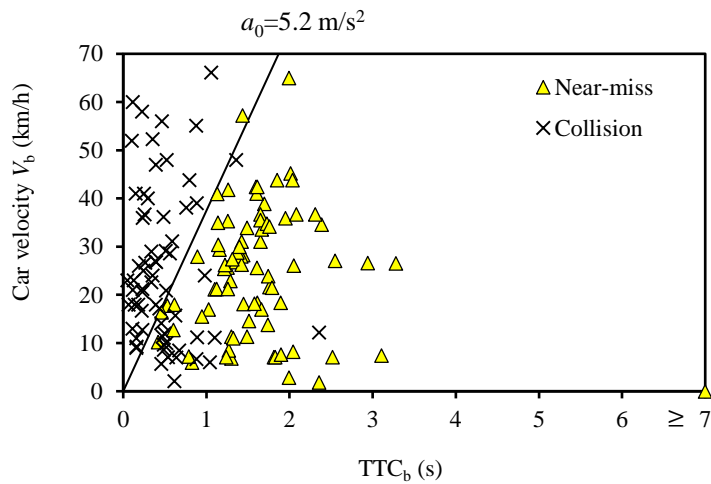
$$P(BRT) = \frac{1}{1 + \exp(1.62 - 2.34BRT)} \quad (2.8)$$

The car braking deceleration  $a = 5.2 \text{ m/s}^2$  corresponds 50% of probability of collision occurrences using the Eq. (2.7). This deceleration  $a$  was the car braking limit, which indicates that the collision could not be avoided when the braking deceleration required to stop the car exceeded the braking limit. Similarly, driver's braking reaction time  $BRT = 0.7 \text{ s}$  corresponds 50% of probability of collision occurrences using the Eq. (2.8).

The car braking deceleration limit of  $5.2 \text{ m/s}^2$  and  $BRT$  of  $0.7 \text{ s}$  is also drawn in the figures. In Fig. 2.8(a), many collisions distributes on the left area of the braking limit, and these cases are already difficult to be avoided when the cyclist was visible. Besides, there are some cases located on the right area of the  $BRT$  limit  $0.7 \text{ s}$ , which indicates that these collisions could be avoided if the drivers could starts braking immediately (e.g., within  $0.7 \text{ s}$ ) after the cyclist was visible to the driver from obstacles. From  $t_a$  to  $t_b$ , all the cases moves to the left, and the near-misses and the collisions are clearly separated by the car braking limit when the car velocity is above  $20 \text{ km/h}$  (Fig. 2.8(b)).



(a) Time when the cyclist is visible ( $t_a$ )

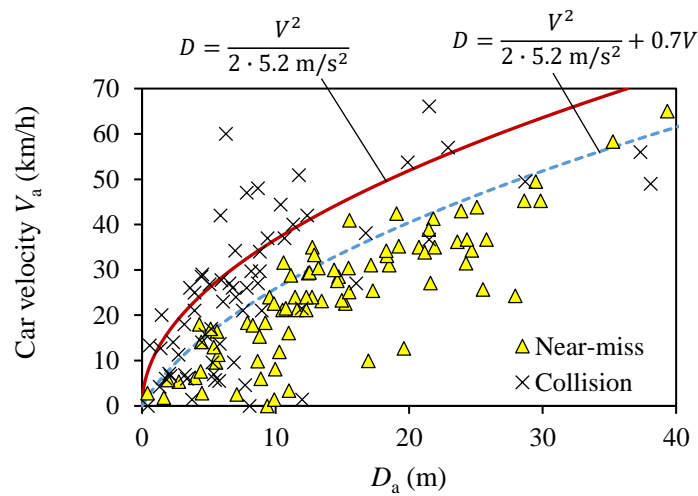


(b) Time of braking onset ( $t_b$ )

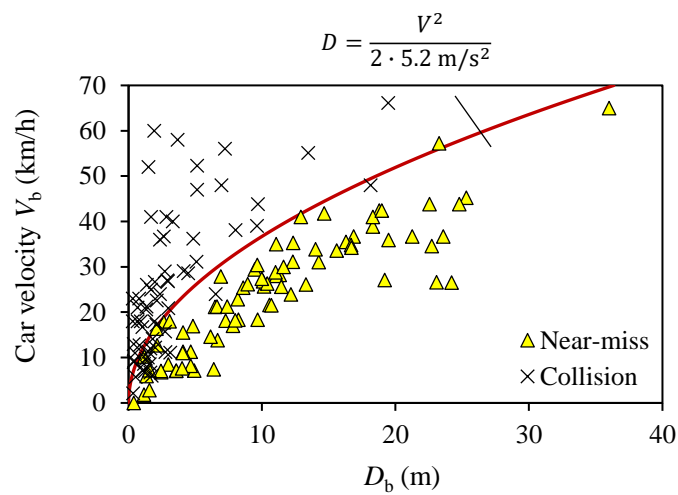
Fig. 2.8 Relationship of car velocity and TTC at the time when the cyclist is visible  $t_a$  and the time of braking onset  $t_b$ .

The relationship between the car velocity and TTC can be also expressed using the car velocity and the distance between the car and the cyclist path. The relationship of the car velocity  $V_a$  and the distance to the collision point  $D_a$  at the time  $t_a$  when the cyclist was visible and the time  $t_b$  of braking onset is shown in the Fig. 2.9. The braking distance limit of the car to avoid collisions can be derived from Eq. (2.4) using the braking deceleration limit  $5.2 \text{ m/s}^2$ . In Fig. 2.9(a), it can be observed that larger car velocity and shorter distance more likely to lead to collisions. Collisions occurs when the required braking distance exceeds the braking limit distance, as shown in the Fig. 2.9(b). There are some collision cases located below

the braking distance limit. This is because these drivers applied braking late or the braking deceleration level is low.



(a) Time when the cyclist is visible ( $t_a$ )



(b) Time of braking onset ( $t_b$ )

Fig. 2.9 Relationship of the car velocity and the distance to the collision point at the time when the cyclist is visible  $t_a$  and the time of braking onset  $t_b$ .

#### 2.3.4. Factors affecting collision occurrence

To identify variables which affect a collision occurrence, a multiple logistic regression analysis was applied to the near-miss and the collision data. Table 2.1 shows the independent parameters  $TTC_a$ ,  $BRT$  and  $A_a$  affecting collision occurrences at the time when the cyclist is visible to the driver using the multiple logistic regression analysis. From the p-value,  $TTC_a$  and  $BRT$  are the two most important factors influencing the occurrence of collisions ( $p < 0.001$ ), and  $A_a$



is not significant in influencing collision occurrences ( $p = 0.208$ ). From the standard partial coefficient, it can be concluded that  $BRT$  is the most important factor influencing the collision occurrences, and smaller  $TTC_a$  and larger  $BRT$  can lead to collision occurrences. The car acceleration ( $A_a$ ) is not significant probably because not all drivers who accelerated in intersections did not pay attention to cyclists with distracted driving.

Table 2.1. Logistic regression of parameters affecting collisions in the drive recorder.

Explanatory variables	Partial regression coefficient	Standard partial coefficient	P-value
Intercept $\alpha$	-1.6829		$p < 0.001$
$TTC_a$	-0.7308	-2.3431	$p < 0.001$
$BRT$	4.9356	3.1009	$p < 0.001$
$A_a$	0.3910	0.3990	0.2083

To easily understand the relationship of  $TTC_a$  and  $BRT$  leading to collision occurrences, two examples are shown in the Fig. 2.10 and Fig. 2.11. In Fig. 2.10, the TTC at the cyclist is visible is 1.45 s, and the  $BRT$  is 1 s. Instituting the car velocity at braking onset 56 km/h,  $BRT$  is larger than  $TTC_a - V_b/2a$ , thus the collision cannot be avoided. In Fig. 2.11, TTC at the cyclist is visible is 1.72 s, and the  $BRT$  is relatively small as 0.3 s. Instituting the car velocity at braking onset 25 km/h, and the  $BRT$  is smaller than  $TTC_a - V_b/2a$ , hence this case could be avoided.

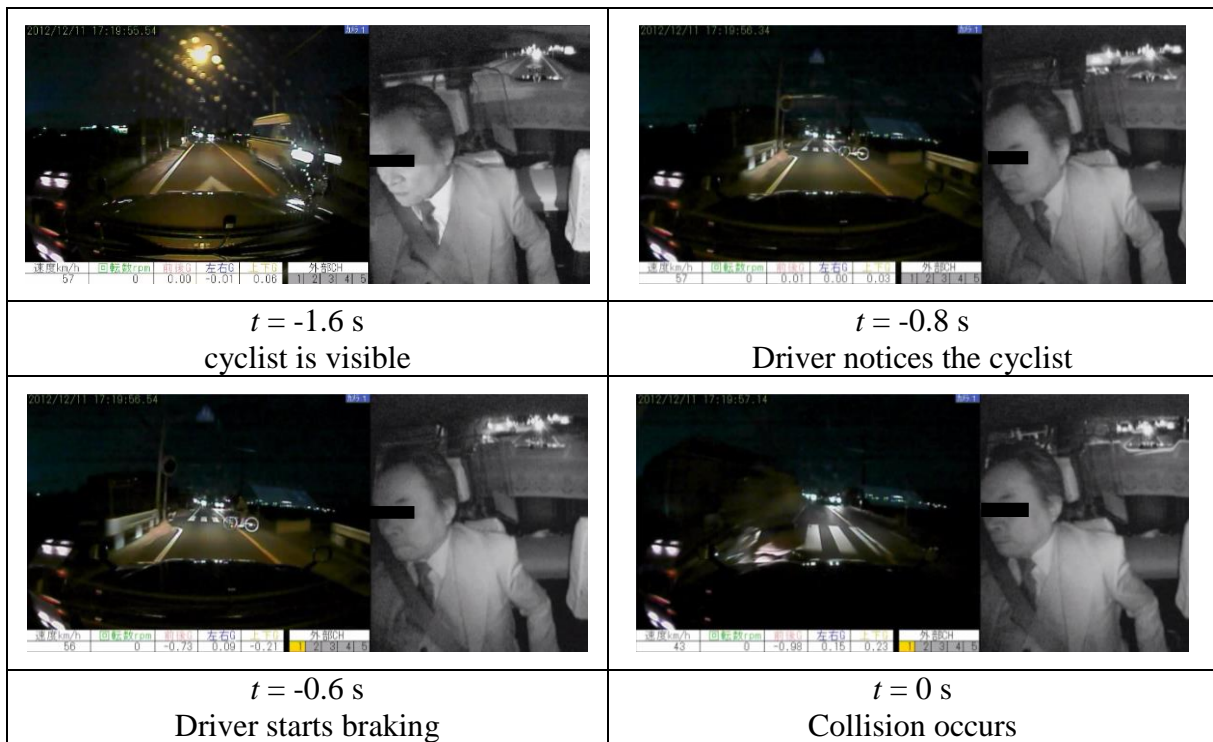


Fig. 2.10 Example of a collision caused by the driver's delayed braking ( $TTC_a$  1.45 s and  $BRT$  1 s,  $t = 0$  represents collision occurs).

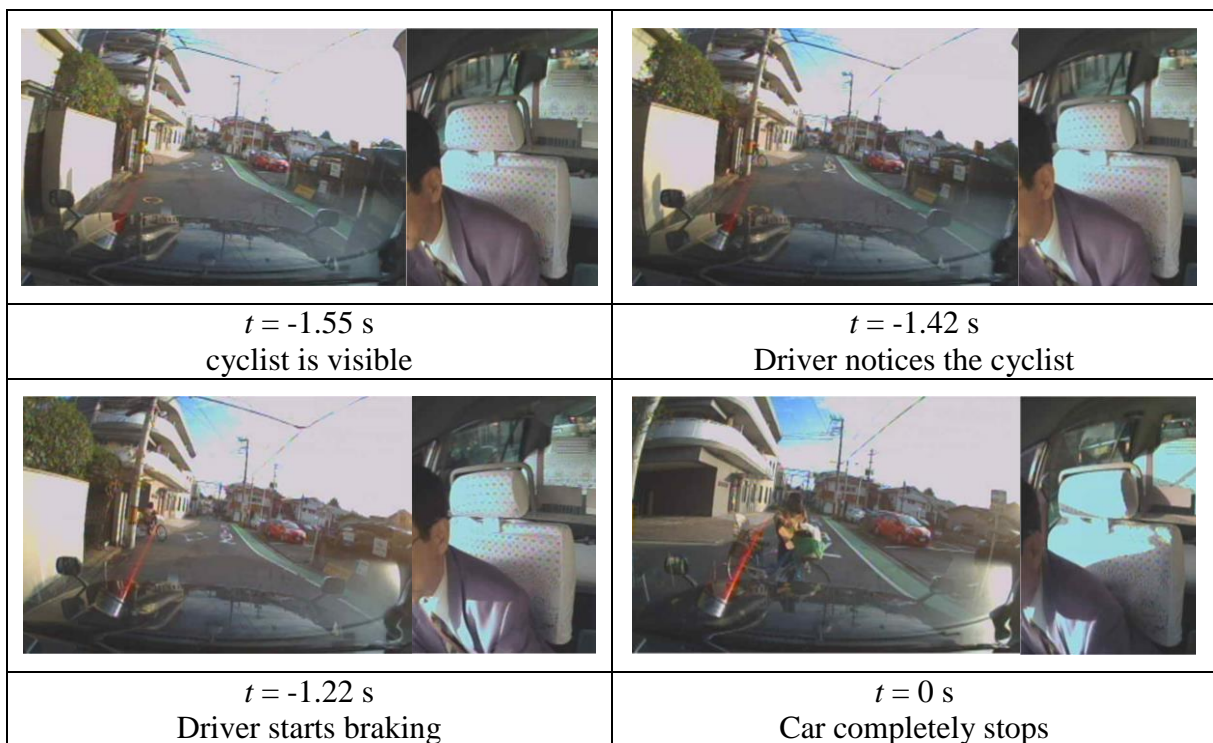


Fig. 2.11 Example of a near-miss avoided by the driver's early braking ( $TTC_a$  1.72 s and  $BRT$  0.3 s,  $t = 0$  represents car completely stops).

## 2.4. Discussion

In this chapter, the parameters of the car environment  $V_a$ ,  $TTC_a$ , and the driver's response  $BRT$ ,  $A_a$  in the perpendicular car-to-cyclist conflicts were compared in the collisions and the near-miss incidents. The average of the parameters was first compared (Fig. 2.5), and  $TTC_a$  in the near-misses (2.15 s) was significantly larger than in the collisions (1.28 s), which indicates that the conflict severity in near-miss incidents was lower than in the collisions. Moreover, the driver's braking response time ( $BRT$ ) was significantly smaller in the near-miss incidents than in the collisions, thereby, the collisions were more likely to be avoided.

These results could be also obtained from Table 2.1. The p-value shows  $TTC_a$  and  $BRT$  were the important parameters affecting the collision occurrences, and the partial regression coefficients suggest that  $BRT$  was the most critical parameter leading to collisions. Matsui (2015) analyzed 166 car-to-cyclist near-miss and calculated the  $TTC$ . They concluded that the average  $TTC$  in the near-misses was 2.1 s, and shortest average  $TTC$  was 1.9 s when the cyclists suddenly appeared from obstacles. In the near-misses of drive recorder data, the  $BRT$  distributed from 0.47 s to 2.13 s with the average 1.02 s. In this study of dissertation,  $BRT$  was 0.43 s and 0.88 s in near-misses and collisions, respectively. Probability of collision occurrences of 50% corresponded to 0.7 s of  $BRT$ . These results were comparable with Makishita and Matsunaga's study (2002), who concluded that  $BRT$  in the conflicts against sudden appearances of pedestrians was small as 0.7 s.

In this chapter, the braking deceleration limit of  $5.2 \text{ m/s}^2$  was newly proposed by comparing the collisions and the near-miss incidents from drive recorders as shown in the Fig. 2.8(b): collisions would occur when the required braking deceleration to stop the car exceeded the braking deceleration limit. From the time  $t_a$  when the cyclist was visible to the time  $t_b$  of driver's braking onset (Fig. 2.8 (a)(b)), there were two types of collisions in terms of collision avoidance: one was that the  $TTC$  was too smaller to be avoided (this type collisions were already in the left unavoidable area of braking deceleration braking in Fig. 2.8 (a)(b)). The second type was that the driver's  $BRT$  was too large and the collision occurred (this type collisions were on the right avoidable area from the braking deceleration limit as shown in Fig. 2.8 (b)).

Based on the above results, the collision occurrence threshold of  $BRT$  can be expressed by  $TTC_a$  according to Eq. (2.5) as follows:

$$BRT \leq TTC_a - \frac{V_b}{2a_0} \quad (2.9)$$

where  $a_0$  is  $5.2 \text{ m/s}^2$  (braking deceleration limit).

Figure. 2.7(a) shows the relationship of  $BRT$  and  $TTC_a$  bounded by the collision threshold at the time when the cyclist was visible. In the area  $1 < TTC_a < 2 \text{ s}$ , the near-misses and the collisions was separated by  $BRT = TTC_a - 1$ . Assuming the typical car velocity  $40 \text{ km/h}$ , the  $V_b/2a$  was  $1.07 \text{ s}$  corresponding the velocity at braking start  $V_b$  of  $40 \text{ km/h}$  and the car braking deceleration  $a$  of  $5.2 \text{ m/s}^2$ . Previous studies show that the driver's  $BRT$  was relative to  $TTC$  at the appearance time of intrusion. Boda et al. (2018) used driving simulator experiments and test track experiments to compare the drivers' response against the crossing cyclists, and they concluded that  $BRT$  and  $TTC$  had a linear relationship. Jurecki and Stańczyk (2014) shows that the driver's  $BRT$  was linear relative to  $TTC$  at the time when the pedestrian was visible. However, the relationship of  $TTC$  and  $BRT$  was examined in the scenarios with lateral intrusions instead of in the emergency situations. In our study, the linear relationship of  $TTC$  and  $BRT$  was examined in the emergency situations, and  $BRT = TTC_a - 1$  was proposed to separate the collisions and the near-miss incidents.

In the area of  $TTC_a > 2 \text{ s}$ , the  $BRT$  no longer increased as  $TTC_a$  increased. Usually, we can consider two types of near-miss incidents in the area with  $TTC_a > 2 \text{ s}$ . One type is that the driver noticed the cyclist when he/she was visible and the driver applies braking to slow down. However, drivers usually did not apply heavy braking, but rather lighter braking to move slowly due to comfortability because the available time  $TTC$  is large enough to avoid collisions. The second type is that drivers started braking as they approached the intersections to observe surroundings, although they did not notice the cyclist until the cyclist was close to the car. Since the driver's foot was already on the braking pedal, they can immediately stop the car to avoid collisions. The driver's slow down behavior at intersection is consistent with the findings of Op den Camp and Montella' research (Montella et al., 2011; Op den Camp et al., 2017). They also observed that many drivers slowed down as they approached the intersection. Since the driver's foot was already on the braking pedal, they can immediately stop the car to avoid collisions. Sharma's research (2020) points out that the driver's response time includes the delay time before the braking onset. During this delay time, some drivers intentionally delay braking to react against the stimulus. In our study, drivers did not intentionally delay braking but avoided

collisions by controlling the braking deceleration probably because the emergency level was high and close to collisions.

In addition, the parameters  $V_a$ ,  $TTC_a$ ,  $BRT$  and  $A_a$  were compared in the near side and the far side shown in Fig 2.6. The driver's response time  $BRT$  was significantly smaller in the near side of 0.64 s than in the far side of 0.98 s. Jurecki and Stańczyk (2014) found that  $BRT$  increased with  $TTC_a$  in response against the lateral pedestrians crossing on the road in the near side and the far side. From their study, the  $BRT$  was expressed as follows:

$$BRT = 0.286 TTC + 0.506 \quad (\text{near side}) \quad (2.10)$$

$$BRT = 0.351 TTC + 0.560 \quad (\text{far side}) \quad (2.11)$$

On the other hand, in this study, the result of drive recorders shows that there was no differences of  $TTC_a$  and  $BRT$  in the near side and the far side of cyclist appearance (Fig. 2.6). This may be because the car-to-cyclist conflicts in the drive recorder data included all collisions and near-misses at all intersections instead of the specific intersections. More study will be necessary to identify differences of the braking reaction time between the near side and the far side.

## 2.5. Conclusions

In this chapter, differences between the car kinematics and driver responses were examined in the perpendicular car to-cyclist conflict configuration. The near-miss and collision cases were newly compared using the real-world data of drive recorders. The results are summarized as follows:

- The average of  $TTC_a$  and drivers' braking reaction time  $BRT$  is significantly different while the car velocity is not significantly different in the near-misses and the collision at the time when the cyclist is visible to the driver.
- $TTC_a$  and  $BRT$  are significant parameters affecting collision occurrences:  $TTC_a$  determines the conflict environment, and  $BRT$  is the critical parameter leading to collisions.
- Collisions cannot be avoided when the required braking deceleration exceeds the braking deceleration limit of  $5.2 \text{ m/s}^2$  at the time of braking onset.
- The collision occurrences can be assessed by the  $TTC_a$ ,  $BRT$ , car velocity and braking deceleration, and the linear relationship of  $TTC_a$  and  $BRT$  can be obtained when substituting the braking deceleration limit and the typical car velocity.

## Chapter 3

### Cyclist Avoidance Behavior Interacting with Drivers

#### 3.1. Introduction

In Chapter 2, the kinematic parameters of the cars and the driver responses between near-miss incidents and collisions were compared to understand the factors affecting car-to-cyclist collision occurrences. From observation of the drive recorder videos, it is implied that the cyclist behavior at intersections can have a significant influence on the collision occurrence. Previous studies of the cyclist behavior usually have used cyclist driving naturalistic data. Landis et al. (2002) indicates that road traffic volume, total outside road width, cyclist's crossing distance, and the number of lanes close to the intersection are the main factors affecting the prediction of risk for cyclists on shared roads. However, the cyclist behavior such as the cyclist traveling velocity or trajectory before collisions are usually obtained from the testimony of cyclists and witness involved in the collisions, or the cyclist behavior is inferred based on the reconstructed accidental scenarios. Thus, basically the cyclist behavior recorded in global accident data as well as in-depth accident database can include uncertainties.

In this chapter, the near-misses and collisions of driver recorders are first classified into two types: near-miss cases avoided by cyclists and cases not avoided by cyclists. The parameters of cyclists are obtained from drive recorders, and the influencing factors that affect the cyclist avoided behavior in emergency situations are identified by analyzing the cyclist parameters and the kinematic parameters of cars in the two types of cases.

#### 3.2. Method

##### 3.2.1. Data of drive recorder

To examine the cyclist avoidance behavior in emergency situations, car-to-cyclist perpendicular incidents were extracted from the near-miss database. The avoidance maneuvers of drivers and cyclists were classified into three types according to who took avoidance behaviors:

- (1) Near-misses avoided by cyclist
- (2) Near-misses avoided by car driver
- (3) Near-misses avoided by both cyclist and driver

In the database, there were 228 near-miss car-to-cyclist perpendicular conflicts. In addition, we compared the near miss incidents with 63 collisions. Collision data of the driver recorder were

collected by this research project from the Aichi taxi association and Nagoya taxi association. Near-miss data were used from the database of Tokyo University of Agriculture and Technology. In order to simplify the analysis and to examine the effective avoidance behaviors against collisions, this study ignored avoidance behaviors of the cyclist and the driver during impact interactions phase in collisions.

### 3.2.2. Definition of parameters

The configuration of car-to-cyclist near-miss incidents at a perpendicular intersection is shown in Fig. 5.1. Cyclists have three positions (right, center, and left) on the road according to the cyclist's direction, and cyclists traveling on the left can be judged as following traffic rules in Japan. In Section 2.2.2, the parameters related to the car were defined in uppercase. Similarly, the cyclist related parameters are defined here in lowercase. The cyclist traveling velocity and the distance to the collision point are defined as  $v$  and  $d$ , respectively. The cyclist velocity and the cyclist distance to the collision point at the time when the cyclist is visible ( $t_a$ ) are denoted as  $v_a$  and  $d_a$ , respectively.

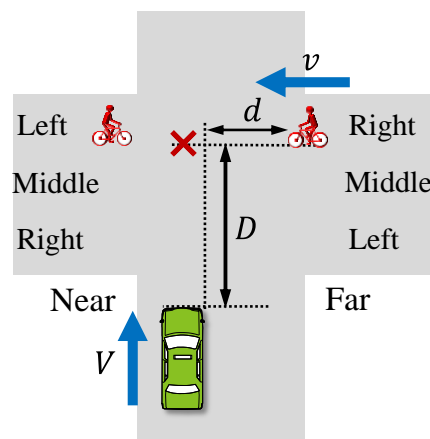


Fig. 3.1 Configuration in the car-to-cyclist perpendicular conflict. The right, middle and left of the road is the location relative to the cyclist traveling direction.

### 3.2.3. Calculation of cyclist velocity and distance

The parameters of the cyclists including the cyclist velocity and the distance from the front tire to the collision point cannot be directly obtained from videos of drive recorders. Thus, video analysis software TUAT-DRM for near-misses and Movias 2.0 for collisions are used to calculate the velocity and the distance of the cyclist. In the two software, there are three

processes to determine the distance. First, the video screen distortion caused by the camera lens is corrected. Second, the perspective transformation is conducted to the screen using 4 corner points on the screen, and the vanishing point on the screen is obtained. Third, a scaling factor from the screen to real dimension is determined. In TUAT-DRM, the distance between the right and left fender mirrors of the taxi is used as the reference, and the horizon distance can be obtained using this reference by a perspective theory. In Movias 2.0, the reference distance is the dimensions of the road signs (i.e., the width of the lines in crosswalks) on the road. Then the position of the front wheel tire's contact point on the road surface is determined in each time frame, and the velocity of the bicycle relative to the taxi can be calculated. By using a fixed point on roads, the absolute velocity of bicycle is calculated, subtracting the fixed point velocity relative to the taxi from the bicycle velocity relative to the taxi.

#### *3.2.4. Identification of cyclist avoidable behavior*

In this study, the cyclist avoidance behavior is identified from the video and divided into 4 types as:

- (1) Brake
- (2) Brake and swerve
- (3) Swerve
- (4) Brake and back

In the cyclist's avoided near-miss, the identification of brake is that the cyclist stops or obviously decelerates before entering the collision area, and the identification of swerve is that the cyclist turns the bicycle's handlebar around (Fig. 3.2). The behavior to avoid collisions is judged to be swerving with brake if the cyclist stops after swerving, and the behavior of cyclists is judged to be swerving if the cyclist rides away after turning the handle. Another identification of cyclist avoidable behavior is when the cyclist stops the bicycle and backs it up until the car passes in front of the cyclist.





(a) Cyclist avoided near-miss by braking



(b) Cyclist avoided near-miss by swerving

Fig. 3.2 Two examples of cyclist avoided collision by braking (a) and swerving (b). Time 0 s represents the time when the car arrives at the cyclist path.

### 3.2.5. Statistical analysis

#### 3.2.5.1. Descriptive statistics

First, independent parameters which can affect the cyclist's and driver's avoidance behavior are selected:  $A_a$ ,  $BRT$ ,  $V_a$ , and  $D_a$  for drivers, and  $v_a$ , and  $d_a$  cyclists involved in the car-to-cyclist near-miss at the time  $t_a$  when the cyclist is visible. Although the  $BRT$  (braking reaction time) is a parameter related to driver responses, cyclists may take actions to avoid collisions through judging the time duration of between their positions and the car braking. Thus,  $BRT$  is included in the data analysis. Second, these parameters are subjected to one-way ANOVA to examine whether there are significant differences in these groups for the cyclist avoided near-miss, cyclist not avoided near-miss and collision groups. When there is a significant difference in the variance in the sets of data, Dunnett's test is applied to calculate the difference among the means of the three avoidance groups. All significant level in the tests are set to 0.05.

### 3.3.5.2. Discriminant analysis

Traveling in the right-of-way road would have different behavioral influences on traffic participants. In car-to-cyclist perpendicular conflicts at intersections, two types of right of way are classified as follows:

- (1) The car has the right of way, and the cyclist needs to yield to the right of way,
- (2) The cyclist has the right of way, and the car driver needs to yields to the right of way.

To examine if the right of way has influences on the parameters of the cyclist avoidable behavior, discriminant analysis is applied. The right-of-way of the car and the cyclist is set as a nonmetric dependent variable (0 represents right of way of the car, and 1 represents right of way of the cyclist). All relevant variables  $A_a$ ,  $BRT$ ,  $V_a$ ,  $D_a$ ,  $v_a$ , and  $d_a$  at the time when the cyclist is visible are selected as explanatory variables. In addition, Fisher's function and Unstandardized function are used as function coefficients in this discriminant analysis.

### 3.2.5.3. Logistical regression analysis

A logistical regression analysis is applied to express the presence/absence of cyclist's avoidance behavior using the parameters of velocity and distance of cars and bicycles. The logistical regression for cyclist avoidance is expressed as:

$$\ln \frac{P}{1-P} = \beta_0 + \beta_1 x_1 + \dots + \beta_n x_n \quad (3.1)$$

where  $P$  is the probability of cyclist avoidance (0: cyclist avoided in near-miss incidents, and 1: the cyclist did not avoid but the driver avoided in near-miss incidents), and  $x_i$  is the explanatory variable, and  $\beta_i$  is the coefficient of explanatory variables ( $i = 1, 2, \dots, 6$ ). The parameters  $A_a$ ,  $BRT$ ,  $V_a$ ,  $D_a$ ,  $v_a$ , and  $d_a$  are explanatory variables to estimate factors influencing the presence/absence of the cyclist avoidance behavior. Parameters with P-values less than 0.05 in the result of logistic regression analysis are extracted for the further logistic regression analysis to obtain more precise equations.

In Chapter 2,  $TTC_a$ ,  $BRT$  and  $A_a$  were employed as explanatory variables in the logistic regression, this is because we focus on the effect of driver behavior on collision occurrences instead of the driver's judgement to cross the cyclist path. In the collected collisions and near-miss data, all the drivers had taken behaviors to avoid collisions for cyclist intrusion (they decide to react to avoid collisions for cyclist intrusion), and thus only driver responses and car parameters were examined. Instead, in the analysis of cyclist behavior in this chapter, we focus

on the factors that influence the cyclist's judgment whether to cross the intersections or not, and thus all factors involving the cyclists crossing intersections are included in the logistic regression analysis.

### 3.3. Results

#### 3.3.1. The number of cyclist avoidance behavior

The number of the near-miss incidents and collisions classified by cyclist and driver avoidance behavior is presented in Table 3.1. There are 85 cases of cyclist avoidance behavior: among them 31 cases are avoided by both cyclist and driver avoidance behavior, and 54 cases are only a cyclist took avoidance behavior (near-miss is successfully avoided by the cyclist avoidance behavior instead of the car driver avoidance behavior). The cyclist does not take avoidance behavior 143 cases: among them the driver's avoidance behavior is observed in 80 cases, and the driver's avoidance behavior is not observed in 63 cases.

Table 3.1 Number of cyclists and drivers with and without avoidance behavior in near-miss incidents and collisions.

		Car driver		Total
		w/ avoidance behavior	w/o avoidance behavior	
Cyclist	w/ avoidance behavior	31	54	85
	w/o avoidance behavior	80	63	143
	Total	111	117	228

Figure. 3.3 shows the relationship of  $TTC_b$  and the car velocity  $V_b$  at the time of car's brake onset  $t_b$  in the cyclist avoided and the cyclist not avoided near-miss incidents. When the required acceleration of the car ( $V_b/2 TTC_b$ ) is higher than the braking performance limit ( $a = 5.2 \text{ m/s}^2$  in the Section 2.3.3 of Chapter 2), the car cannot stop before reaching the collision point. The cyclists who do not take avoidance behavior is distributed in the right area of the car's braking performance limit ( $V_b/2 TTC_b < 5.2 \text{ m/s}^2$ ), and car drivers can avoid the collision by car braking. In this area, the cyclists do not take avoidance behavior probably because  $TTC_b$  is still large to take avoidance behavior for cyclists.

Of the 85 near-miss incidents in which the cyclists took avoidance behavior, 14 cyclists are beyond the car's braking limit. These 14 cases would have resulted in a collision if the cyclist

had not taken avoidance behavior, indicating that cyclist avoidance behavior is effective in avoiding collisions.

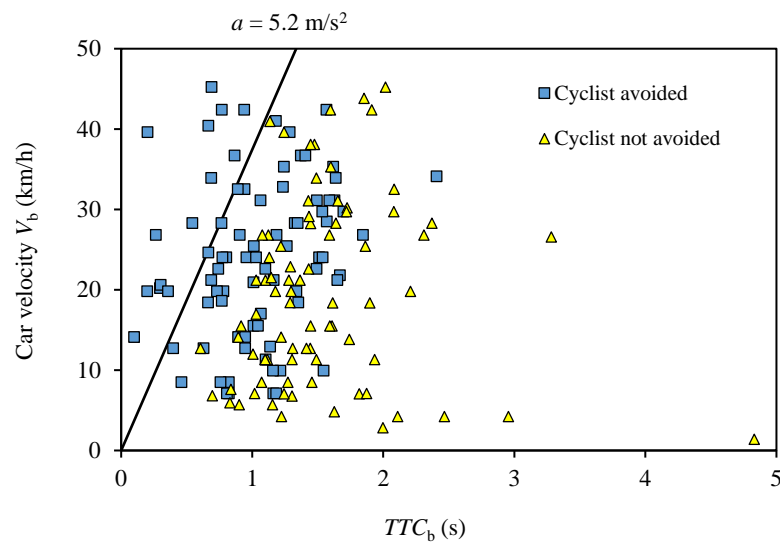


Fig. 3.3 Relationship between  $TTC_b$  and the car velocity  $V_b$  at the time of brake onset  $t_b$  with/without cyclist avoidance behavior in near-miss incidents (the line shows the braking limit). Note: collisions are not included.

### 3.3.2. Descriptive parameters of car and driver

Figure. 3.4 shows the mean of the parameter  $A_a$ ,  $V_a$ , and  $D_a$  of the car at the time when the cyclist is visible ( $t_a$ ). Statistical differences using one-way ANOVA is also added. All parameters are significantly different among groups except for  $BRT$  ( $F(2, 224) = 2.228$ ,  $p = 0.11$ ). The mean acceleration of the car  $A_a$  in the near-miss group is lower than in the collision group. The p-value of the difference of the car velocity  $V_a$  between the cyclist avoided near-miss and the cyclist not avoided near-miss is close to the significant level ( $p = 0.054$ ). The distance of the car  $D_a$  does not show significant difference in between the cyclist avoided near-miss and the cyclist not avoided near-miss ( $p = 0.005$ ).

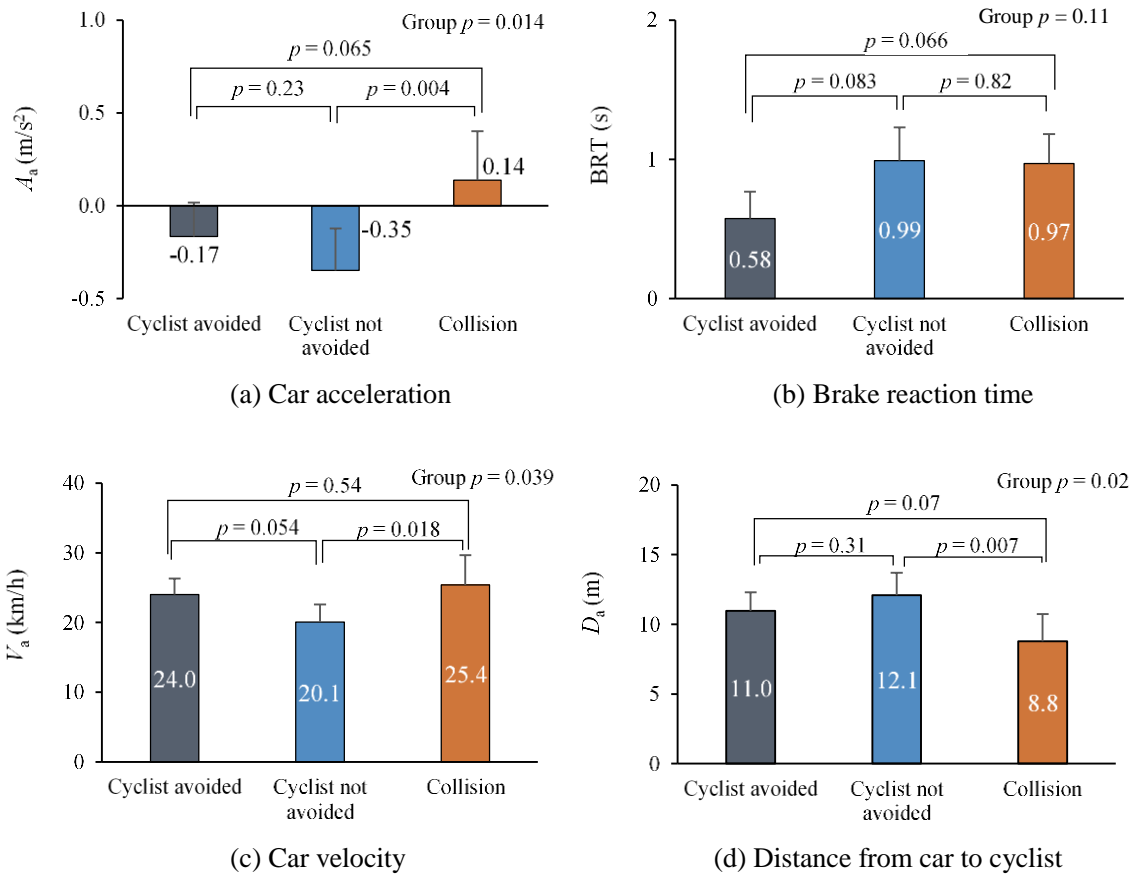


Fig. 3.4. Mean values of  $V_a$  and  $D_a$  in cyclist avoided near-misses and cyclist not avoided near-miss incidents. The error bars represent 95% confidence interval.

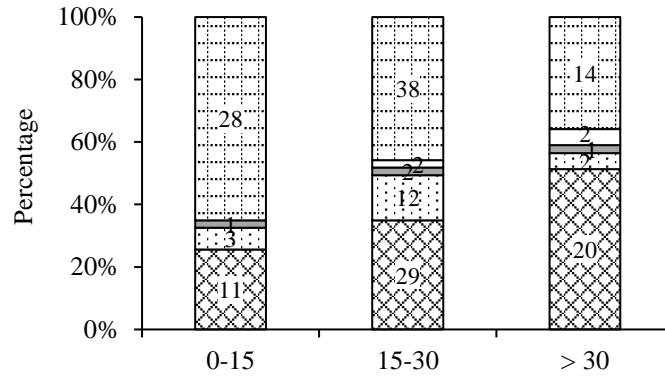
### 3.3.3. Cyclist avoidance behavior

#### 3.3.3.1. Behavior classification

The percentage of the cyclist behavior with different car velocities  $V_a$  at the time when the cyclist is visible  $t_a$  is shown in Fig. 3.5(a). The percentage of avoidance behavior increases while that of no avoidance behavior of cyclists decreases as the car velocity increases. Among types of cyclist avoidance behavior, the primary behavior of the cyclists is bicycle braking. Some cyclists use swerving or applied both braking and swerving to avoid collisions. In addition, 4 cyclists applies braking and go back the bicycle to avoid accidents.

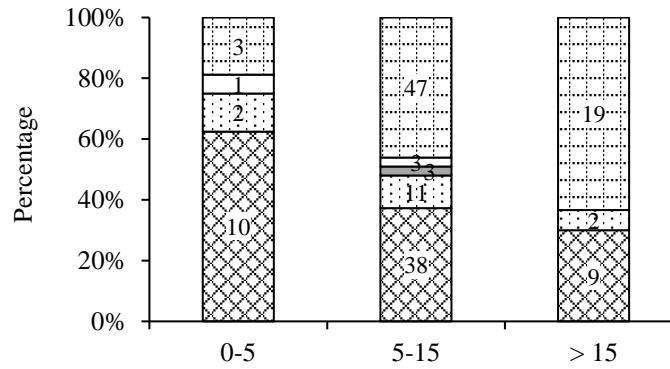
Figure. 3.5(b) shows the percentage of the cyclist behavior with cyclist velocity  $v_a$ . The trend of cyclist behavior with the cyclist velocity is contrary to that with the car velocity. The percentage of the avoidance behavior decreases, and that of no avoidance increases as the cyclist velocity increases. Hence, it can be summarized that cyclists tend to take avoidance behavior as the car velocity is high and the cyclist velocity is low.

Brake
  Brake and swerve
  Swerve
  Brake and back
  No avoidance



(a) Vehicle velocity  $V_a$  (km/h)

Brake
  Brake and swerve
  Swerve
  Brake and back
  No avoidance



(b) Cyclist velocity  $v_a$  (km/h)

Fig. 3.5 Cyclist avoidance behavior with different car velocity  $V_a$  and cyclist velocity  $v_a$  when the cyclist is visible ( $t_a$ ).

### 3.3.3.2. Cyclist direction and location relative to the car

Table 3.2 presents the ratio of cases with cyclist's traveling location and intruding direction relative to the car in the cyclist avoided near-miss, cyclist not avoided near-miss and the collision group. Traffic violation of the cyclists is also included in this table. The ratio of cyclist's intruding from the far side is larger than that from the near side, particularly in the cyclist not avoided near-miss incidents. On the other hand, more cyclists violate traffic rules (traveling in the right side of the road) in collisions (61%) than in near-miss incidents (53% and 46%).

Table 3.2. Proportion of intruding direction and location of cyclists relative to the car and traffic violation of the cyclists.

Side	Cyclist avoided (near-miss)		Cyclist not avoided (near-miss)		Collision	
	Near	Far	Near	Far	Near	Far
Left	0.27	0.20	0.24	0.30	0.21	0.30
Center	0.04	0.16	0.04	0.16	0.02	0.07
Right	0.14	0.19	0.10	0.16	0.20	0.28
Total	0.45	0.55	0.38	0.63	0.43	0.57
Violation	0.53		0.46		0.61	

### 3.3.3.3. Cyclist velocity and distance

The mean velocity of the cyclist in the cyclist avoided, cyclist not avoided and collision groups at the time when the cyclist is visible is compared in Fig. 3.6(a). The mean velocity of cyclists in the cyclist avoided near-miss, cyclist not avoided near-miss and collision group is 9.8 km/h, 12.7 km/h and 13.5 km/h, respectively ( $F(2, 198) = 12.393, p < 0.001$ ). The p-value indicates that the velocity of the cyclist's avoided near-miss is significantly lower than that of the cyclist's not avoided near-miss and the collision. Figure. 3.6(b) shows the distance from the bicycle to the collision area. The distance  $d_a$  in the cyclist's not avoided near-miss is significantly larger than in the cyclist's avoided near-miss and the collision. Hence, cyclists tend to take avoidance behavior as the cyclist velocity is low and the distance to the car is small. On the other hand, collisions tend to occur as the cyclist velocity is high and the distance to the car is small.

The distribution of cyclist velocity at the time when the cyclist is visible in the cyclist avoided near-misses, cyclist not avoided near-misses and collisions is shown in Fig. 3.7. The accumulation of cyclist velocity in the cyclist avoided near-misses is higher than the cyclist not avoided near-misses and the collision group, which imply that the overall cyclist velocity in cyclist avoided near-misses is smaller than the other two groups. The distribution and cumulative curve of the collision show that the percentage of high cyclist velocity in the collisions is larger than the other two groups.

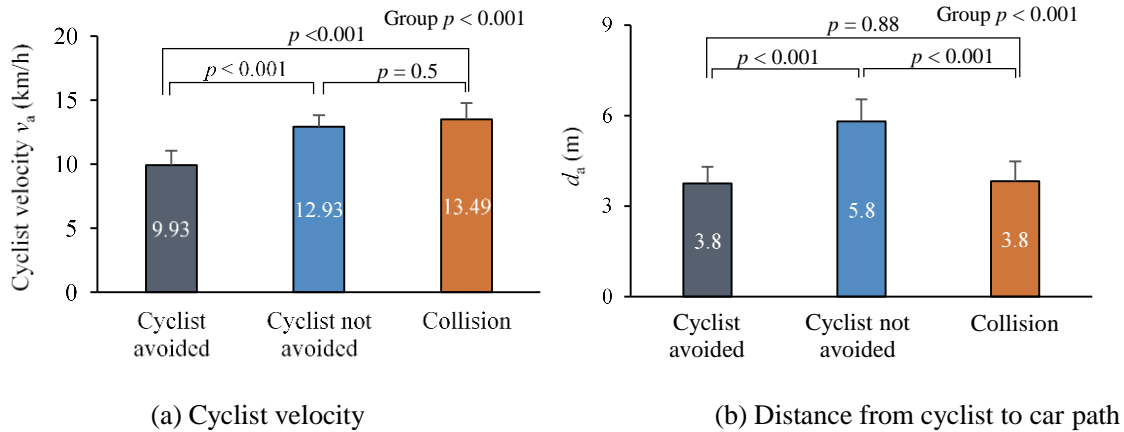


Fig. 3.6 Cyclist velocity and distance at the time when cyclist is visible classified by cyclist avoidance behavior.

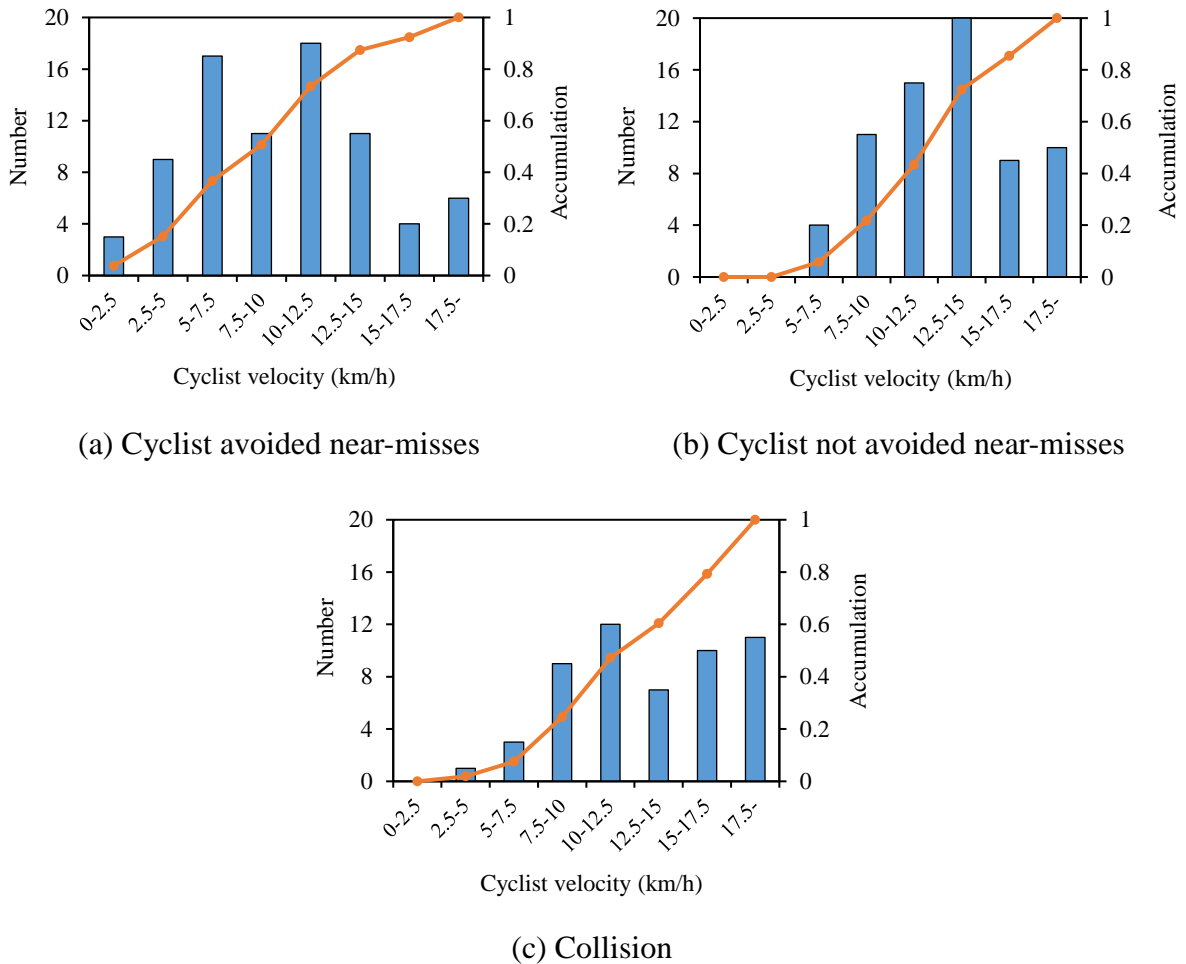


Fig 3.7 Distribution of cyclist velocity at the time when the cyclist is visible in cyclist avoided collision group, cyclist not avoided group and collision (cases where cyclist velocity cannot be calculated were not included).



### 3.3.4. Effects of right of way

Table 3.3 presents the influences of the right of way of drivers or cyclists on the parameters  $A_a$ ,  $BRT$ ,  $V_a$ ,  $D_a$ ,  $v_a$ , and  $d_a$  using logistic regression analysis. The car deceleration  $A_a$  ( $p = 0.023$ ), the car velocity  $V_a$  ( $p = 0.004$ ), and the cyclist distance to the collision point  $d_a$  ( $p = 0.007$ ) is significant to discriminate the right of way of the car and the cyclist. Based on the sign of the partial regression coefficients, the car acceleration and the car velocity is higher, while the distance between the cyclist and the collision point is smaller when the car has the right of way at the time when the cyclist was visible.

Table 3.3 Effects of right of way using discriminant analysis. (0 represents right of way of the car and 1 represents right of way of the cyclist).

Explanatory variables	Discriminant coefficient	Wilks' lambda	F-value	P-value
$A_a$	0.3341	0.9675	5.3060	0.0226
$BRT$	-0.1401	0.9963	0.5882	0.4443
$V_a$	0.0603	0.9497	8.3620	0.0044
$D_a$	0.0395	0.9912	1.4068	0.2374
$v_a$	0.0064	0.9997	0.0517	0.8204
$d_a$	-0.1639	0.9551	7.4284	0.0071

### 3.3.5. Parameter determining taking avoidance behavior

Table 3.4 presents the partial coefficients and p-values of explanatory variables for the presence or absence of cyclist's avoidance behavior in the logistic regression analysis. Car velocity  $V_a$ , car distance  $D_a$ , and cyclist velocity  $v_a$  at the time when the cyclist is visible, are primary parameters for determining cyclist's taking avoidance behavior in near-miss incidents based on the p-value ( $P < 0.05$ ). The partial regression coefficient indicates that the cyclist is more likely to take maneuvers to avoid collisions when  $V_a$  is higher,  $D_a$  is smaller, and  $v_a$  is lower.

Significant parameters such as  $V_a$ ,  $D_a$ , and  $v_a$  are chosen based on p-value  $< 0.05$  in Table 3.4, and applied to the logistic regression, again. Table 3.5 presents the coefficients and p-value of the logistic regression. Fitting the partial regression coefficient, the probability of avoidance by cyclists is expressed as follows:

$$P = \frac{1}{1 + \exp(-1.006 - 0.1348 V_a + 0.1996 D_a + 0.1448 v_a)} \quad (3.2)$$

In Eq. (3.2), the probability of cyclist avoidance increases as the car velocity is higher and the distance between the cyclist and the collision point is smaller. Thus, we can set up a hypothesis that a cyclist may avoid collisions based on TTC ( $= V/D$ ). Hence, a logistic regression was conducted using  $TTC_a$  instead of  $V_a$  and  $D_a$ . The regression coefficients of cyclist avoidance is presented in Table 3.6, and the probability of avoidance by cyclists using TTC can be expressed simply as follows:

$$P = \frac{1}{1 + \exp(-2.2738 + 0.3131 TTC_a + 0.1376 v_a)} \quad (3.3)$$

The prediction accuracy of the regression is the same level as 70.9% in Eq. (3.2) and Eq. (3.3).

Table 3.4 Probability of presence/absence of cyclist avoidance behavior in logistic regression analysis (cyclist avoided near-misses ( $P = 1$ ) and the cyclist not avoided near-misses ( $P = 0$ )). The prediction accuracy is 71.5%.

Explanatory variables	Partial regression coefficient	Standard error	Standard regression coefficient	P-value
$A_a$	0.2855	0.2331	0.2698	0.2207
$BRT$	0.3829	0.2749	0.3846	0.1636
$V_a$	0.1443	0.0402	1.6135	<0.001
$D_a$	-0.2170	0.0654	-1.4866	<0.001
$v_a$	-0.1095	0.0428	-0.5390	0.0105
$d_a$	-0.1458	0.0956	-0.4578	0.1272
Constant	1.0754	0.6887		0.0983

Table 3.5. Reduced parameters of  $V_a$ ,  $D_a$ , and  $v_a$  of the cyclist avoidable behavior using logistic regression analysis. The prediction accuracy is 70.9%.

Explanatory variables	Partial regression coefficient	Standard error	Standard regression coefficient	P-value
$V_a$	0.1348	0.0316	1.5082	<0.001
$D_a$	-0.1996	0.0523	-1.3675	<0.001
$v_a$	-0.1448	0.0403	-0.7124	<0.001
Constant	1.0060	0.5748		0.0801

Table 3.6. Reduced parameters  $TTC_a$  and  $v_a$  of the cyclist avoidable behavior using logistic regression analysis. The prediction accuracy is 70.9%.

Explanatory variables	Partial regression coefficient	Standard error	Standard regression coefficient	P-value
$TTC_a$	-0.3131	0.1326	-0.5005	0.0182
$v_a$	-0.1376	0.0376	-0.6773	< 0.001
Constant	2.2738	0.5476		< 0.001

### 3.4. Discussion

In this chapter, the cyclist behavior in emergency situations was examined through comparing between the cyclist collision avoided group and the cyclist not collision avoided group using videos in the drive recorders. In chapter 2, the driver responses to cyclist intrusions at intersections were compared in collisions and near-miss incidents after the drivers had determined to take actions to avoid cyclist collisions. The data where the driver decided to cross the cyclist path after the driver judged all parameters involving the car and the cyclist could not be collected by drive recorder in this study (the car does not have large decelerations in the lateral and the longitudinal directions in this situation, and data cannot not be uploaded). Thus, only the  $TTC_a$ ,  $BRT$  and  $A_a$  relative to the car and the driver as explanatory variables were used in logistic regression analysis to investigate the factors influencing the collision occurrences. Unlike the analysis of driver behaviors in Chapter 2, the cyclist motivation to cross the car path at intersections to avoid collisions could be obtained from drive recorder data. Thus all parameters  $A_a$ ,  $BRT$ ,  $V_a$ ,  $D_a$ ,  $v_a$ , and  $d_a$  relative to the judgements by cyclist were examined in the logistic regression analysis to investigate the factors influencing the cyclist decide to avoid collisions. Besides, the avoidance behavior taken by cyclists was more effective than taken by drivers, because the cyclist could stop or swerve in a short time. Hence this chapter did not focus on the behavior after the cyclists decided to take actions to avoid the collisions.

In this chapter, the parameters of cars such  $V_a$ ,  $D_a$ ,  $A_a$  and  $BRT$ , as well as the kinematic parameters of cyclists  $v_a$  and  $d_a$  at the time when the cyclist was visible were firstly compared in the cyclist avoided group and the cyclist not avoided group. The results show that the car velocity  $V_a$ , the cyclist velocity  $v_a$  and the cyclist distance to the collision point  $d_a$  were significantly different in the two groups (Fig. 3.4 for cars and Fig. 3.6 for cyclists). These parameters were further examined to understand the influences affecting the cyclist avoidance

behavior using logistical regression analysis. The car velocity  $V_a$ , the distance of the car to the collision point  $D_a$  and the cyclist velocity  $v_a$  were the critical factors affecting the cyclist avoided behavior. As  $V_a$  increased,  $D_a$  decreased and the  $v_a$  decreased, then cyclists were more likely to avoid and stop (Table 4).

These results imply that there is some basis for a cyclist to judge to cross intersections when a car approaches. It is likely that cyclists judged whether they could pass an intersection based on car's approaching velocity and distance. Besides, cyclists also did not tend to take avoidance behavior if cyclist's traveling velocity was high probably because they did not recognize hazard for crossing the intersection.

Figure. 3.3 shows the effectiveness of cyclist's avoidance behavior in preventing collisions from occurring. The 14 cases in which avoidance behavior was taken by cyclists are distributed on the left side above the braking limit of the car. On the other hand, all cases in which no avoidance behavior was taken by cyclists are distributed on the right side below the braking limit. This suggests that cyclists may have thought that there was a possibility of a collision if they did not take avoidance behavior by themselves. Previous studies have investigated only the avoidance behavior of car drivers in emergency situations. However, the results of this study show that even if a car cannot stop due to braking restrictions, a collision can still be avoided if the cyclist notices emergencies and applies braking and stops.

It should be noted that near-miss incidents in drive recorder is recorded by the trigger (threshold) of braking deceleration. Therefore, the drive recorder data do not include near-miss incidents that drivers did not take any maneuvers but only cyclists took avoidance behaviors. This can underestimate the effectiveness of cyclist avoidance behavior in the analysis using drive recorder.

One of the highlights of this study is that we calculated the cyclist velocity at intersections in the conflicts by using video processing software. The average cyclist velocity in the cyclist avoided and cyclist not avoided group was 9.9 km/h and 12.9 km/h. The average cyclist velocity in the collisions was slightly higher as 13.5 km/h. Some previous studies calculated the cyclist velocity in the naturalistic traveling. Thompson (1997) shows that the average cyclist velocity was 14.8 km/h on the road without motor vehicles. Balevski and Lyubenov (2018) calculated the average cyclist velocity 14-15 km/h and 12 km/h on the narrow road. Pein et al. (1997) calculated the cyclist velocity of 12.7 km/h crossing intersections. In this dissertation, the cyclist's velocity was measured when the cyclist was approaching to the intersection, thereby

the average velocity was probably lower than the normal cycling on the road without intersections. The cyclist velocity on the cyclist avoided group was lower than in the cyclist not avoided group (see Fig. 3.6(a)), this is because the cyclists who took the avoidance behavior determined to decelerate recognizing the conflict configuration.

The cyclist can have various velocity distributions depending on the road type. However, in this research study, the road of the cyclists traveled was not classified, and the data included all road types in the collisions and near-misses such as pavements as well as vehicle and pedestrian shared roads. Besides, Blanc et al. (2016) showed that the facilities and the width of roads have influences on cycling comfort, thus this result in Japan cannot be applied to road environments in foreign countries.

In this chapter, errors may occur when calculating the cyclist velocity: although the video was calibrated before using TUAT-DRM and Movias 2.0, errors may be included when the cyclist appeared from the edge of the screen with high distortion of the screen. At the time when the cyclist was visible, the cyclist was far from the drive recorder camera, and the wheel of bicycle sometimes was not be clearly extracted in the screen, which may also lead to errors. Moreover, in the near-miss incidents, the collision point was determined based on the assumption of the cyclist trajectory.

### **3.5. Conclusions**

The avoidance behavior of cyclists in the near-miss incidents was investigated based on the observation of videos of driver recorders. The conclusions are as follows:

- Among the 85 near-miss incidents where cyclist shows avoidance behavior, 14 cases are found to be effective to avoid actual collisions. These cases are included in the area which exceed the car braking limit.
- The velocity of the cyclists in the cyclist collision avoided group is significantly smaller than that of the cyclist not taking avoidance behavior in near-miss incidents and collisions.
- The right of way of the road has a significant influence on the car deceleration and the distance from the bicycle to the collision point: the car on the road with the right of the way tends to have high acceleration and high velocity, and small distance of cyclist to the collision point.

- The probability of taking avoidance behavior by cyclist is expressed with logistic regression by using vehicle  $TTC_a$  and the cyclist velocity  $v_a$ : smaller  $TTC_a$  and lower  $v_a$  lead to high probability of cyclist to take avoidance behavior.

## Chapter 4

### Study of Driver Response in Avoiding Collisions Using Driving Simulator

#### 4.1. Introduction

Many cyclists are involved in collisions against cars every year. Hence, understanding the driver responses in an emergency car-to-cyclist scenario is necessary to develop active safety systems such as autonomous emergency braking (AEB) and advanced driver assistance system (ADAS) to reduce the injuries and fatalities in collisions involving cyclists.

Driving simulators can effectively and safely reflect drivers' behavior in the real world (Underwood et al., 2011). Driving simulators are used as a useful method to understand driver's responses in the traffic conflicts (Markkula et al., 2019). Some studies investigated driver behavior using driving simulators and test tracks in the car-to-car and car-to-pedestrian conflicts, showing that braking is the primary response in avoiding collisions, and driver also combines with swerving to avoid collisions in scenarios where there is small time-to-collision due to lateral intrusions (Morita et al., 2013; Jurecki and Stańczyk, 2014; Li et al., 2019). However, there is no research examining the driver responses interacting with intruding cyclist from both right and left directions in collisions.

The driver responses and car kinematics in collisions and near-miss incidents from drive recorder data were compared in chapter 2. In this chapter, three typical collisions are extracted from drive recorder data and reconstructed to examine responses of different drivers in the three scenarios using a driving simulator. The driver responses and car kinematics in the scenarios involving the cyclist intruding from the near side and the far side with various time-to-collisions (TTC) at the time when the cyclist is visible are examined. In addition, gaze distributions of drivers are measured by an eye track system in the driving simulator experiments to determine the driver's gaze location and hazard recognition ability for cyclist intruding from different sides. The time when the driver notices the cyclist is measured, and the driver responses is investigated by the TTC when the driver notices the cyclist.

#### 4.2. Methods

##### 4.2.1. Driving simulator and participants

An immersive driving simulator from Nagoya University is used to examine the driver's reactions in emergency situations as shown in Fig. 4.1. This driving simulator is surrounded by

five 240-inch high-brightness displays to provide the driver with a 315 degrees wrap-around driving experience. The front compartment of a mini car is mounted on a 6-axis motion pedestal with 6 degrees of freedom, which can provide the driver with the sensation of accelerating and decelerating the vehicle in both linear and rotational modes.



Fig. 4.1 Immersive driving simulator.

#### 4.2.2. Test procedure

Three typical collisions are extracted from drive recorder data and were reconstructed using UC/win Road software in the driving simulator. Table 4.1 and Fig. 4.2 show the parameters and reconstructed scenarios. In scenario N1, the cyclist model is illegally traveling on the right on his/her way at a velocity of 10 km/h and appearing from the left side (near side) with respect to the car in an intersection. The participants are asked to drive the car at 40 km/h and the distance to the path of the cyclist is 17 m, resulting in  $TTC_a$  of 1.5 s at the time when the cyclist is visible.

In scenario N2, the cyclist intrudes into an intersection from the left side (near side) with a velocity of 10 km/h relative to the driver. The cyclist model is illegally riding on the right side of his/her road. The participants are asked to drive at a velocity of 30 km/h. The distance to the cyclist path is 7 m at the time when the cyclist appears from the obstacle, and  $TTC_a$  is small as 0.8 s.

In scenario F, the cyclist model emerges from the right side (far side) relative to the driver, and the cyclist is traveling at a velocity of 15 km/h on the left side of his/her road. The participants are asked to drive the car at 40 km/h. The distance from the front of the car to the cyclist traveling trajectory is 23 m when the cyclist was visible, resulting in relatively larger  $TTC_a$  of 2.0 s.

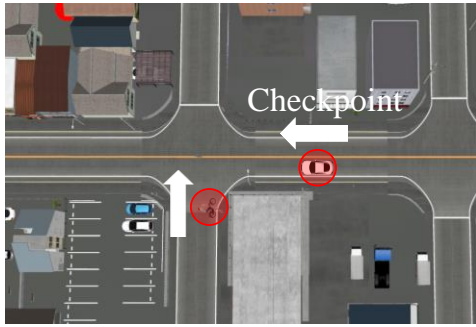


The cyclist appears at the 7th, 3rd, and 9th intersection, and the distance from the starting point to the cyclist traveling path is 311 m, 186 m, and 756 m in the scenario N1, N2, and F, respectively (Fig. 4.3). When the car passes the checkpoint, the cyclist model is set to start to move, and  $TTC_a$  could be consistent with the expected  $TTC_a$  if the driver drove at an instructed velocity.

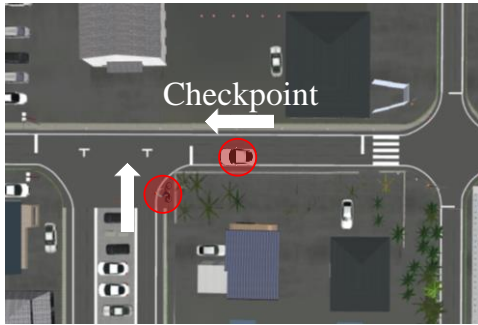
Before the participants starts the three scenarios, the participants are asked to drive at 50 km/h on the practice trial with 4 intersections over 900 m. In the practice trial, the participants are instructed to drive in compliance with traffic rules to adapt to accelerate/decelerate and follow the front car of them. Three scenarios are randomly allocated to the participants after completing the practice trial.

Table 4.1 Parameters in the driving simulator experiments

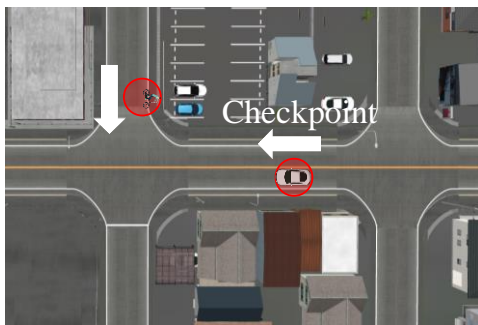
Scenario	$TTC_a$ (s)	Car velocity $V_a$ (km/h)	Cyclist velocity $v$ (km/h)	Distance from the car to the cyclist $D_a$ (m)	Cyclist side
N1	1.5	40	10	17	Near
N2	0.8	30	10	7	Near
F	2.0	40	15	23	Far



(a) Scenario N1



(b) Scenario N2



(c) Scenario F

Fig. 4.2 Three reconstructed test scenarios in the driving simulator.



(a) Scenario N1



(b) Scenario N2



(c) Scenario F

Fig. 4.3 Top view of three scenarios. The distance from the starting point to the cyclist path of scenario N1, scenario N2, and scenario F is 311 m, 186 m, and 756 m, respectively.

#### 4.2.3. Eye track

Figure. 4.4 shows the Smart Eye Pro DX system installed in the driving simulator as a gaze track system. This system consists of four cameras: three cameras are installed on the instrument panel and one is installed above the mirror. The system measures the driver's gaze with 160 degrees by calculating the driver's head movement, direction of gaze, eye position, and eye opening degree in the video. Calibration is required before each participant starts the experiment. First, the participants are asked to hold up a cardboard with a chessboard in the front of the cameras for camera lens calibration. Next, the participants are asked to stare at the red point in the center of the screen for gaze calibration.

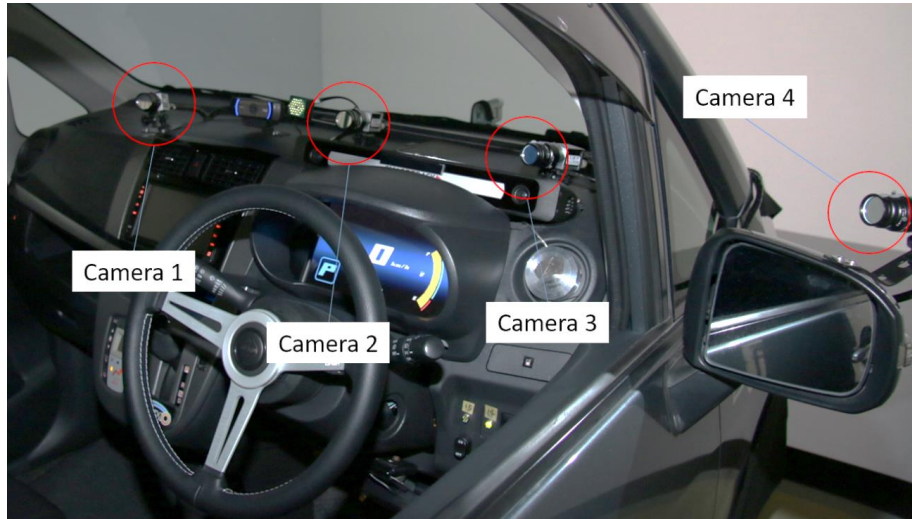


Fig. 4.4 Eye track system installed in the car

#### 4.2.4. Participants

Thirty-one participants with driver's licenses are recruited through the Nagoya University website, including 29 males and 2 females. The age distributions are 14 participants in their 20s, 1 participant in their 30s, 5 participants in their 40s, 6 participants in their 50s, 3 participants in their 60s, and 2 participants in their 70s. The mean age is 40.3 years old with the standard deviation of 17.2 years old. Moreover, the work or study of all participants is not relevant to this research. This experiment is approved by the Ethics Committee of Nagoya University Graduate School of Engineering (No. 20-1).

#### 4.2.5. Statistical analysis

The same statistical analysis is applied in the driving simulator experiment as in the Section 2.2.2. The difference of mean values of the car kinematic parameters  $TTC_a$  and  $V_a$  and the parameters of the driver's response  $BRT$  and  $A_a$  at the time  $t_a$  when the cyclist is visible are examined in the avoidance and the collision groups. Moreover, the sample in the driving simulator is small, and thus normality is examined before t-test. If the data do not satisfy the normal distribution, Mann-Whitney test (non-parametric test) is applied instead of t-test.

A decision tree is applied to hierarchically clarify the factors influencing the collision occurrence. The independent parameter  $TTC_a$ ,  $BRT$  and  $A_a$  was used in the IBM SPSS Statistic as explanatory variables. The growth method of classification regression tree (CRT) is selected for the decision tree.

A logistic regression analysis is employed in the three scenarios to calculate the values of drivers' braking response  $BRT$  and braking deceleration  $a_0$  to determine the threshold of the collision occurrence. The logistic regression is expressed as follows:

$$\ln \frac{P}{1-P} = \beta_0 + \beta_1 x_1 \quad (4.1)$$

where  $P$  is the probability of collision occurrence (0 was avoidance and 1 was crash),  $x_1$  is explanatory variable  $BRT$  or  $a_0$ , and  $\beta_i$  is its coefficients ( $i = 1, 2$ ).

#### 4.2.6. Threshold of collision occurrence

The collision occurrence/avoidance can be expressed using TTC, BRT, velocity, and braking deceleration (see Eq. (2.5)). The threshold of collision avoidance can be obtained if the drivers apply braking to avoid collisions.

$$TTC_a - BRT - \frac{V_b}{2a_0} > 0 \quad (4.2)$$

The value of  $BRT$  and  $a_0$  corresponding 50% probability can be calculated from Eq. (4.1), and this value is substituted into Eq. (4.2) to obtain the threshold of collision occurrence.

In addition to applying driver's braking to avoid collisions, there are also situations where drivers can avoid collisions by accelerating or maintaining velocity at the intersection: the driver passes the collision point before the cyclist reaches the collision point. In this situation, it takes time  $d_a/v_a$  for the cyclist to arrive at the collision point, and this time duration  $d_a/v_a$  is smaller than the time duration  $TTC_a + L/V_a$  for the rear end of the car (car length  $L$  in Fig. 2.3) to pass the collision point. Hence, the threshold to avoid collisions can be expressed as follows:

$$TTC_a + \frac{L}{V_a} - \frac{d_a}{v_a} < 0 \quad (4.3)$$

The collision occurrences can be examined using Eqs. (4.2) and (4.3).

### 4.3. Results

#### 4.3.1. Driver avoidable results

The driver responses to avoid cyclists in the car-to-cyclist conflicts at a perpendicular

intersection was examined by the driving simulator. Figure. 4.5 shows the number of driver's avoidance/collision is shown with classification of driver's responses in the driving simulator. In scenario N1, 8 drivers avoids collisions, and 23 drivers collide with the cyclist. In scenario N2, 10 drivers avoid collisions, and 21 drivers have collisions against the cyclist. In scenario F, 18 drivers avoid collisions, and 13 drivers do not avoid collisions. The driver has 4 types of behaviors to avoid collisions: braking, braking with swerving, swerving only, and no response. No response is that the driver maintains the behaviors after the cyclist is visible. In addition, driver's braking and swerving but impacting with the cyclist is also included in the avoidance behavior.

Most drivers applied braking to avoid collisions in all scenarios. In the collision group, more drivers apply braking with swerving and only swerving compared to the avoidance group. The drivers take more evasive maneuvers in the near side than in the far side. In scenario N1, 10 drivers apply braking with swerving and 3 drivers take swerving only in the collision group, and there is only 1 driver applies braking with swerving in the avoidance group. In scenario N2, 7 drivers employ braking with swerving and 1 driver employs swerving only in the crash group, and 3 drivers apply braking with swerving in the avoided group. In scenario F, 3 drivers apply braking with swerving and 1 driver applies only swerving in the crash group, and only 1 driver applies braking with swerving and 1 driver applies only swerving in the avoided group. In all scenarios, there are 6 driver apply only swerving, and 5 drivers of them do not avoid collisions, which suggests that only swerving is not effective for avoiding collisions.

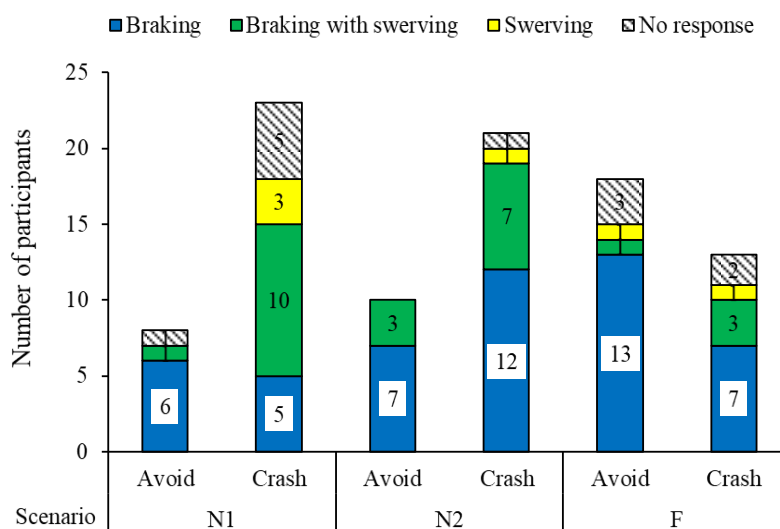


Fig. 4.5 Result of the driving simulator experiment in scenario N1, N2, and F.

#### 4.3.2. Descriptive statistics

The mean of the parameter for  $TTC_a$ ,  $V_a$ ,  $BRT$ , and  $A_a$  in the driving simulator experiments is shown in Fig. 4.6. In scenario N1,  $V_a$  ( $t(8) = -2.34, p = 0.045$ ) and  $BRT$  ( $U = 2, p < 0.001$ ) is significantly different in the avoidance and the collision group.  $TTC_a$  in the avoidance group is larger than in the collision group, although the p-value is close to the significant level 0.05 ( $t(7) = 2.24, p = 0.06$ ). This indicates that the driver travels at a lower velocity and applies braking earlier if the drivers avoided collisions in scenario N1.

In scenario N2,  $TTC_a$  ( $U = 25, p < 0.001$ ),  $V_a$  ( $U = 30, p = 0.006$ ) and  $BRT$  ( $U = 4, p < 0.001$ ) shows significant differences between the avoided group and the crash, which suggests that all parameters need to satisfy a lower velocity, larger  $TTC_a$  and early braking for avoiding collisions in the scenario with small  $TTC_a$ .

In scenario F, only  $BRT$  shows the significant differences in the avoided group and the crash group ( $t(21) = -5.15, p < 0.001$ ). This indicates that the driver needs to apply braking early for avoiding collisions in this scenario F where the cyclist travels from the far side with relatively large  $TTC_a$ .

In addition,  $BRT$  in all scenarios shows the significant differences between the avoidance group and the collision group, and the mean of avoidance group is significantly smaller than of the collision group. The car acceleration in all scenarios does not show the differences in the avoidance group and the collision group, which indicates that the car acceleration at the time when the cyclist is visible, is not the critical parameter affecting the collision occurrence in emergency situations.



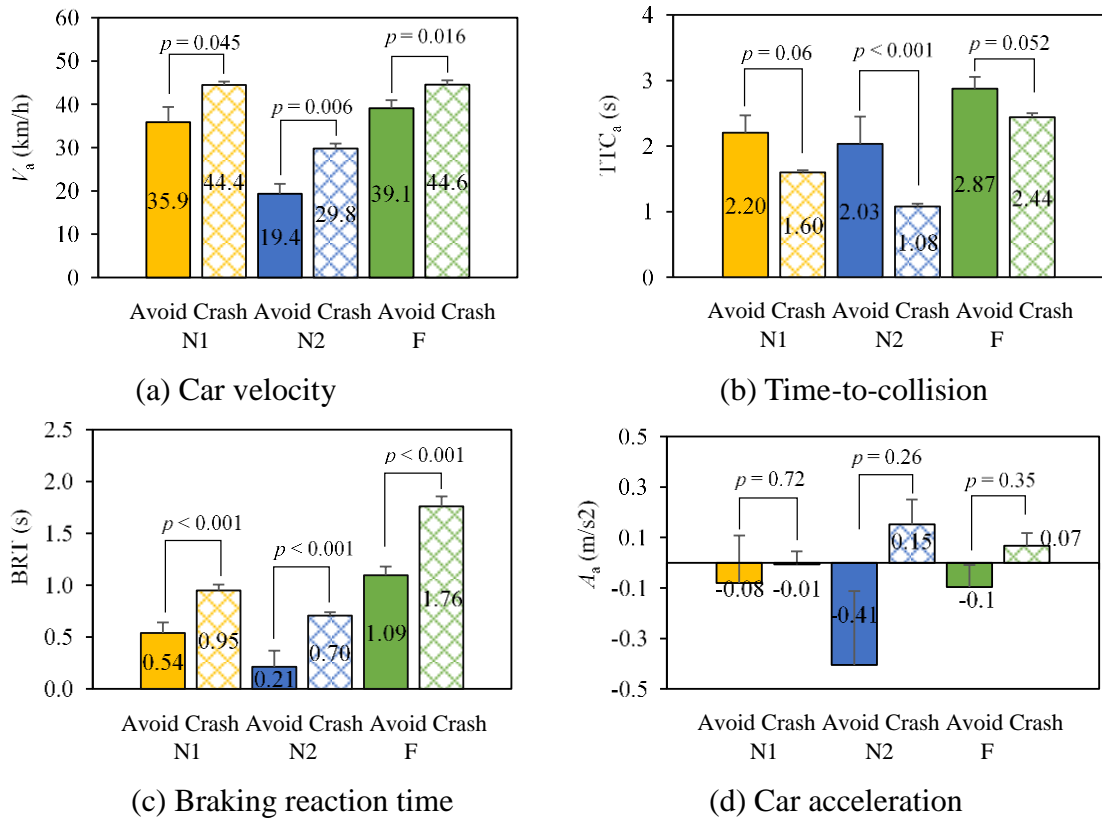


Fig. 4.6 Mean of parameters  $TTC_a$ ,  $V_a$ ,  $BRT$ , and  $A_a$  in the driving simulator experiments (error bar represents standard errors).

It is shown from Fig. 4.6 that  $BRT$  is as a key factor which influenced the collision occurrences. Thus,  $BRT$  is examined particularly in the different intruding sides of cyclist. Figure. 4.7 shows the mean value of  $BRT$  in the near side and the far side. The mean of  $BRT$  in the near side and far side is 0.65 s and the 1.35 s, respectively. The p-value shows that the driver response time in near side is significantly smaller than in the far side ( $U = 109, p < 0.001$ ).

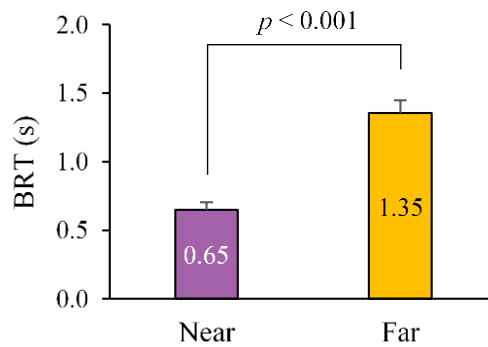


Fig. 4.7 Mean of driver reaction time  $BRT$  in the near side and the far side.



To understand the structure of collision occurrence parameters, a decision tree is applied to collision occurrence using parameters as  $TTC_a$ ,  $BRT$ , and  $A_a$  (Fig. 4.8). The classification regression tree (CRT) is selected as the method of pruning tree.

The result shows that  $TTC_a$  as the most important parameter to divide cases into two parts with  $TTC_a \leq 2.2$  s and  $TTC_a > 2.2$  s with the collision occurrence probability difference of 75% and 15%.  $BRT$  as the second parameter divides case into  $BRT \leq 0.56$  s and  $BRT > 0.56$  s under  $TTC_a \leq 2.2$  s, and  $BRT \leq 1.5$  s and  $BRT > 1.5$  s under  $TTC_a > 2.2$  s. This result shows that collisions can be avoided when  $TTC_a$  is greater than 2.2 s and  $BRT$  is less than 1.5 s. The overall prediction accuracy of the decision tree is 87.1%.

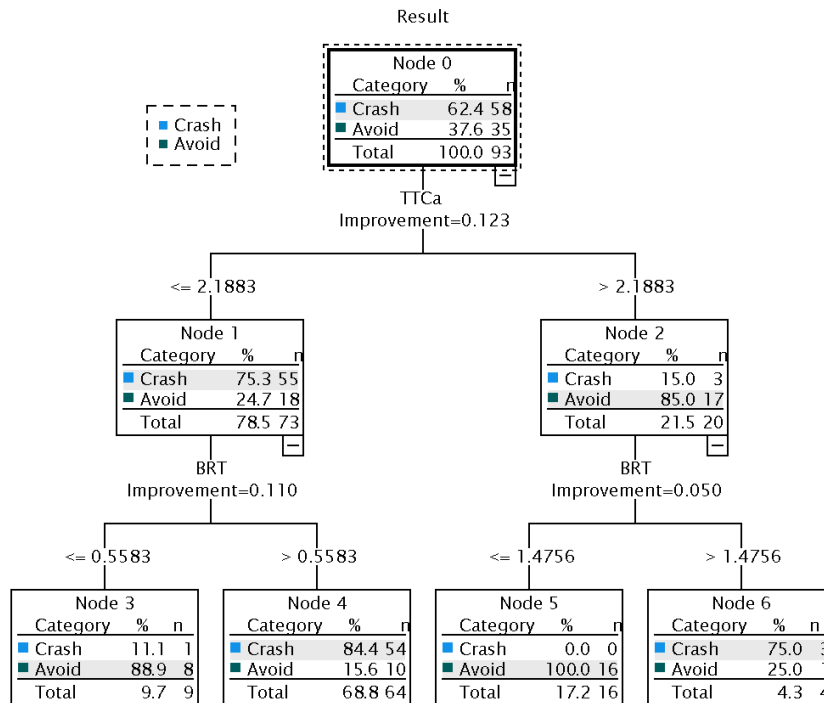


Fig. 4.8 Collision occurrence using decision tree.

#### 4.3.3. Cyclist trajectory

Figure. 4.9 shows the trajectories of the front end of the bicycle relative to the front end of the car from time  $t_a$ . The slope of the bicycle trajectory is given by the ratio of the car velocity to the cyclist velocity  $V(t)/v(t)$ . In collision avoided cases, the trajectories of the bicycle are not included in the area of the car. When a collision is avoided by braking of the car, the trajectory of the bicycle is plotted laterally in front of the car.

In scenario N1 (Fig. 4.8(a)), there are many cases that the cyclists collide the side of the car because many participants drive more than 40 km/h (instructed velocity). There is one collision-avoided case where the cyclist go behind the left rear corner of the car. In this case, the participant drive at a high velocity and passes the crash point before the cyclist arrives. In scenario N2 (Fig. 4.8(b)), the TTC is so small that most drivers are unable to decelerate enough in time and collide with the bicycle at the front of the car. Because the TTC is so small that the collision cannot be avoided driving at a high velocity through passing the bicycle.

In scenario F (Fig. 4.8(c)), the cyclist trajectories distribute widely from the front, right side and rear of the car. This is because TTC is large in the far side and driver responses varies depending on the recognition time of the cyclist. There are 3 participants who avoid a collision without car deceleration: they do not notice the cyclist model until they pass the cyclist.

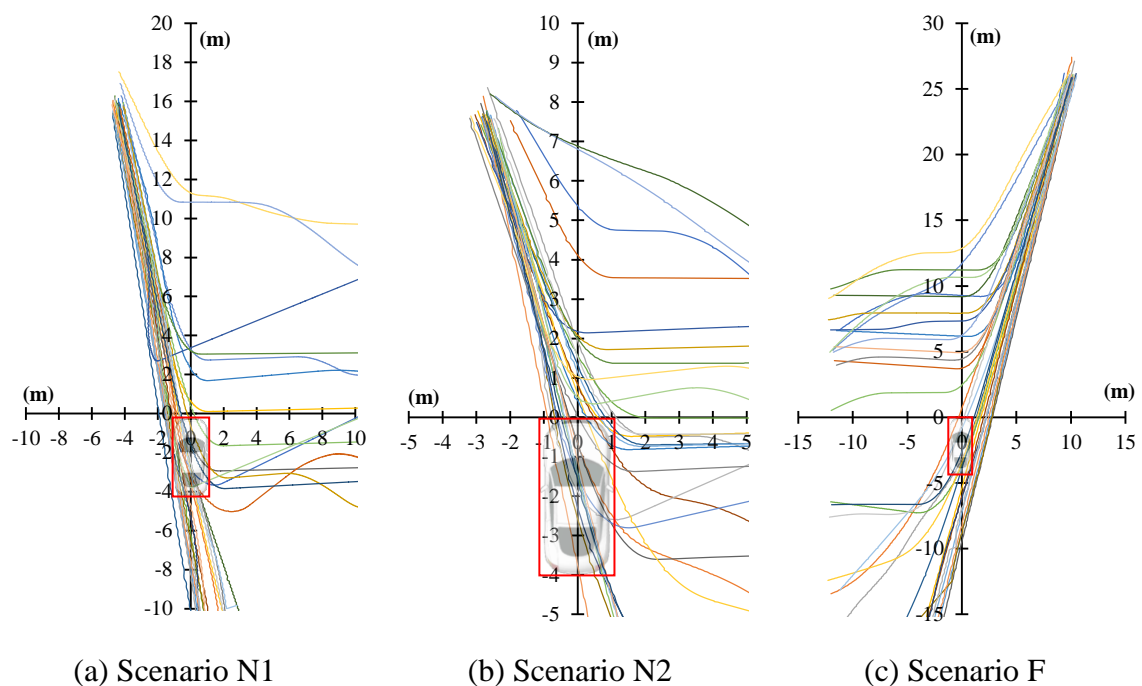


Fig. 4.9 Trajectory of the front end of the bicycles relative to the front end of the car in the driving simulator experiments.

#### 4.3.3. Gaze analysis

Figure. 4.10 shows the percentage of the driver's gaze distributions on the screen before the cyclist is visible. The percentage is cumulative frequency of gaze positions summed for all drivers in all frames from the start of the scenario until the cyclist becomes visible. Generally, the drivers mostly look at the center of their lane (future path), and the gaze points distributes

in the horizontal direction to monitor pedestrians and cyclists on the pavements. Since we asked the participants to travel at the target velocity, the gaze is also distributed in the area of the speedometer. Besides, the gaze points of participants are located relatively to the left from the center in all three scenarios before the cyclist appears from behind obstructions.

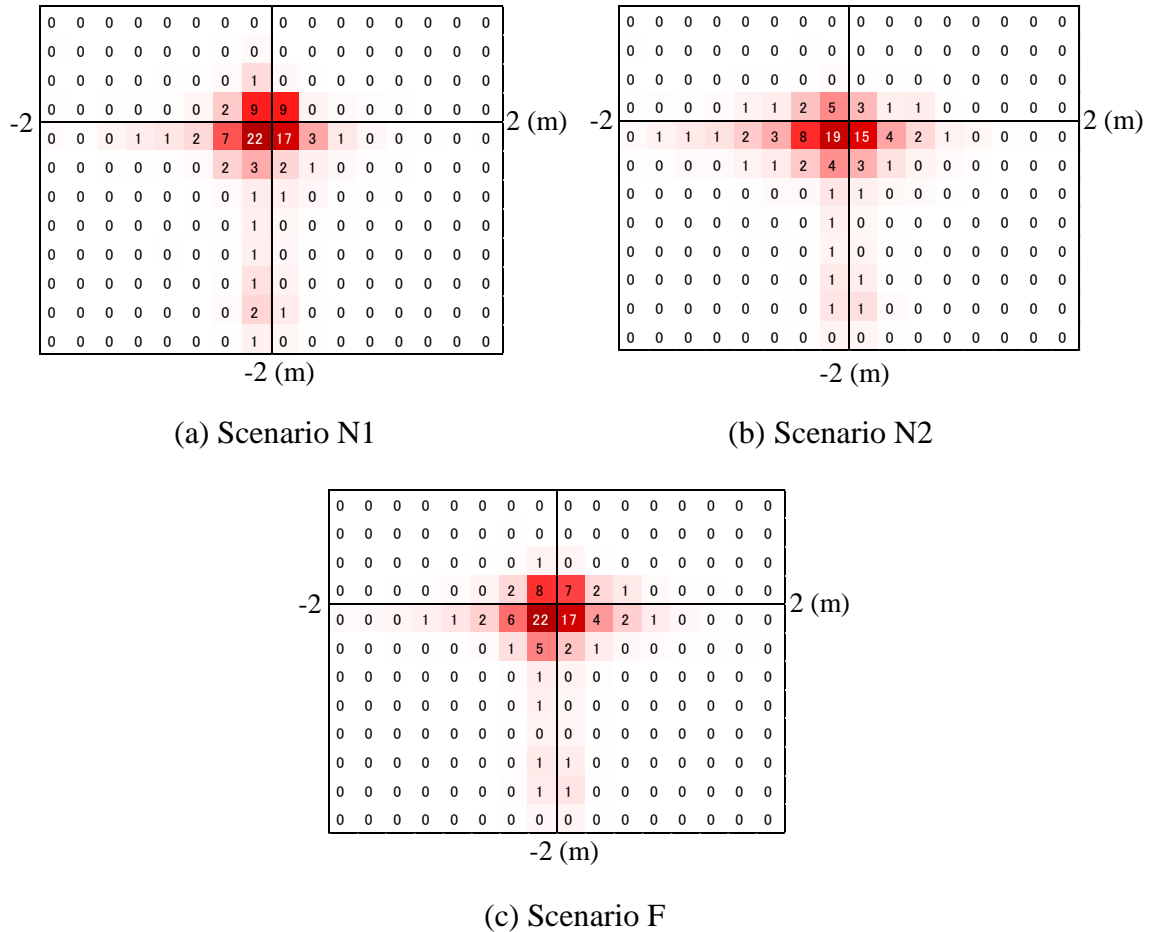


Fig. 4.10 Percentage of gaze point distributions on the screen before the cyclist is visible in the driving simulator experiments.

The driver's looking point on the screen at the time when the cyclist is visible at  $t_a$  is shown in Fig. 4.11. The point is where the driver looks on the screen, and the color represents different *BRTs*. The blue rectangle represents the speedometer on the dashboard of the car. Most of drivers look the front road (future path), and some drivers look the speedometer, resulted in relatively large *BRT*. In all scenarios, many drivers look at the left of the crossing road at the intersection probably because they predict hazard at the intersection. Particularly in the scenario N2 with a T-junction, most drivers look to the left of the road because they can concentrate on the direction where hazards might occur. It is likely that this driver's gaze behavior makes large

BRT in the far-side scenario (see Fig. 4.6).

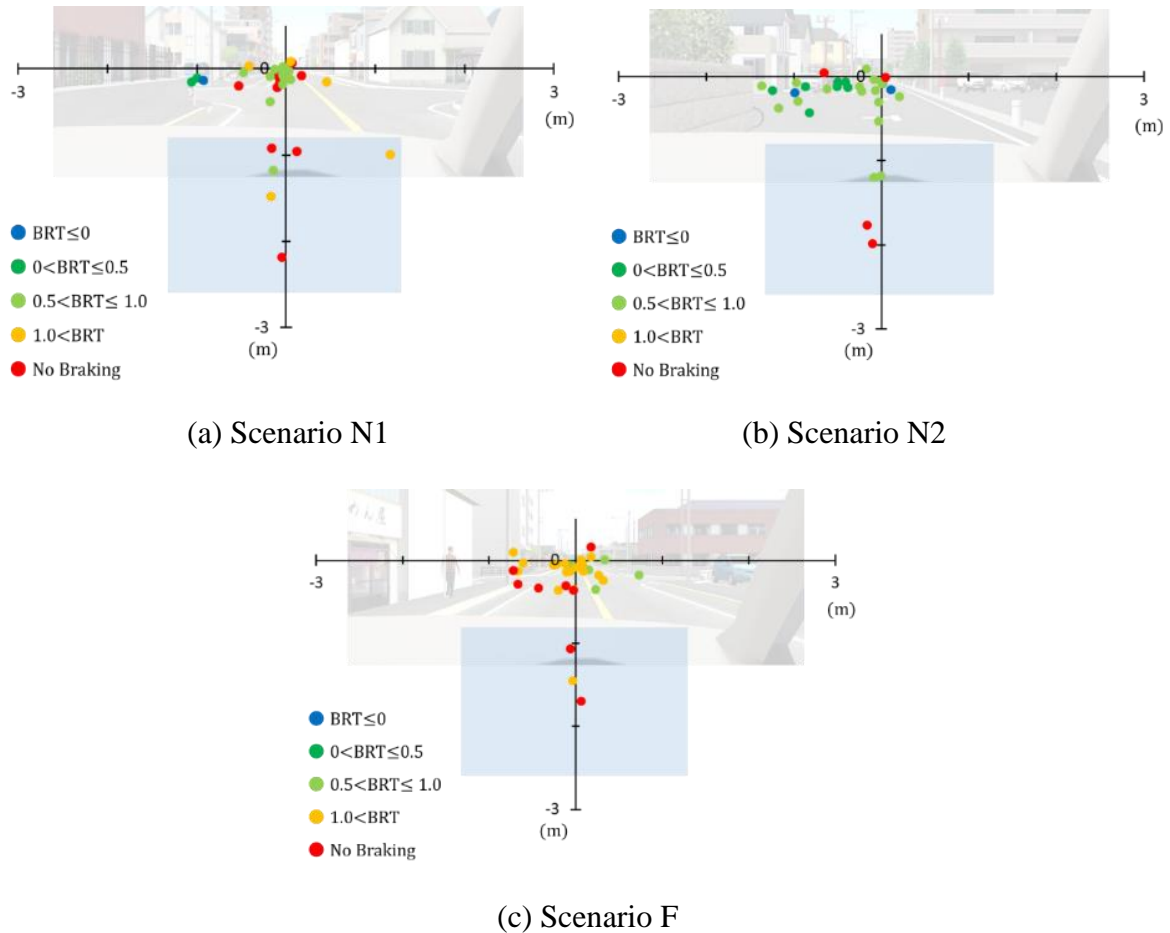


Fig. 4.11 Position of the drivers' looking point with different  $BRT$  at the time when the cyclist is visible in the driving simulator.

When the driver notices the cyclist model, the gaze location suddenly change and continue to look at the cyclist model. Then, the driver starts to response of braking and steering. By this gaze analysis, we can identify the driver's notice time  $t_n$  of the cyclist.

The braking reaction time of drivers can be divided into two parts: notice time from the time when the cyclist is visible  $t_a$  to the time when the cyclist is noticed by drivers  $t_n$  ( $t_n - t_a$ ); and the pedal change time from the accelerator pedal is released and the foot is put on the brake pedal after the driver notices the cyclist ( $t_b - t_n$ ) (see Fig. 2.1). In Fig. 4.12, the mean values of notice time and pedal change time of the avoided group and the crash group are compared. There were significant differences in the notice time between the avoidance group and the collision group in all scenarios (scenario N1:  $t(29) = -3.54, p = 0.001$ ; scenario N2:  $U = 44, p = 0.01$ ; scenario F:  $t(29) = -3.35, p = 0.002$ ). Meanwhile, the difference in pedal change time

between the avoidance and the collision group is not significant in the scenarios N1 ( $U = 32, p = 0.22$ ) and F ( $t(21) = -1.11, p = 0.28$ ). In combination with the mean of  $BRT$  in Fig. 4.6, this implies that the  $BRT$  is affected by the notice time instead of the pedal change time in the scenarios with a relatively large  $TTC_a$  such as in scenarios N1 and F.

In the scenario N1 and F1 with relatively large TTC, driver's notice time is significantly different while the pedal change time is not significantly different between avoidance and collision groups. In the scenario N2, significant differences are found for both driver's notice time and the pedal change time ( $U = 27, p = 0.004$ ), indicating that a collision cannot be avoided simply by shortening the notice time after the cyclist is visible in such scenarios with such a very small  $TTC_a$ . In other words, it is important to apply braking immediately or even decelerate in small TTC situation in advance of approaching the intersection before the cyclist appears behind obstructions.

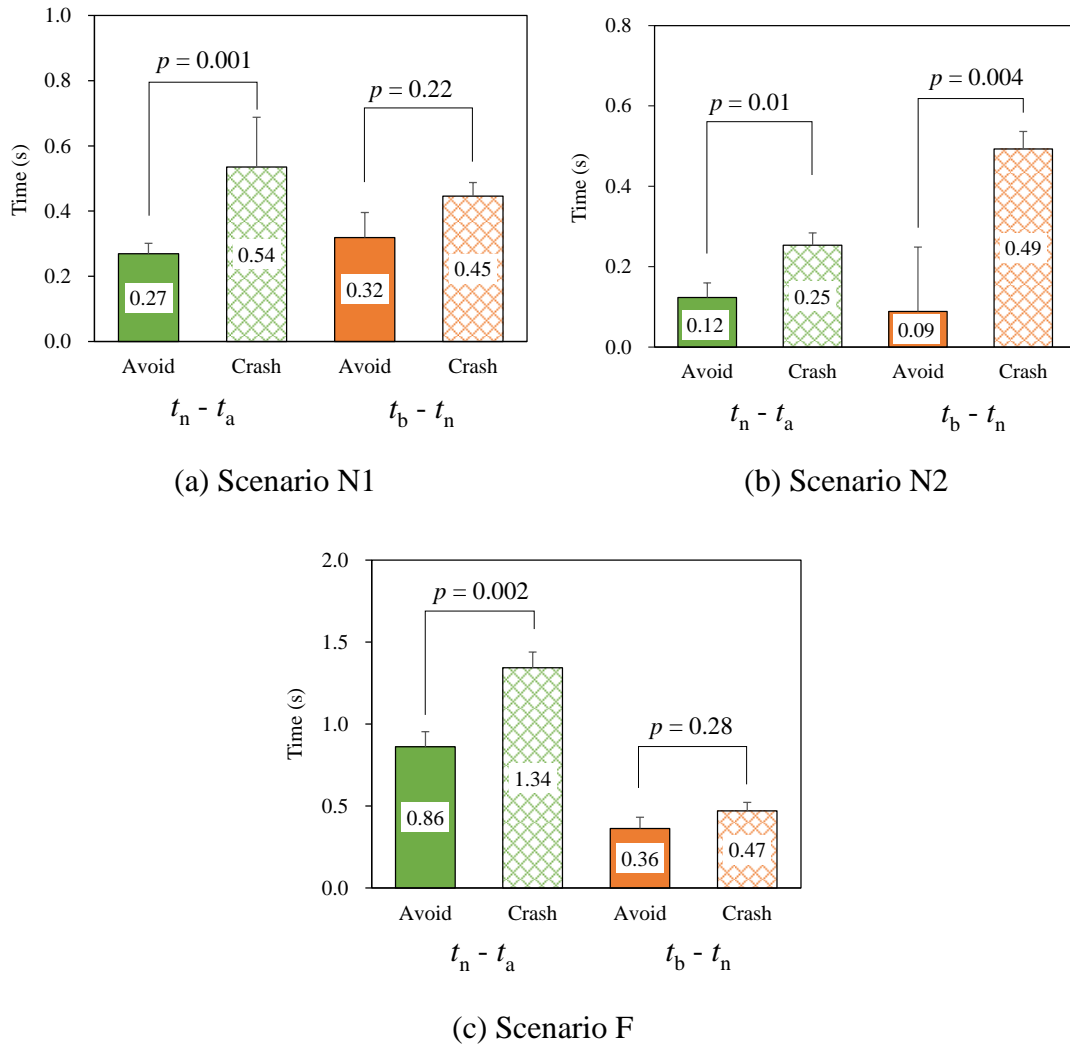


Fig. 4.12 Mean values of the notice time ( $t_n - t_a$ ) and the pedal change time ( $t_b - t_n$ ) of the avoided and the crash group in the driving simulator experiments.

The relationship of the notice time ( $t_n - t_a$ ) and the gaze angle between the cyclist and the gaze direction at the time when the cyclist is visible is shown in Fig. 4.13. There is a tendency that the notice time increased as the gaze angle increased across all scenarios. The notice time distributes below 1.0 s for scenario N1 and below 0.5 s for scenario N2. Besides, the distributions of the notice time in scenario F is wider, ranging from 0.3 s and 2.0 s.

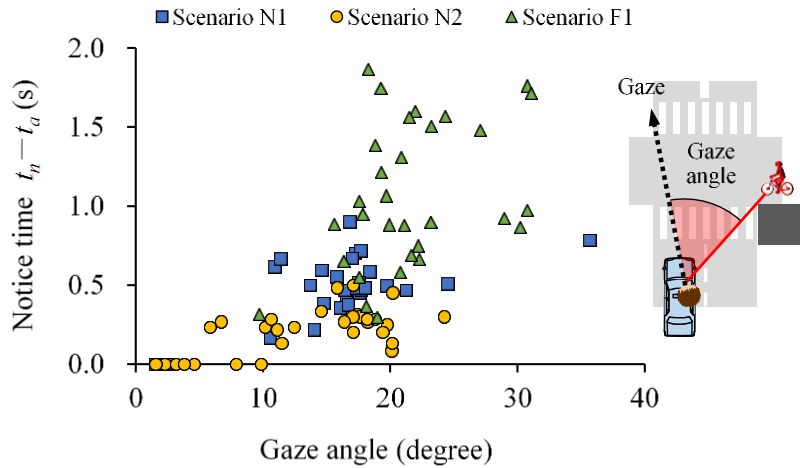


Fig. 4.13 Relationship between the notice time ( $t_n - t_a$ ) and the gaze angle of the cyclist and the gaze at the time when the cyclist is visible.

Because the notice time distributes differently in the three scenarios from the Fig. 4.13, the *BRT* components of notice time ( $t_n - t_a$ ) and the pedal change time ( $t_b - t_n$ ) are separately compared in the near side and the far side as shown in Fig. 4.14. The notice time in the near side and the far side is 0.29 s and 0.94 s, showing the significant differences ( $t(28) = -7.4, p < 0.001$ ). The pedal change time is 0.45 s and 0.49 s in the near side and the far side, the p-value does not show differences between them ( $t(73) = -0.56, p = 0.57$ ). This indicates that the difference of *BRT* between the near side and the far side is due to the difference of notice time, not the driver's pedal change time.

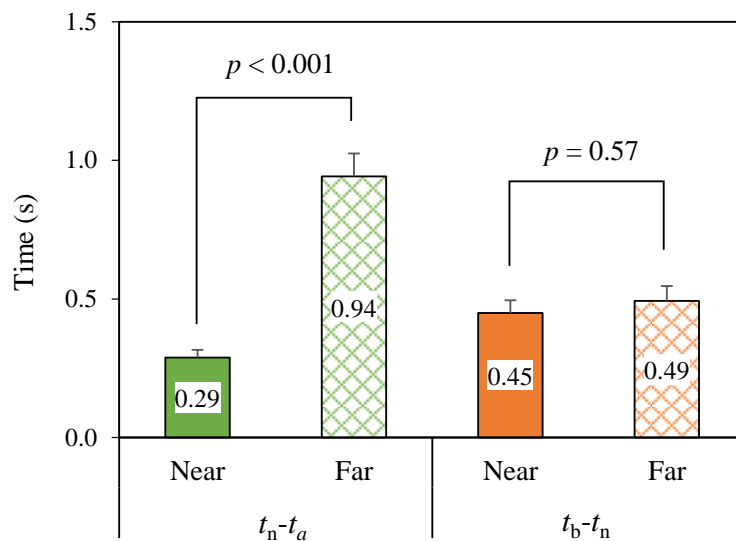


Fig. 4.14 Mean of the notice time ( $t_n - t_a$ ) and the pedal change time ( $t_b - t_n$ ) in the near side and the far side.

From the gaze analysis, it can be obtained that the time when the driver notices the cyclist is a critical factor influencing the collision occurrence. Hence, the driver's response to avoid conflicts in emergency situations with different  $TTC_n$  is examined again using the notice time, as shown in the Fig. 4.15. Clear trends of driver responses are observed using the notice time. The percentage of driver applies braking increases consistently as the  $TTC_n$  increases. As the  $TTC_n$  decreases, the driver's response in avoiding collisions changes from braking to braking with swerving. Moreover, there are 10 cases that the driver does not change their behaviors (no response) with the  $TTC_n$  smaller than 1.0 s. This is because the driver does not have enough time to respond after they notices the cyclists.

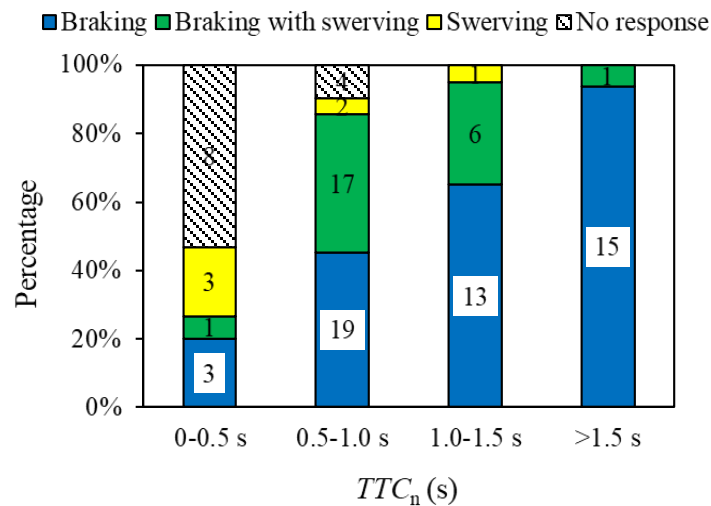


Fig. 4.15 Drivers' response to avoid collisions with different  $TTC_n$ .

#### 4.3.4. Braking and swerving response

Figure. 4.16 shows the boxplot of driver's braking reaction time  $BRT$  ( $t_b - t_a$ ), swerving reaction time  $SRT$  ( $t_s - t_a$ ), and gas release time  $GRT$  ( $t_r - t_a$ ) in the cases where the driver applies braking with swerving. The mean of  $BRT$ ,  $SRT$  and  $GRT$  is 0.99 s, 0.74 s and 0.7 s. The p-value shows the significant differences between the  $BRT$  and  $SRT$  ( $U = 182.5$ ,  $p = 0.012$ ), and there are no differences between the  $SRT$  and  $GRT$  ( $U = 312$ ,  $p = 0.99$ ). This indicates that the driver releases the gas pedal and simultaneously applies swerving, and the time difference between  $BRT$  and  $GRT$  is the time that the driver's foot changes from the gas pedal to the braking pedal.



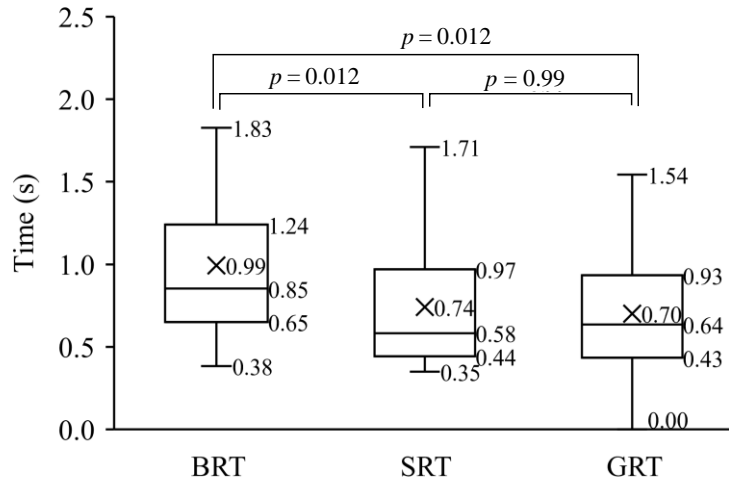


Fig. 4.16 The driver's braking reaction time  $BRT$  ( $t_b - t_a$ ), swerving reaction time  $SRT$  ( $t_s - t_a$ ), and gas release time  $GRT$  ( $t_r - t_a$ ) in the cases where the driver applies braking with swerving. The number of participants applying braking with swerving is 25.

#### 4.3.5. Threshold of collision occurrence

Figure. 4.17 shows the relation between collisions/avoidances by braking (the cases where the driver swerves or no responses are omitted) and the allowance time  $TTC_a - BRT - V_b/2a_0$  calculated using parameters in each test based on Eq. (4.2). The value of  $a_0$  is the average car deceleration over the time duration from the start to end of braking by each participant. All the participants who have positive allowance time of driver response ( $TTC_a - BRT - V_b/2a_0 > 0$ ) avoided collisions, and all the participants who have negative allowance time for driver responses ( $TTC_a - BRT - V_b/2a_0 < 0$ ) collide with the cyclists. Therefore, the allowance time  $TTC_a - BRT - V_b/2a_0$  is confirmed to be a reliable parameter to predict collision occurrences.

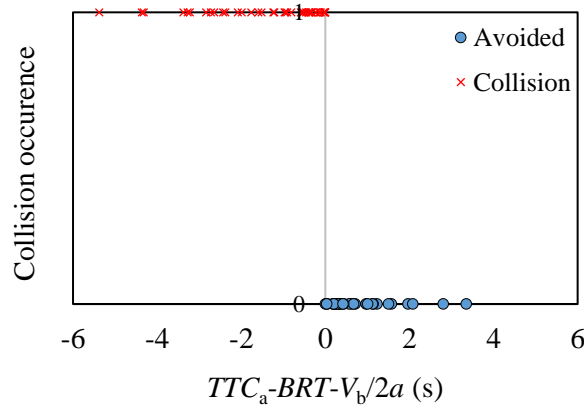


Fig. 4.17 Prediction of collision occurrence/avoidances as a function of the allowance time for driver response at the time of cyclist emergence. The avoided case is 0 and the collision case is 1 in the vertical axis.

Figure. 4.18 shows the relationship between  $BRT$  and  $TTC_a$  at the time when the cyclist becomes visible. The line based on Eq. (4.2) in the figure clearly separates the avoided cases and collision cases. When the  $BRT$  is above this line ( $BRT > TTC_a - 0.63$ ) collisions occurred: Longer  $BRT$  can be acceptable for avoiding collisions in emergency cases with long  $TTC_a$ .

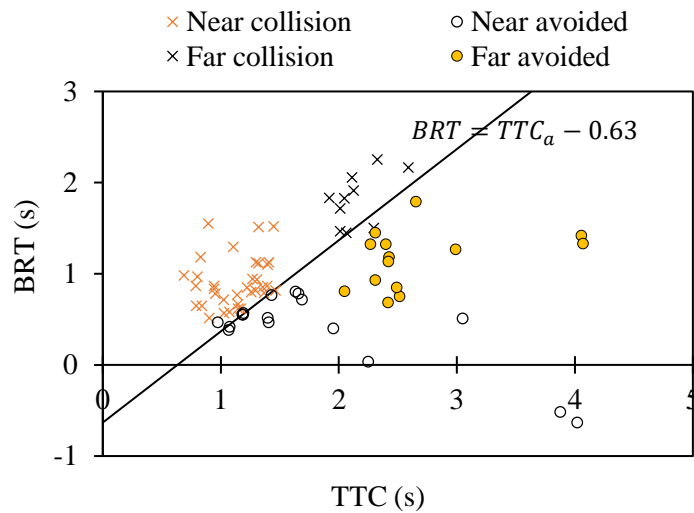
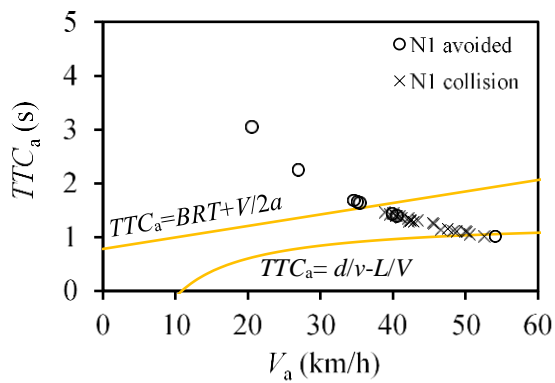


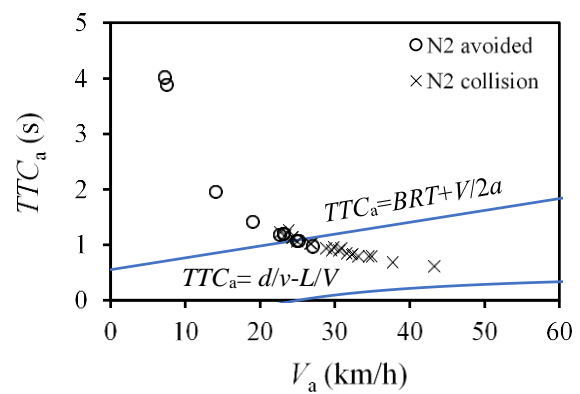
Fig. 4.18 Relationship of  $BRT$  and  $TTC_a$  at the time when the cyclist is visible.

Figure. 4.19 shows the relationship between the car velocity  $V_a$  and  $TTC_a$  at the time when the cyclist becomes visible for thresholds with/without braking to avoid collisions in each scenario. The  $TTC_a$  needs to be larger than  $BRT + V_b/2a_0$  when drivers apply braking to

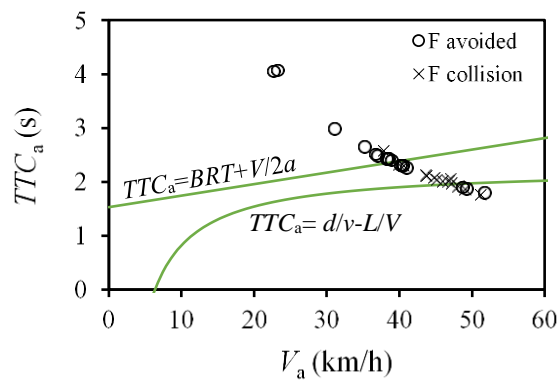
avoid collisions (see Eq. (4.2)). The  $BRT$  (0.78 s, 0.55 s and 1.53 s in scenario N1, N2 and F) and the car braking deceleration  $a_0$  ( $6.5 \text{ m/s}^2$ ) substituted in each scenario is calculated from 50% probability of collision occurrence in the logistic regression. For the cases where the driver does not apply braking to avoid collisions before arriving at the cyclist path,  $TTC_a$  needs to be smaller than  $d/v - L/V$  (see Eq. (4.3)). Hence, collision risks are high in the area bounded by the two lines shown in the figure. Most avoided cases are located above the braking line and the collisions distributed below the line in each scenario. There are a total of 5 cases in large TTC scenarios (1 case in scenario N1 and 4 cases in scenario F) where the participants do not brake but accelerates to avoid collisions. On the other hand, in scenario N2 (Fig. 4.19(b)), the cyclist emerges in front of the car with a very small  $TTC_a$  that there are no cases where collisions are avoided by acceleration or by keeping high velocity.



(a) Scenario N1



(b) Scenario N2



(c) Scenario F

Fig. 4.19 Collision occurrences shown by vehicle velocity and TTC at the visible time of cyclists. The upper boundary is thresholds of collision occurrence with braking (Eq. (4.2)) and the lower boundary is without braking (Eq. (4.3)).

#### 4.4. Discussion

This chapter examined drivers' response in three scenarios with different  $TTC_a$  using driving simulator experiments. The driver behavior interacting with the cyclist intruding from the near and far side in the conflicts was examined (Fig. 4.5). The parameters such as  $V_a$ ,  $TTC_a$ ,  $BRT$  and  $A_a$  at the time when the cyclist was visible were then compared in the avoidance group and collision group (Fig. 4.6). Independent parameters as  $TTC_a$ ,  $BRT$  and  $A_a$  were also examined to investigate the structural influence of collision occurrences using a decision tree (Fig. 4.8).

Previous studies show that braking was applied as the primary means of collision avoidance, followed by the braking with swerving (Muttart, 2005; Li et al., 2019). In the cases where the driver applied braking with swerving, the driver started braking and started swerving simultaneously, and the time difference between  $BRT$  and  $SRT$  was due to the driver's foot moving from the braking pedal to the gas accelerator pedal. This conclusion was consistent with Toxopeus's conclusion (2018). Moreover, in this study, a total of 6 drivers applied only swerving, and 5 of them were involved in collisions. Therefore, swerving alone was not effective in avoiding collisions. On the other hand, since the driver applied swerving, the position of the cyclist contact with the car may change from the front of the car to the side of the car. This may result in reducing the car's longitudinal impulse on the cyclist.

In driving simulator experiments in this study, there were many cases where the car arrived earlier at the collision point than the cyclist, and the cyclist impacted the side of the car (Fig. 8). Accident analysis shows that the front, right side, left side and rear of the bicycle were impacted in 45.6%, 28.3%, 22.1% and 3.9%, of the cases, respectively when classified by the impact location of the bicycle in these collisions (Maki et al. 2000). Hence, it is probable that such collision occurrences (the front of the bicycle impacting the side of the car) are common in real-world events. In real-world crashes, cyclists will not be impacted substantially against car's side impact compared to car's frontal impact. Besides, cyclist may detect crossing cars ahead of them and apply braking to avoid such collisions. Thus, cyclists may not be injured seriously in such impacts against the side of a car. More research will be necessary to investigate such events that occur.

In this driving simulation experiment, there were two ways to avoid a collision with braking or not braking (keeping the original velocity after the cyclist appeared from the obstacles). The collision occurrence was formulated by  $TTC_a$  instead of  $TTC_n$ , this is because the  $TTC_a$  as a

car kinematic parameter was easier to be measured than  $TTC_n$  even though the  $TTC_n$  was found to be related to the driver responses (Fig. 4.15). For the cars without eye track systems, using  $TTC_a$  to investigate the collision occurrence could be applied in general scenarios and experimental equipment. Morita et al., (2013) used the braking distance to predict the collision occurrence. When the braking distance required for stopping the car was greater than  $V_b \cdot BRT + V_b^2/2a$ , collisions cannot not be avoided. He substituted the average  $BRT$  of 0.45 s and the average braking deceleration of  $6.9\text{m/s}^2$  into collision occurrence threshold to verify the accuracy of this threshold with 77%. In this study, we used time (e.g. TTC) instead of distance, which will be useful to activate the driver assistant systems. Moreover we applied parameters independently in each scenario to predict collision occurrence using Eq. (4.2) and Eq. (4.3).

The results show that  $TTC_a$  and  $BRT$  were important determinants of collision occurrence.  $TTC_a$  determined the conflict environment before contact (i.e., the near side and the far side in this study) and the driver's reaction time  $BRT$  determined collisions occurred or not. This result was consistent with the results we obtained from drive recorder data in Chapter 2. Li et al. (2019) examined driver behavior in car-to-pedestrian collision conflict scenarios with different  $TTC$  in a driving simulator. Their finding shows that in the car-to-pedestrian scenarios, drivers' braking reaction time  $BRT$  and the maximum swerving radian were the primary factors affecting the collision occurrence. However the results was obtained from the configuration where the pedestrian running from only the near side. In this study, the effects of  $TTC_a$  and  $BRT$  was concluded from the conflict configurations where the cyclist intruding from the near and far side at an intersection, thus this study was more informative for broader scenarios.

Drivers' gaze distribution was measured by an eye track system in the driving simulator. The driver responses actually started after they notice the cyclist, and thus the time when the driver noticed the cyclist  $t_n$  was introduced in this study. Green (2000) showed that driver' peripheral retina was used when the intrusions came from the lateral directions. This could be explained by the driver's gaze angle between the cyclist position and the looking direction at  $t_a$  in this study. Driver's gaze angle in the near scenarios was smaller than in the far side (Fig. 4.13), thus the time difference (notice time) from the cyclist was visible  $t_a$  to the time the cyclist was noticed  $t_n$  was larger in the far side than in the near side. Moreover, the  $TTC_n$  at the time when the driver noticed the cyclist was also newly introduced, and driver responses to cyclists intruding from braking to swerving as  $TTC_n$  decreased (Fig. 4.15).  $TTC_a$  determines the

crash environment that cannot be changed by drivers, but the  $TTC_n$  determines the remaining time that could react before collisions. For the collisions led by driver's long BRT, the  $TTC_n$  in this type of collisions was small, and thus collisions also occurred although the  $TTC_a$  was relatively large.

In the research of driver reactions to intrusions from different sides, Jurecki's research (2014) shows that drivers' *BRT* response to pedestrians was greater in far side than in near side intrusion into a road. Their study agrees with this study that drivers' *BRT* in the near side and the far side was 0.65 s and 1.35 s, respectively, with significant differences (Fig. 4.7, Fig 4.11 and Fig 4.13). However, Jurecki et al. (2014) did not show the reason of *BRT* difference in near and far side intrusion. In the experiments in this dissertation, the drivers were looking towards the future road (Fig. 4.11), and the angle between the driver's gaze and the cyclist in the scenario where the cyclist intruded from far side was larger than that the cyclist from the near side (Fig. 4.13). As a result, the driver's *BRT* in the far side was larger than that in the near side. In this study, we also analyzed in more detail about the components of the *BRT* in the near side and far side (Fig. 4.12 and Fig 4.14). The difference of the *BRT* in the near side and far side was caused by the notice time ( $t_n - t_a$ ) rather than pedal change time ( $t_b - t_n$ ).

In the driving simulator experiments, the drivers were asked to drive at the instructed velocity. However, since each driver have different driving manner, experiences and abilities to anticipate hazards, the car's velocities at the time at the intersection when the cyclist was visible were different, which resulted in that the TTC was not well controlled. In addition, only two females participated this experiment, and the age distribution was also not balanced enough. Thus, this may lead to biases in the driver's response compared to other researches.

#### 4.5. Conclusions

The driver's response in the three scenarios with different TTCs was examined using driving simulator experiments. The car's kinematics and driver's response was investigated in the near side and the far side. This study also used eye track system to analyze the effect of the driver's gaze on response in emergency situations. The conclusions are listed as follows:

- Drivers' braking reaction time *BRT* in the near side is significantly smaller than in the far side, and the difference of *BRT* caused by the notice time from the cyclist is visible to the driver notices the cyclist.
- The driver applies braking and swerving simultaneously, the time difference between the

braking reaction time  $BRT$  and the gas pedal releasing time  $GRT$  is the time for drivers changing foot from the gas acceleration pedal to the braking pedal.

- $TTC_a$  and  $BRT$  are the critical parameters affecting the collision occurrence:  $TTC_a$  determines the conflict severity, and  $BRT$  determines a collision occurred or not.
- When  $TTC$  at the time of notice of a cyclist by the driver is larger, driver response to avoid collisions changes from control action of swerving to braking.
- Collisions are avoided when drivers applied the brakes or when the driving velocity exceeds the target velocity specified to the subjects. Collision avoidance by braking and driving without deceleration is predicted using expression involving  $TTC$ ,  $BRT$  and car deceleration.

## Chapter 5

### Evaluation Effectiveness of AEB for Cyclist Protection Using Drive Recorder

#### 5.1. Introduction

In order to decrease the number of collision occurrences, assisted driving is increasingly used in automobiles today. Autonomous emergency braking (AEB) system is a technology that automatically stops a vehicle in an emergency to avoid collisions. Previous study focused on the topic of the effectiveness of AEB for pedestrian protection. Rosen et al. (2013) and Rosen (2010) calculated the effectiveness of AEB for pedestrians using GIDAS data, and they found that the effectiveness of AEB for pedestrian protection was 40% at a field of view (FOV) of 40°, brake deceleration of 0.6 g, and 1 s of initial time. However, cyclists travel at higher speeds and enter the FOV immediately than pedestrians, thus, the AEB for pedestrian protection is probably no longer appropriate for cyclists.

According to the findings in Chapters 2 and 4 as well as the study by Ito et al. (2018), car-to-cyclist collisions could be divided into two types: one type includes collisions caused by the driver's large brake reaction time (BRT), and the other type is that the cyclists' sudden appearance. The purpose of this chapter is to evaluate the effectiveness of AEB in protecting cyclists from both types of collisions. In this chapter, all car-to-cyclist perpendicular collisions and turning collisions are reconstructed first, and then the reconstructed collisions are recalculated with AEB by changing the AEB parameters.

#### 5.2. Methods

##### 5.2.1. Collision reconstruction

Collisions from drive recorder is reconstructed using an accident reconstruction program, PC-Crash. The time when the cyclist contacted with the car is set to  $t_c$ , as it is used in the drive recorder analysis. In this study, in the reconstruction of car-to-cyclist collisions, the paths of the cyclist and the car are set from  $t_c$  rewinding to the time  $t_a$  when the cyclist appears from obstacles. Using the collision video of drive recorder, it is possible to determine the paths of the cyclists and the cars based on their relative positions to the road and surrounding buildings and houses.

It is then necessary to input the kinematics of the car and the cyclist before collisions including car and cyclist braking in PC-Crash. The acceleration or deceleration can be



determined directly from the driver recorder video. However, the acceleration and deceleration of the car are fluctuating, and it will be not realistic to exactly reconstruct the acceleration or deceleration shown in the drive recorder video every time step in the PC-Crash reconstruction. For this reason, it is sufficient when the acceleration and deceleration of the car in the reconstructed matched the average value in the drive recorder video every time step duration (i.e., 1 s). Based on the surrounding landmarks, the acceleration or deceleration of the car during the reconstruction are adjusted to confirm that positions and velocity of the car with time basically coincided that observed in the original video. For the cyclist, since the kinematics cannot be obtained directly from the video, the velocity of the cyclist is set temporarily based on velocity distributions of cyclists (i.e., 10 km/h at the intersection), and then the velocity is adjusted based on the position of the cyclist relative to the surroundings in the video. In this study, 63 car-to-cyclist perpendicular collisions and 51 left and right turning collisions are reconstructed using PC-Crash.

### 5.2.2. AEB algorithm

The time-to-collision ( $TTC = V/D$ ) is used to activate the AEB in the algorithm. In perpendicular collision configurations, assuming that the car decelerates with constant deceleration  $a$ , the deceleration can be expressed by the car velocity  $V$  and the distance to the cyclist path  $D$  as following:

$$V^2 = 2aD \quad (5.1)$$

Substitute the definition of TTC into Eq. (5.1), and the deceleration can be expressed by  $V$  and  $TTC$ :

$$V = 2a \cdot TTC \quad (5.2)$$

Cars using the AEB cannot stop to avoid collisions when the deceleration  $a$  calculated by Eq. (5.2) exceeds the braking limit. In this study, the upper limit of the braking deceleration is set to  $\mu g$  ( $a \leq \mu g$ ), where  $\mu$  is the friction coefficient between the tire and the road and  $g$  is 9.8 m/s<sup>2</sup>. The AEB deceleration  $a$  can be smaller than the braking limit when there is enough distance for the car to stop. In this study, the friction coefficient  $\mu$  is set to 0.8 in the dry condition and 0.2 in the wet condition.

In the turning configuration, the cyclists have two positions relative to the cars: same direction with the car and opposite direction from the car (Fig. 5.1(b)). In the reconstructions of

left and right turning collisions involving cars equipped with AEB, the collision point is not known for the car (the collision point is the crossing path of the car and the cyclist in the perpendicular collision), thus, the TTC is calculated as a function of the relative distance and relative velocity between the cyclist and car to determine the time of AEB onset shown in the Fig. 5.1(b). The relative vector velocity of the cyclist relative to the car  $V_R$  is calculated by the car velocity  $V$  and cyclist velocity  $v$  as follow:

$$V_R = v - V \quad (5.3)$$

Assuming that  $V_R$  forms an angle  $\theta$  of with respect to the direction of travel from car to cyclist (the angle between the relative velocity and the line of the car and the cyclist), the effective velocity of the cyclist closing in on the car is equal to  $V_R \cdot \cos \theta$  ( $V_R$ : the magnitude of  $V_R$ ). As a result, TTC in turning collisions can be expressed as follows:

$$TTC = \frac{D_R}{V_R \cdot \cos \theta} \quad (5.4)$$

where  $D_R$  is the relative distance between the car and the cyclist.

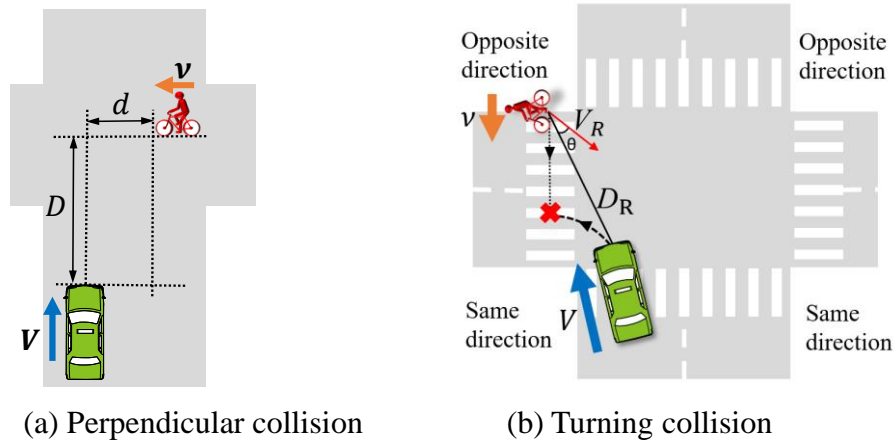


Fig. 5.1. Relative position of the car and the cyclist and TTC in a perpendicular collision and in a turning collision.

AEB algorithm for cyclists and the car deceleration in the time sequence is shown in Fig. 5.2, and the relative position of the car and the cyclist in the time sequence is shown in Fig. 5.3. When the cyclist enters the field of view (FOV) of AEB (Fig. 5.3(b)), the AEB starts to calculate the  $TTC$  between the car and the cyclist after the sensor delay time (SDT). Once  $TTC$  is

smaller than 1.4 s (Fig. 5.3(c)), the AEB starts braking with a braking deceleration  $a$ . It takes time for the AEB system to the car's start braking because of the process of braking: the pressure of the brake system is increased, and the brake rotter moves until the brake pad contacting the brake disc. This required time is brake pre-charge time (BPT). The time it takes for the car to start braking to the maximum deceleration  $a$  is brake boost time (BBT). In this study, the SDT, BPT and BBT is set to 0.4 s, 0.1 s and 0.15 s, respectively. The delay time (DT) of this AEB system consists of SDT and BPT, and the delay time is set to 0.5 s. Besides, the cyclist can be included in the FOV from a long distance, thus the time  $t_e$  when the cyclist enters an intersection is introduced in the turning collisions. In this study, the AEB is set to start detecting after  $t_e$ .

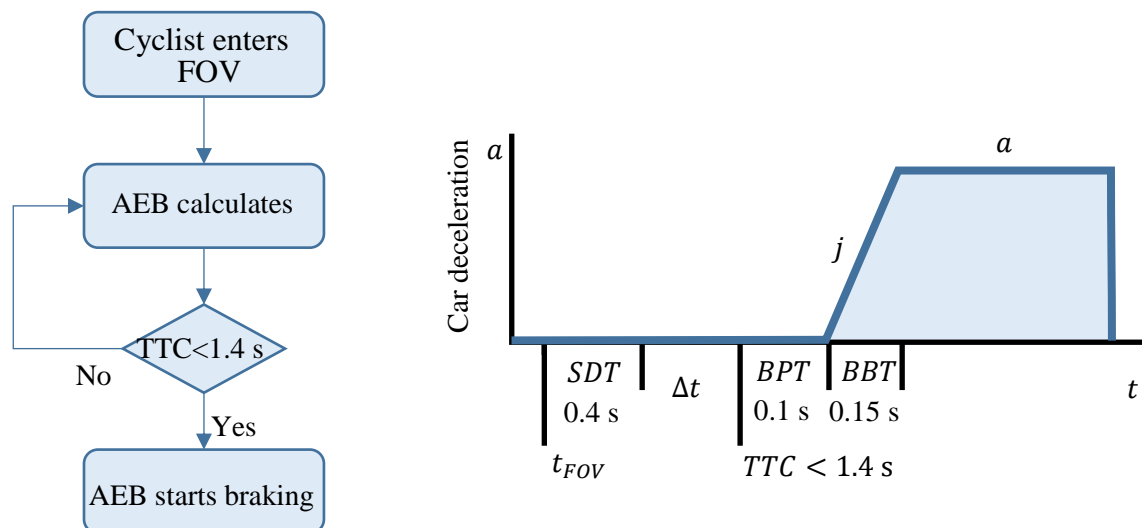


Fig. 5.2. AEB algorithm and car deceleration changing with time.

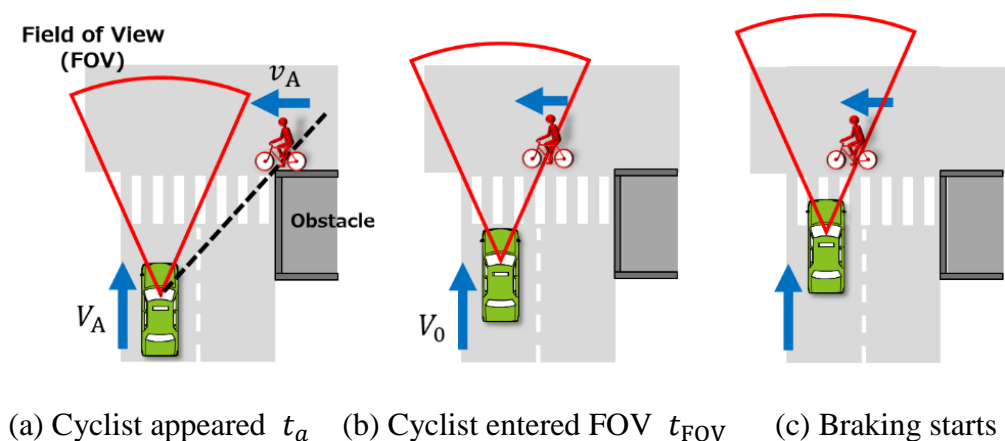


Fig. 5.3. Relative position of the car and the cyclist with time.

### 5.2.3. AEB parameter change

Three types of FOVs of AEB is used to examine effectiveness for avoiding collision with cyclists in this study. The camera of AEB is installed at the top of the windshield (see Fig. 5.4), and the camera is assumed to be unaffected by weather and light. First one is 50° FOV applied in the current cars for preventing pedestrian collisions: The angle of FOV is 50° ( $\pm 25^\circ$ ), and the sensing distance of this AEB is 50 m. The second type is 90° FOV where the sensing angle is 90° ( $\pm 45^\circ$ ) and the sensing distance is 75 m. This FOV 90° is required to ensure that sensors detect the cyclist by AEB in Euro NCAP cyclist AEB test configurations. The last one is the 360° FOV where the sensing angle is 360° ( $\pm 180^\circ$ ) and the sensing distance is 75 m. The ideal AEB used in this study is that the FOV angle is 360° and the delay time of AEB is 0 s.

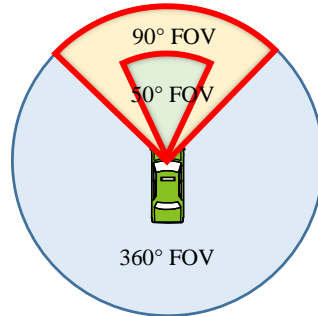


Fig. 5.4. Three field of views (FOVs) used in this research.

## 5.3. Results

### 5.3.1. Effectiveness of AEB in perpendicular collisions

The effectiveness of AEB for preventing cyclist collisions using the AEB designed for pedestrians (50° FOV and DT 0.5 s) is examined first. The relationship of the car velocity  $V_a$  and the  $TTC_a$  at the time when the cyclist is visible is shown in Fig. 5.5. Based on Eq. (5.2), the relationship between  $V_a$  and  $TTC_a$  with the braking deceleration upper limit 0.8 g is also shown in the figure.

Among 63 car-to-cyclist perpendicular collisions, only 14 collisions are avoided by the AEB with 50°FOV. 12 collisions are not avoided by the AEB and the car collides with the cyclist, even though the AEB is active. 37 AEBs are not active in collisions because the cyclist does not enter the relatively small FOV of AEB for pedestrians and AEB does not reach the process to start braking. This result indicates that the AEB for pedestrians is not so effective for cyclists

since cyclists have a higher traveling velocity compared to pedestrians. Thus, more robust AEB is needed for preventing car-to-cyclist collisions effectively.

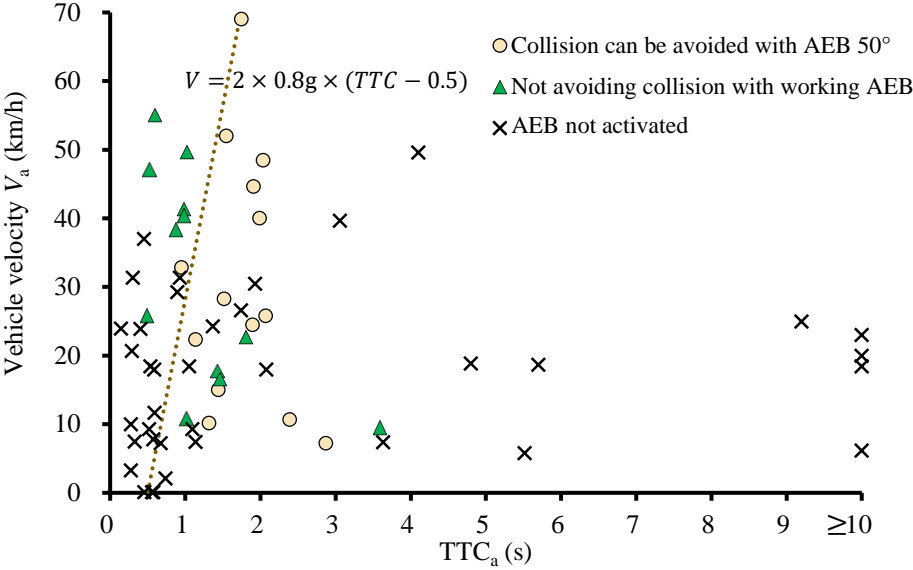


Fig. 5.5. Result of AEB effectiveness in car-to-cyclist perpendicular collisions using the 50°FOV for pedestrians.

Figure. 5.6 shows the position of the cyclist with respect to the car at the time when the cyclist is visible. The results of collision avoidances are also included by the AEB system of increasing FOV angle (50° FOV, 90° FOV and 360° FOV) with DT 0.5 s. Six collisions avoided by AEB with 50° FOV locate in the 50° FOV, and 8 collisions avoided by 50° FOV locate out of 50° FOV. Then, 9 collisions avoided by AEB with 90° FOV locate in the area of 90° FOV, and 6 collisions locate out of 90° FOV. Finally, 8 collisions are avoided by AEB with 360° FOV. Though this figure shows the relative positions of the car and the cyclist at the time when the cyclist is visible, and the relative position may change after the cyclist is visible. This is the reason why some collisions can be avoided, despite being located outside the FOV. For the collisions that cannot be avoided by AEB with 360° FOV (including collisions with reduced impact velocity as well as collisions with AEB not active), most of them locate 10 m in front of the car.

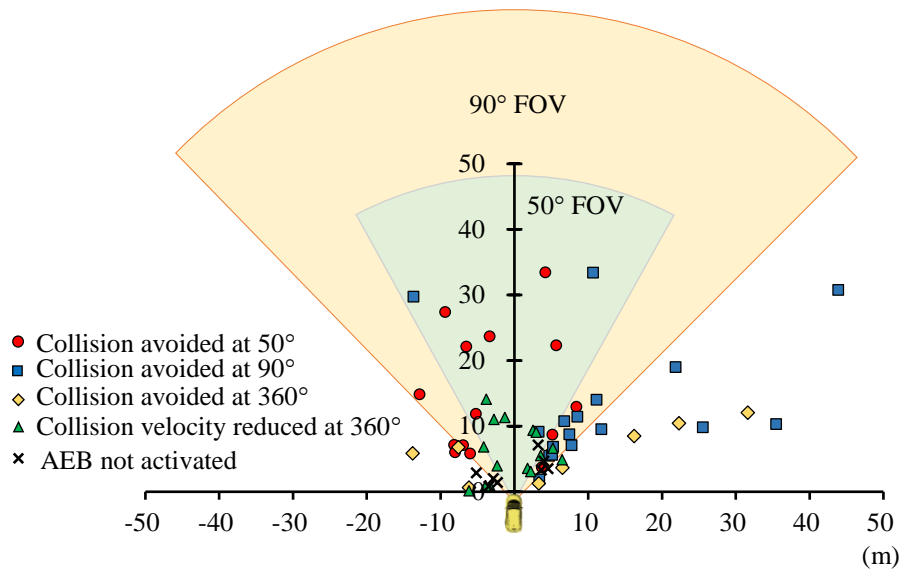


Fig. 5.6 Position of the cyclists with respect to the car using 50°FOV, 90° FOV and 360°FOV with DT 0.5 s at the time when the cyclist is visible in car-to-cyclist perpendicular collisions.

Figure. 5.7 shows the relationship between the car velocity and  $TTC_a$  using AEB with 50°FOV, 90° FOV and 360°FOV with DT 0.5 s at the time when the cyclist is visible. The blue dotted line and the brown dotted line represent the braking limit of the car with no braking delay (DT) and with 0.5 s braking delay, respectively.

All the avoided collisions distribute on the right of the braking limit with no braking delay (blue dotted line), and all the collisions with AEB not active distribute on the left side of the braking limit. Some collisions that are not avoided by AEB with 360° FOV but impact velocities reduced are distributed between two dotted lines. This indicates that this type of collisions could be avoided if the braking delay time decreased. In the area where  $TTC_a$  is greater than 3 s, there are 6 collisions avoided by AEB with 90° FOV with car velocity less than 30 km/h and 4 collisions avoided by AEB with 360° FOV with car velocity less than 10km/h. This is because car velocity is low and the relative angle between the cyclist and the car is relatively large, which makes it difficult for the cyclist to enter the FOV. Hence, this type of collisions require an AEB with larger FOV to avoid collisions.

All the collisions are then investigated using an ideal AEB with 360° FOV and DT 0 s, and the relationship of car velocity and  $TTC_a$  is shown in Fig. 5.8. Eleven collisions cannot be avoided even using an ideal AEB, and 9 of them distribute on the left of the braking limit and 2 of them is close to the braking limit.  $TTC_a$  of these 11 collisions is smaller than 0.9 s.

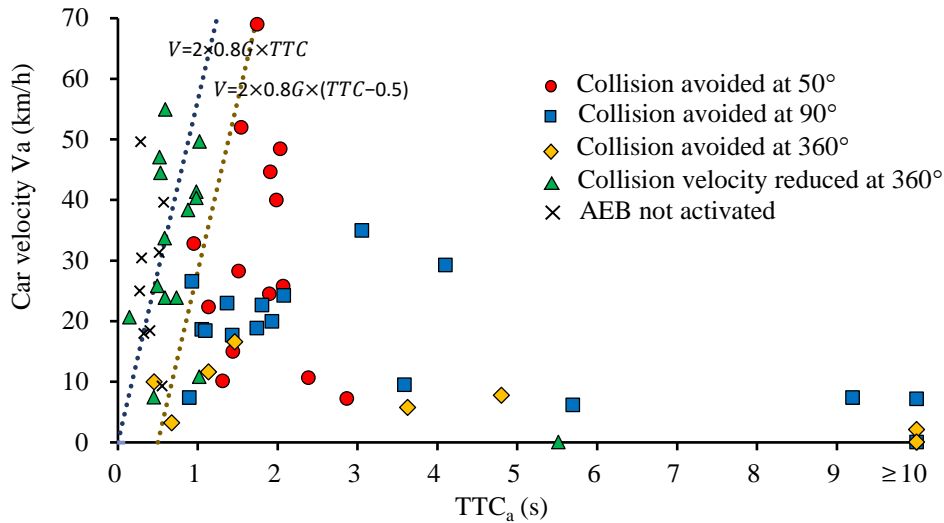


Fig. 5.7 Relationship of car velocity and  $TTC_a$  using  $50^\circ$ FOV,  $90^\circ$  FOV and  $360^\circ$ FOV with DT 0.5 s at the time when the cyclist is visible in car-to-cyclist perpendicular collisions.

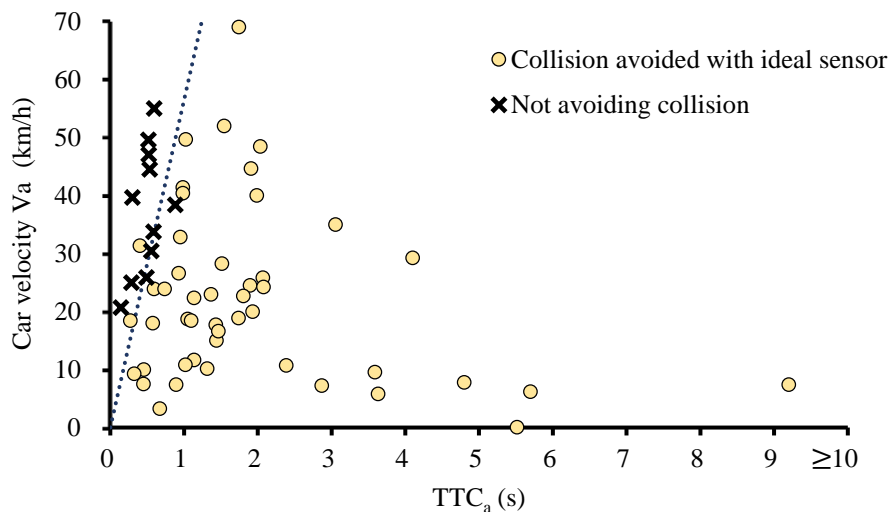


Fig. 5.8 Relationship of car velocity and  $TTC_a$  in avoiding collisions using an ideal AEB with  $360^\circ$ FOV and DT 0 s in car-to-cyclist perpendicular collisions.

The effectiveness of the three AEBs with  $50^\circ$  FOV,  $90^\circ$  FOV and  $360^\circ$  FOV in avoiding perpendicular car-to-cyclist collisions are examined and shown in the Fig. 5.9. As the FOV increases, the effectiveness of collision avoidance increases. The effectiveness of AEB in preventing cyclists using AEB for pedestrians ( $50^\circ$  FOV and DT 0.5 s) is only 22.2%, and AEB is not activated in 58.7% of collisions. Thus, the AEB currently installed in vehicles for pedestrian protection is not effective enough for prevention of car-to-cyclist collisions. This effectiveness increases to 50.8% when the FOV angle increases to  $90^\circ$ , while 27% of collisions is not still avoided since the AEB is not activated. Even though the ideal AEB ( $360^\circ$  FOV and

DT 0 s) is applied to car-to-cyclist collisions, there are still 17.5% collisions that cannot be avoided.

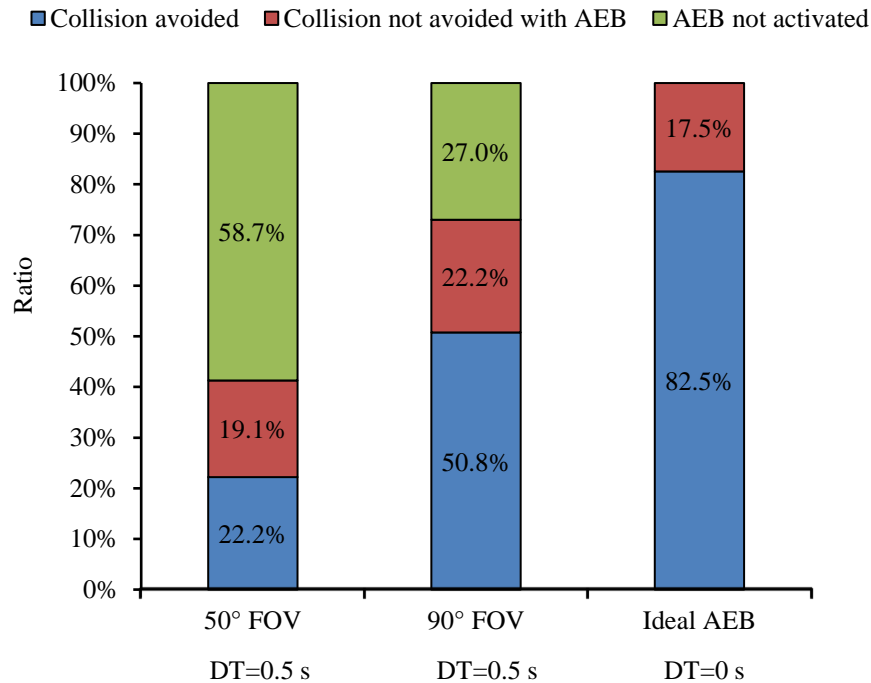


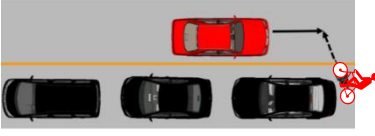
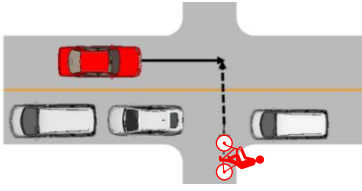
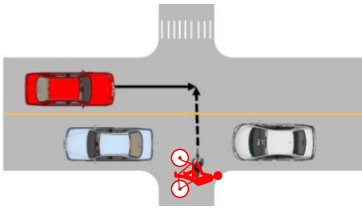
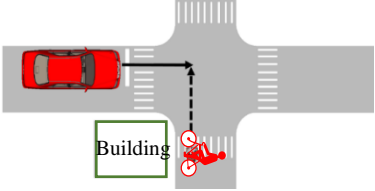
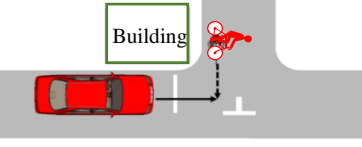
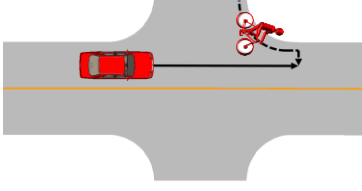
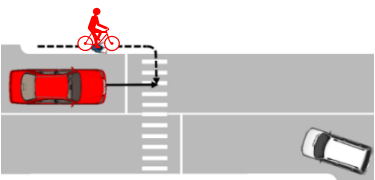
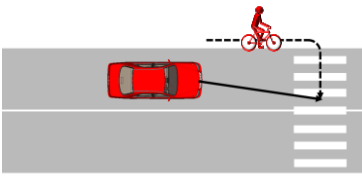
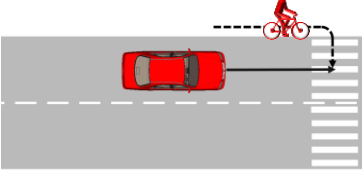
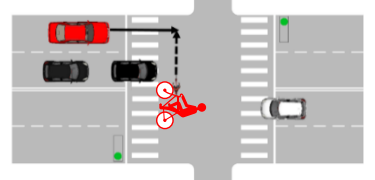
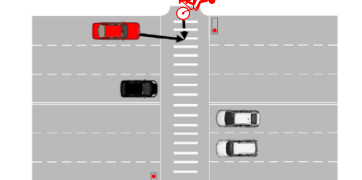
Fig. 5.9 Effectiveness of AEB with 50°FOV, 90° FOV and 360°FOV in avoiding collisions in car-to-cyclist perpendicular collisions.

The configuration of crash and car kinematic of the 11 unavoidable collisions are shown in the Table 5.1. 9 of 11 unavoidable collisions occur at intersections without traffic signals, and the other 2 collisions occur at larger intersections with traffic lights. These 11 collisions can be divided into three categories. The first category is the sudden appearance of the cyclists from behind cars and buildings (No. 1. 2. 3. 4. 5): the cyclists in No. 1, No. 2 and No. 3 suddenly intrude into roads from the opposite lanes (far side); the cyclists in No. 4 and No. 5 appear from buildings, and the  $TTC_a$  in No. 5 where the cyclist intrudes from near side is the smallest (0.287) in the first category. The second category is that the cyclist suddenly changed his/her travelling direction from the near side (No. 6. 7. 8. 9), and 3 of 4 collisions are that the cyclists change their directions to cross the crosswalks. The car velocity in the second category of collisions is relatively higher (No. 6, No. 8, and No.9), this may be explained by that the drivers do not expect the cyclist changing their directions and thus keep high velocities. The third category is that the cyclist (No.10) or the car driver (No. 11) violated traffic rules. Although



these 11 collisions are not avoided by ideal AEB, the impact velocity of the cars are all reduced.

Table 5.1 Collisions that cannot be avoided by ideal AEB with 360°FOV and DT 0 s.

<p>No. 1 <math>TTC_A</math> 0.880 s <math>V_A</math> 38.4 km/h Impact velocity: w/o AEB 30 km/h w/ AEB 6.5 km/h</p>	<p>No. 2 <math>TTC_A</math> 0.517 s <math>V_A</math> 49.6 km/h Impact velocity: w/o AEB 35 km/h w/ AEB 32.3 km/h</p>	<p>No. 3 <math>TTC_A</math> 0.555 s <math>V_A</math> 30.5 km/h Impact velocity: w/o AEB 8 km/h w/ AEB 4.6 km/h</p>
		
<p>No. 4 <math>TTC_A</math> 0.587 s <math>V_A</math> 33.8 km/h Impact velocity: w/o AEB 10 km/h w/ AEB 7.0 km/h</p>	<p>No. 5 <math>TTC_A</math> 0.287 s <math>V_A</math> 25.0 km/h Impact velocity: w/o AEB 25 km/h w/ AEB 14.5 km/h</p>	<p>No. 6 <math>TTC_A</math> 0.595 s <math>V_A</math> 55.0 km/h Impact velocity: w/o AEB 50 km/h w/ AEB 25.8 km/h</p>
		
<p>No. 7 <math>TTC_A</math> 0.144 s <math>V_A</math> 20.7 km/h Impact velocity: w/o AEB 15 km/h w/ AEB 10.5 km/h</p>	<p>No. 8 <math>TTC_A</math> 0.535 s <math>V_A</math> 44.5 km/h Impact velocity: w/o AEB 32 km/h w/ AEB 15.3 km/h</p>	<p>No. 9 <math>TTC_A</math> 0.522 s <math>V_A</math> 47.1 km/h Impact velocity: w/o AEB 20 km/h w/ AEB 16.2 km/h</p>
		
<p>No. 10 <math>TTC_A</math> 0.299 s <math>V_A</math> 39.7 km/h Impact velocity: w/o AEB 35 km/h w/ AEB 25.3 km/h</p>	<p>No. 11 <math>TTC_A</math> 0.493 s <math>V_A</math> 25.9 km/h Impact velocity: w/o AEB 15 km/h w/ AEB 11.3 km/h</p>	
		

### 5.3.2. Effectiveness of AEB in turning collisions

AEBs with 50° FOV, 90° FOV and 360° FOV are also applied in reconstruction of car-to-cyclist turning collisions to examine the effectiveness of AEB. The positions of the cyclists relative to the car at the time when the cyclist enters intersections is shown in Fig. 5.10. The cyclists in turning collisions locate closer to the car compared to perpendicular collisions (see Fig. 5.6), and most of them distribute within 20 m in the front of the car. There are some collisions locate outside the FOV but can be avoided by the corresponding AEB (i.e., 11 collisions avoided by AEB with 50° FOV locate outside 50° FOV), and this is because positions of the cyclists relative to the car change during the car turns.

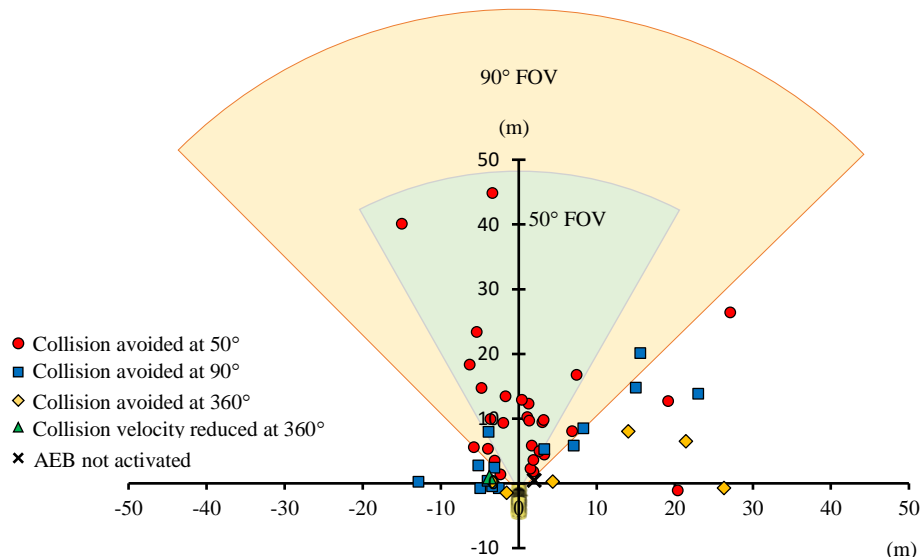


Fig. 5.10 Position of the cyclists relative to the car using AEB with 50°FOV, 90°FOV and 360°FOV at the time when the cyclist enters intersections ( $t_e$ ) in car-to-cyclist turning collisions.

Figure. 5.11 shows the relationship between the car velocity and  $TTC_e$  at the time when the cyclist enters intersections. The collision avoidances using AEB with 50° FOV, 90° FOV and 360° FOV are also included. Unlike the performance of AEB in perpendicular collisions, the car velocity during car turning is below 30 km/h, which results in a wider distribution of  $TTC_e$ . In addition, more collisions with larger  $TTC_e$  can be avoided by AEB with 50° FOV. All collisions locate on the right area of the braking limit, indicating that failure to avoid collisions during car's turning is not because the required braking deceleration to stop the car exceeds the braking limit.

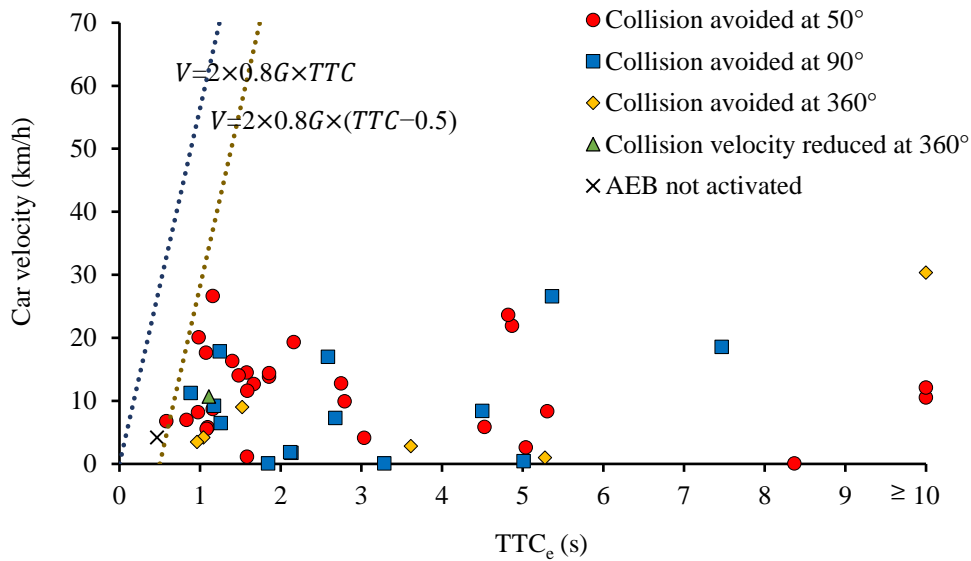


Fig. 5.11 Relationship of car velocity and  $TTC_e$  with different FOV at the time when the cyclist enters intersections in car-to-cyclist turning collisions.

Figure. 5.12 shows the result of AEB with 50° FOV, 90° FOV and 360° FOV in avoiding car's left turning collisions. In general, the collisions when the cyclist approaches in the same direction of the car is difficult to be avoided because the cyclist approaches from the rearward of the car. In the collisions using AEB with 50° FOV and DT 0.5 s, the AEB is not effective for the cases where the cyclist comes from same direction. Only 1 collision can be avoided, and the AEB in 8 collisions is not active since the cyclist does not enter the FOV of AEB until the car collides with the cyclist. However, the same AEB is effective for preventing the collisions where the cyclist approaches from the opposite direction. When the FOV increases to 90°, the AEB is able to protect the majority of the cyclists coming from the same or the opposite direction. The ideal AEB with 360°FOV and DT 0 s is effective for preventing all collisions except 1 collision where the cyclist travels from the opposite direction.

The result of AEB effectiveness in avoiding right turning collisions is shown in Fig. 5.13. The trend is comparable with AEB specifications (FOV and DT) and the cyclist direction (same opposite) between the right and left turning collisions (Fig. 5.12 and Fig. 5.13). As with AEB in left turning collision, the 50° FOV is not effective in protecting the cyclist approaching from the same direction in right turning collisions, and only 2 collisions are avoided. The majority of collisions can be avoided AEB with 90° FOV, irrespective of the cyclist approaching direction (same or opposite). When the FOV increases to 360° FOV and the DT decreases to 0 s, the AEB is effective for all collisions except 1 collision where the cyclist comes from opposite direction.

In left turning and right turning collisions, the 2 collisions that cannot be avoided by the ideal AEB is that the cyclist suddenly enters the pedestrian crosswalk occurs on the side of the car. Since the low velocity of the car in the turning, the braking of the car because of AEB makes the impact position change from the rear of the side to the front of the side.

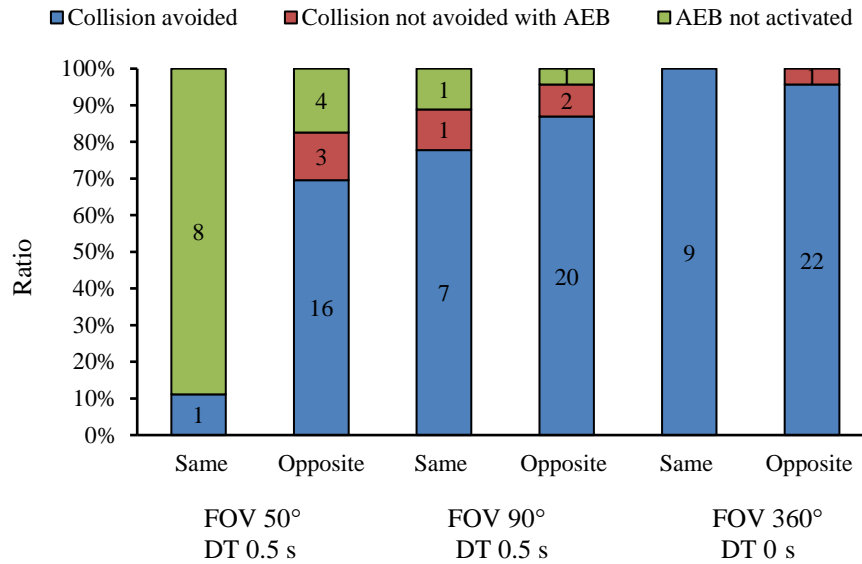


Fig. 5.12 Effectiveness of AEB with 50°FOV, 90°FOV and 360°FOV in left turning collisions.

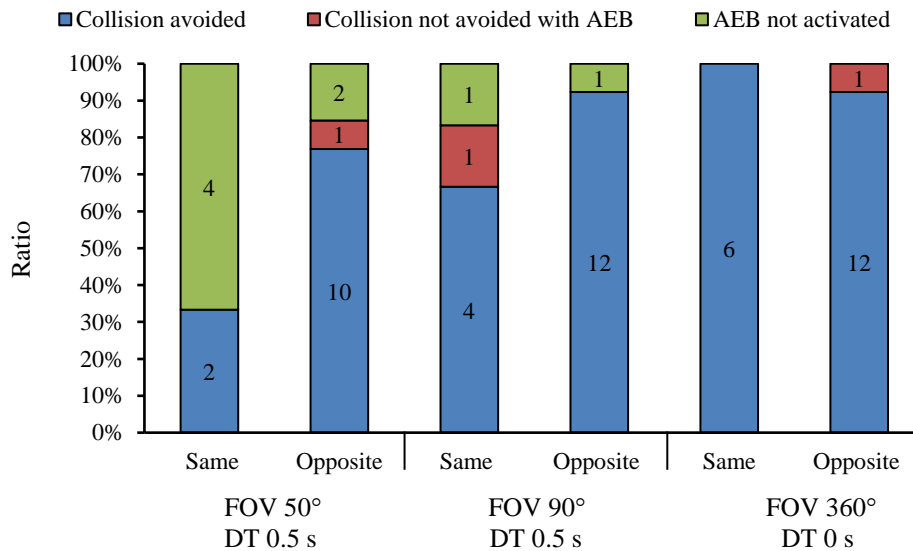


Fig. 5.13 Effectiveness of AEB with 50°FOV, 90°FOV and 360°FOV in right turning collisions.

## 5.4. Discussion

This chapter examined the effectiveness of AEB in protecting cyclists in perpendicular collisions and turning collisions by reconstructing the accidents obtained from the car drive recorder. The advantage of using collisions collected from drive recorders instead of the in-depth data or police data used in past studies is that the kinematic parameters of the cars and the behavior of the cyclists could be accurately determined, especially before the collisions occurred. This is because the parameters of the cars and the cyclists are usually inferred from tire skid marks and testimonies of the persons involved in the collisions or eyewitness in in-depth accident data or police data, and thus these data contain uncertainty in the information.

In this study, the results show that AEB for pedestrians ( $50^\circ$ FOV and DT 0.5 s) was insufficient in preventing occurrences of perpendicular and turning car-to-cyclist collisions. This finding is consistent with Lenard's study (2018) showing that cyclists appear at a wider angle relative to cars than pedestrians, thus a larger FOV is required to avoid car-to-cyclist collisions. In this study, the effectiveness of AEB was greatly improved when FOV increased to  $90^\circ$  (Fig. 5.9, Fig. 5.12 and Fig. 5.13), and this result coincides with other studies indicating that the effectiveness of AEB increases as angle of FOV increases (Fredriksson et al., 2015; Sander and Lubbe, 2018; Gruber et al., 2019).

In this study, it was shown that the effectiveness of delay time for avoiding collisions is not larger than widening the angle of FOV. Fig. 5.6 shows 11 unavoidable collisions with  $360^\circ$  FOV and DT 0.5 s and 8 collisions with AEB not activated distributed 10 m in front of the car at the time when the cyclist was visible in the perpendicular collisions. In these cases, the braking distance left for the car after delay time was insufficient, thus it is necessary to shorten the delay time for the collision where the cyclist appeared in close to the car. This result was verified in Fig. 5.8 showing that the number of the collisions was decreased to 11 using the AEB without delay time (DT 0 s). Since the required braking deceleration exceeded the braking limit (Table 5.1), the 11 collisions could not be avoided by ideal AEB with  $360^\circ$  FOV and DT 0 s. Based on these results, this study demonstrated a new finding that it is worth noting that these collisions would also occur in autonomous driving. In the first category of unavoidable collisions, the collisions were difficult to be detected and avoided since the cyclists suddenly intruded from view blocking obstructions, causing small  $TTC_a$ . To avoid this type of collisions, it may be necessary to discuss to obey traffic rules for drivers and cyclist to prevent sudden appearance into the road or inter-vehicle communication including car-to-cyclist communication. In the

second category of collisions, the cyclists travelling along the roads were visible, but the driver could not perceive the cyclist's motivation of sudden changing directions. Similarly, the sudden intruding behavior of cyclists was also difficult to be judged by autonomous cars. Thus, enhancing the cyclist's education is a better approach to avoid collisions in this situation. For example, the cyclist shows clearer motivations of crossing intersections at the proper time.

In Figure 5.7, the car with higher velocity seems more likely to be avoided by AEB, and AEB with a larger FOV was needed to avoid collisions when the car velocity was below 20 km/h. This is because the relative angle between the cyclist and the car was large when the car traveled with low velocity, causing more difficulty for the cyclist to enter the FOV of AEB.

In the turning collisions, lower velocities of cars during turning resulted in the cars to stop more easily though the cyclists appeared laterally and closer to the car compared to perpendicular collisions. Sander (2017) calculated the effectiveness of AEB in avoiding left turning car-to-car collisions using GIDAS accident database, and they concluded that AEB could hardly avoid collisions when the car velocity exceeds 40 km/h. In addition, for the conflict configuration where the object was straight going vehicles (equivalent to the opposite direction in the right turning collision in this study), an AEB with 40°FOV could avoid 80% of the collisions. This is consistent with the results in this dissertation showing that AEB was effective for the cyclist traveling from the opposite direction (Fig. 5.13). However, small FOV of AEB was insufficient for the cyclists traveling at lower velocity or coming from the same direction since the cyclist velocity is close to parallel to the car. Thus, it is necessary to enhance the FOV of AEB to protect the cyclist coming from the same direction.

To sum up, the AEB with FOV 50° ( $\pm 25^\circ$ ) and DT 0.5 s designed for pedestrians was not insufficient for cyclists no matter in the perpendicular configuration or the turning configuration because cyclists have higher traveling velocity compared to pedestrians. Moreover, traffic situations are more complex in the real world, for instance, non-motorized vehicles including electric bicycles and electric two-wheelers are also traveling at same time, which have higher traveling speed. Thus, the AEB applied in the future is necessary to technically increase FOV and decrease the delay time as much as possible for preventing traffic users from various crash configurations.

In this study, the trajectory of the cars could be determined from the videos, but the trajectory of the cyclists was determined by comparing the cyclist position with landmarks in the video since the parameters of the cyclists were not directly available. This may include errors in the

results of AEB activation. Besides, intentions and behaviors of the cyclists were not taken into account in the simulation with AEB (cyclists may stop when they hear the braking noise of the AEB), thus the results in this study may be different from the results using AEB to avoid collisions in the real world.

## **5.5. Conclusions**

This chapter estimated the effectiveness of AEB in the reconstruction of car-to-cyclist perpendicular collisions and turning collisions obtained from the drive recorder videos. The conclusions are summarized as follows:

- The AEB designed for pedestrians is not effective in preventing cyclists from the perpendicular collisions because FOV range of AEB is not enough to detect cyclists who travels at high velocity than pedestrians.
- The number of cases to avoid collisions by AEB increases as the field of view (FOV) of AEB widened and delay time decreases. The FOV of the AEB is more effective to avoid collisions than reducing the delay time.
- Ideal AEB is not effectiveness in the collisions with small time-to-collision where the cyclist suddenly appears from the obstacles. Probably, these collisions cannot be avoided in autonomous cars.
- In turning collisions, the cyclist traveling from the same direction with the car is difficult to enter FOV of AEB because the cyclist approaches from the behind of the car. Widening the FOV angle range of AEB can also effective to avoid this type of collisions.

## Chapter 6

### General Discussion and Conclusions

#### 6.1. General discussion

This dissertation investigated causes of collision occurrences in car-to-cyclist conflicts including the driver behavior and the cyclist behavior in emergency situations using videos of drive recorders. The cyclist and driver behaviors were identified with time in videos which is advantage compared to research study using police data and in-depth data. The driver reactions in three typical scenarios reconstructed from the drive recorder data was then investigated using a driving simulator. Finally, an AEB with different field of view and sensor delay time was applied to all collisions in drive recorder videos in order to examine the effectiveness of advanced driver-assistance systems in protecting cyclists from collisions.

As far as the author knows, this is first research to identify causes of car-to-cyclist collisions by comparing driver behaviors in near-miss incidents and collisions using videos of drive recorders. Many research studies investigated collision occurrences using near-miss incidents of drive recorders, however, collision videos have not been used. The collision data of drive recorder was newly corrected in this study, and they were compared to the near-miss database.

In the collisions that could not be avoided by drivers, the required braking deceleration to stop the cars before collisions was beyond the braking performance limit ( $5.2 \text{ m/s}^2$ ). This was identified as the boundary of near-miss and collisions. Two typical configurations were observed in car-to-cyclist collisions. The first configuration is the cyclist suddenly intruding behind the obstacles such as stopping cars or buildings. TTC was too small for cars to stop when the cyclist was visible. The second configuration is the delay of driver's reaction with long brake reaction time.

One of the highlights of this study was that driver's gaze was newly examined combining with driver reactions to intruding cyclists from the side direction at an intersection, though driver's gaze has been analyzed by previous research studies in car following scenarios. In driving simulator experiments, it was found that drivers usually looked to their lane where they were driving (future path). Driver had longer braking reaction time in cyclist's intruding from the far side than from the near side because the gaze to the cyclist from the far side required a larger gaze angle to notice. This can be different collision occurrence mechanism compared to that in the longitudinal direction (rear-end collisions). The gaze analysis made it possible to



identify notice of the cyclist. Drivers were more likely to use swerving instead of braking when driver's notice time of the cyclist is smaller. Moreover, the drivers released the accelerating pedal and turned the steering wheel at the same time, indicating that the drivers applied braking and swerving simultaneously when the driver applied braking combining with swerving.

Another highlight is that this is a first study that investigated the cyclist behavior to avoid collision by comparing the near-miss incidents by the cyclist avoided and not incidents avoided based on drive recorder videos. It was demonstrated that cyclist avoidance behavior was effective to avoid collisions particularly for cases that the cyclist intruded into the area that car could not stop to avoid collisions. The cyclist velocity was calculated according to the real world near-misses and the collisions, showing that the cyclist velocity in the near-miss incidents was significantly lower than in the collisions. Previous studies show that the cyclist avoided the car at intersection was related to the car acceleration at the time when the cyclist was visible. In this study, the regression analysis indicates that the cyclist showed avoidance behavior as the TTC was smaller and the cyclist velocity is lower. This cyclist avoidance behavior needs to be investigated to develop cyclist models which can predict collisions in driving models.

AEB was applied to all collision cases in the videos of drive recorders. The collision configuration with relatively large TTC with long brake reaction time of the driver could be avoided effectively using an AEB system. However, the collision configurations with small TTC ( $< 1.0$  s) such that the cyclist suddenly appeared were difficult to be avoided. 18% of collisions were still not be avoided even using an ideal AEB system with  $360^\circ$  FOV without delay time. This result implies that collisions will continue to occur in autonomous cars with AEB. Thus, other technical solutions such as vehicle-to-cyclist communication and education of cyclists will be necessary. This study probably demonstrated firstly that some types of accidents still occur in autonomous cars while some people considered that accidents can be zero in autonomous cars.

The limitation of this study is that the number of collisions in drive recorders is smaller compared to the in-depth data and police-reported accident data, and the data do not include records of post-crash injuries. Because the drivers in the collected data are experienced and professional taxi drivers, their reactions in emergency situations will not be representative of all drivers. Besides, the majority of taxi drivers in Japan is males, therefore, the data in gender and gender are unbalanced. Moreover, the drivers in the drive recorder experiments might be more attentive with no distraction than those in naturalistic driving. The driver avoidance

reactions might be stronger than in naturalistic driving because they did not have to consider the physical influences of sudden hard braking and steering on the oncoming and following cars. Finally, the cyclist behavior analyses may include errors because the cyclist was visible from a distance was sometimes not clear in the videos.

## **6.2. Conclusions**

The objective of this study is to identify causes of collision occurrences in the car-to-cyclist perpendicular conflicts at intersections using the drive recorders and to determine the effectiveness of AEB for preventing the cyclist from collisions. The conclusions of this study are as follows:

1. Collisions and near-miss incidents can be distinguished whether the cyclist enters the braking performance limit of the car ( $5.2 \text{ m/s}^2$ ). If the cyclist enters this area, the car cannot stop before the cyclist path while a collision can be avoided only by cyclist avoidance.
2. Time-to-collision (TTC) and braking reaction time (BRT) are the most critical parameters in collision occurrences: TTC can determine the conflict environment, and BRT determines the collision occur or not.
3. Applying braking is primary reaction of drivers in emergency situations, and drivers are more likely to change their reaction from braking to swerving as the TTC decreases. However, applying swerving alone is not effectiveness in avoiding collisions.
4. Drivers apply braking and swerving simultaneously in the cases where the drivers take braking combining with swerving, and the time difference of BRT of swerving reaction time SRT is the time that the driver change the foot from the accelerating pedal to the braking pedal.
5. Driver braking reaction time in interacting with the cyclist intruding from the far side is larger than from the near side, and this difference is caused by the notice time of drivers from the time of cyclist visible to the driver notices the cyclist.
6. Cyclists avoided behavior is effective in avoiding collisions that cannot be avoided by drivers since the required braking deceleration of these collisions exceeds the braking limit of the car.
7. The cyclist avoided behavior is associated with the car TTC to the cyclist path and the cyclist velocity at the time when the cyclist is visible: smaller TTC and higher cyclist velocity results in high probability of cyclist to take avoidable maneuvers.

8. The effectiveness of AEB in preventing cyclists from collisions increases with the field of view (FOV) increases and the sensor detecting delay time (DT) decreases in both perpendicular collisions and turning collisions, and increasing FOV is more effective to avoid collisions than decreasing DT.
9. Ideal AEB is not effectiveness to avoid collisions for cyclist sudden appearance from obstacles with small TTC, even though the car velocity impacted with cyclist is reduced by the ideal AEB.

### **6.3. Future work**

In this thesis, fundamental responses of drivers were understood in car-to-cyclist perpendicular conflicts, which led to collisions. Further analysis of driver responses in systematic method is necessary to apply its outcomes for driving assistant systems. First, the future work needs to include responses of drivers and cyclists in the emergency configurations in various traffic conflicts, such as car left and right turn interacting with cyclists at intersections and car overtaking cyclists. Second, driver gaze in the lateral direction was found to affect driver recognition of cyclists to avoid lateral collisions. Thus, the sequence of driver's gaze and recognition is necessary to be understood in the mechanism of collision occurrences. This analysis needs to include individual differences of drivers because drivers showed various scans of gazes during driving simulator experiments. Moreover, recognitions and responses of elderly drivers and cyclists also needs to be studied because this study did not take into account the effects of ages. Besides, the driver's responses in the rural and urban areas for cyclist's intrusions may be different, and thus the different responses of drivers need to be examined in the future.

## References

- Arai, Y., Nishimoto, T., Ezaka, Y., Yoshimoto, K. (2001). Accidents and near-misses analysis by using video drive-recorders in a fleet test (No. 2001-06-0001). *SAE Technical Paper*.
- Aust, M. L. (2010). Generalization of case studies in road traffic when defining pre-crash scenarios for active safety function evaluation. *Accident Analysis & Prevention*, 42(4), 1172-1183.
- Bella, F., Silvestri, M. (2018). Survival model of drivers' speed reduction time at bicycle crossroads: a driving simulator study. *Journal of Advanced Transportation*, 2018, 4738457.
- Bernardi, S., & Rupi, F. (2015). An analysis of bicycle travel speed and disturbances on off-street and on-street facilities. *Transportation Research Procedia*, 5, 82-94.
- Bíl M, Bílová M, Müller I. Critical factors in fatal collisions of adult cyclists with automobiles. *Accident Analysis & Prevention*. 2010 Nov 1;42(6):1632-6.
- Billot-Grasset, A., Amoros, E., & Hours, M. (2016). How cyclist behavior affects bicycle accident configurations?. *Transportation Research Part F: Traffic Psychology and Behaviour*, 41, 261-276.
- Blaizot, S., Papon, F., Haddak, M. M., Amoros, E. (2013). Injury incidence rates of cyclists compared to pedestrians, car occupants and powered two-wheeler riders, using a medical registry and mobility data, Rhône County, France. *Accident Analysis & Prevention*, 58, 35-45.
- Blanc, B., & Figliozzi, M. (2016). Modeling the impacts of facility type, trip characteristics, and trip stressors on cyclists' comfort levels utilizing crowdsourced data. *Transportation Research Record*, 2587(1), 100-108.
- Boda, C. N., Dozza, M., Bohman, K., Thalya, P., Larsson, A., & Lubbe, N. (2018). Modelling how drivers respond to a bicyclist crossing their path at an intersection: How do test track and driving simulator compare?. *Accident Analysis & Prevention*, 111, 238-250.
- Calvi, A., D'amico, F. (2013). A study of the effects of road tunnel on driver behavior and road safety using driving simulator. *Advances in Transportation Studies*, (30).
- Chajmowicz, H., Saadé, J., & Cuny, S. (2019). Prospective assessment of the effectiveness of autonomous emergency braking in car-to-cyclist accidents in France. *Traffic Injury Prevention*, 20(sup2), S20-S25.
- Chang, X., Li, H., Qin, L., Rong, J., Lu, Y., Chen, X. (2019). Evaluation of cooperative systems

- on driver behavior in heavy fog condition based on a driving simulator. *Accident Analysis & Prevention*, 128, 197-205.
- Chen, M., Zhu, X., Ma, Z., Li, L., Wang, D., Liu, J. (2016, June). Brake response time under near-crash cases with cyclist. In *2016 IEEE Intelligent Vehicles Symposium (IV)* (pp. 80-85). IEEE.
- Cheng, B., Lin, Q., Song, T., Cui, Y., Wang, L., Kuzumaki, S. (2011). Analysis of driver brake operation in near-crash situation using naturalistic driving data. *International Journal of Automotive Engineering*, 2(4), 87-94.
- Cicchino, J. B. (2017). Effectiveness of forward collision warning and autonomous emergency braking systems in reducing front-to-rear crash rates. *Accident Analysis & Prevention*, 99, 142-152.
- Coelingh, E., Eidehall, A., Bengtsson, M. (2010, September). Collision warning with full auto brake and pedestrian detection-a practical example of automatic emergency braking. In *13th International IEEE Conference on Intelligent Transportation Systems*, pp. 155-160. IEEE.
- Crundall, D. E., Underwood, G., Chapman, P. R. (1998). How much do novice drivers see? The effects of demand on visual search strategies in novice and experienced drivers. In *Eye guidance in reading and scene perception*, pp. 395-417.
- Den Camp, O. O., Ranjbar, A., Uittenbogaard, J., Rosen, E., & Buijssen, S. H. H. M. (2014). Overview of main accident scenarios in car-to-cyclist accidents for use in AEB-system test protocol. In *Proceedings of International Cycling Safety Conference*.
- Den Camp, O. O., van Montfort, S., Uittenbogaard, J., Welten, J. (2017). Cyclist target and test setup for evaluation of cyclist-autonomous emergency braking. *International Journal of Automotive Technology*, 18(6), 1085-1097.
- Dill, J., & Gliebe, J. (2008). Understanding and measuring bicycling behavior: A focus on travel time and route choice. Final report OTREC-RR-08-03 prepared for Oregon Transportation Research and Education Consortium (OTREC), December 2008.
- Dozza, M., & Werneke, J. (2014). Introducing naturalistic cycling data: What factors influence bicyclists' safety in the real world?. *Transportation Research Part F: Traffic Psychology and Behaviour*, 24, 83-91.
- Duivenvoorden, K., Hogema, J., Hagenzieker, M., Wegman, F. (2015). The effects of cyclists present at rural intersections on speed behavior and workload of car drivers: a driving simulator study. *Traffic Injury Prevention*, 16(3), 254-259.

- Edwards, M., Nathanson, A., Wisch, M. (2014). Estimate of potential benefit for Europe of fitting autonomous emergency braking (AEB) systems for pedestrian protection to passenger cars. *Traffic Injury Prevention*, 15(sup1), S173-S182.
- Eiríksdóttir, H. H. (2016). *Quantitative analysis of rear-end crash causation mechanisms based on naturalistic crash data* (Master's thesis).
- El-Geneidy, A., Krizek, K. J., Iacono, M. (2007, January). Predicting bicycle travel speeds along different facilities using GPS data: A proof of concept model. In Proceedings of the 86th annual meeting of the transportation research board, compendium of papers. TRB Washington, DC, USA.
- Euro NCAP, AEB car-to-cyclist. <https://www.euroncap.com/en/vehicle-safety/the-ratings-explained/vulnerable-road-user-vru-protection/aeb-cyclist/>
- Euro NCAP, AEB car-to-pedestrian. <https://www.euroncap.com/en/vehicle-safety/the-ratings-explained/vulnerable-road-user-vru-protection/aeb-pedestrian/>
- Euro NCAP, AEB car-to-car. <https://www.euroncap.com/en/vehicle-safety/the-ratings-explained/safety-assist/aeb-car-to-car/>
- Fildes, B., Keall, M., Bos, N., Lie, A., Page, Y., Pastor, C., Tingvall, C. (2015). Effectiveness of low speed autonomous emergency braking in real-world rear-end crashes. *Accident Analysis & Prevention*, 81, 24-29.
- Fredriksson, R., Ranjbar, A., Rosén, E. (2015, June). Integrated Bicyclist Protection Systems- Potential of Head Injury Reduction Combining Passive and Active Protection Systems. In *24th International Technical Conference on the Enhanced Safety of Vehicles (ESV)*, Gothenburg, SE.
- Fruhen, L. S., Flin, R. (2015). Car driver attitudes, perceptions of social norms and aggressive driving behaviour towards cyclists. *Accident Analysis & Prevention*, 83, 162-170.
- Fruhen, L. S., Rossen, I., Griffin, M. A. (2019). The factors shaping car drivers' attitudes towards cyclist and their impact on behaviour. *Accident Analysis & Prevention*, 123, 235-242.
- Fu, T., Miranda-Moreno, L., Saunier, N. (2018). A novel framework to evaluate pedestrian safety at non-signalized locations. *Accident Analysis & Prevention*, 111, 23-33.
- Green, M. (2000). "How long does it take to stop?" Methodological analysis of driver perception-brake times. *Transportation human factors*, 2(3), 195-216.
- Gruber, M., Kolk, H., Tomasch, E., Feist, F., Klug, C., Schneider, A., Fredriksson, A. (2019, June). The effect of P-AEB system parameters on the effectiveness for real world pedestrian

- accidents. In *Proceedings of the 26th ESV Conference Proceedings*.
- Habibovic, A., Tivesten, E., Uchida, N., Bärgrman, J., Aust, M. L. (2013). Driver behavior in car-to-pedestrian incidents: An application of the Driving Reliability and Error Analysis Method (DREAM). *Accident Analysis & Prevention*, 50, 554-565.
- Hamdane, H., Serre, T., Masson, C., Anderson, R. (2015). Issues and challenges for pedestrian active safety systems based on real world accidents. *Accident Analysis & Prevention*, 82, 53-60.
- Hamdar, S. H., Qin, L., Talebpour, A. (2016). Weather and road geometry impact on longitudinal driving behavior: Exploratory analysis using an empirically supported acceleration modeling framework. *Transportation Research Part C: Emerging Technologies*, 67, 193-213.
- Hankey, J. M., McGehee, D. V., Dingus, T. A., Mazzae, E. N., & Garrott, W. R. (1996, October). Initial driver avoidance behavior and reaction time to an unalerted intersection incursion. In *Proceedings of the Human Factors and Ergonomics Society Annual Meeting* (Vol. 40, No. 18, pp. 896-899). Sage CA: Los Angeles, CA: SAGE Publications.
- Harms, L. (1991). Variation in drivers' cognitive load. Effects of driving through village areas and rural junctions. *Ergonomics*, 34(2), 151-160.
- Haus, S. H., Sherony, R., Gabler, H. C. (2019). Estimated benefit of automated emergency braking systems for vehicle-pedestrian crashes in the United States. *Traffic Injury Prevention*, 20(sup1), S171-S176.
- Isaksson-Hellman, I. (2012, October). A study of bicycle and passenger car collisions based on insurance claims data. In *Annals of Advances in Automotive Medicine/Annual Scientific Conference* (Vol. 56, p. 3). Association for the Advancement of Automotive Medicine.
- Isaksson-Hellman, I., & Lindman, M. (2012, October). The effect of a low-speed automatic brake system estimated from real life data. In *Annals of Advances in Automotive Medicine/Annual Scientific Conference* (Vol. 56, p. 231). Association for the Advancement of Automotive Medicine.
- Isaksson-Hellman, I., & Lindman, M. (2016). Evaluation of the crash mitigation effect of low-speed automated emergency braking systems based on insurance claims data. *Traffic Injury Prevention*, 17(sup1), 42-47.
- Ito, D., Hayakawa, K., Kondo, Y., Mizuno, K., Thomson, R., Piccinini, G. B., & Hosokawa, N. (2018). Difference between car-to-cyclist crash and near crash in a perpendicular crash

- configuration based on driving recorder analysis. *Accident Analysis & Prevention*, 117, 1-9.
- Japan Electronics and Information Technology Industries Association (JEITA), 2021. <https://www.jeita.or.jp/japanese/stat/drive/2020/>
- Jeppsson, H., & Lubbe, N. (2020). Simulating automated emergency braking with and without Torricelli vacuum emergency braking for cyclists: Effect of brake deceleration and sensor field-of-view on accidents, injuries and fatalities. *Accident Analysis & Prevention*, 142, 105538.
- Jeppsson, H., Östling, M., Lubbe, N. (2018). Real life safety benefits of increasing brake deceleration in car-to-pedestrian accidents: Simulation of Vacuum Emergency Braking. *Accident Analysis & Prevention*, 111, 311-320.
- Johnson, M., Charlton, J., Oxley, J., Newstead, S. (2010, January). Naturalistic cycling study: identifying risk factors for on-road commuter cyclists. In *Annals of advances in automotive medicine/annual scientific conference* (Vol. 54, p. 275). Association for the Advancement of Automotive Medicine.
- Jurecki, R. S., & Stańczyk, T. L. (2014). Driver reaction time to lateral entering pedestrian in a simulated crash traffic situation. *Transportation Research Part F: Traffic Psychology and Behaviour*, 27, 22-36.
- Jurecki, R. S., Stańczyk, T. L. (2014). Driver reaction time to lateral entering pedestrian in a simulated crash traffic situation. *Transportation Research Part F: Traffic Psychology and Behaviour*, 27, 22-36.
- Kaplan, S., Vavatsoulas, K., Prato, C. G. (2014). Aggravating and mitigating factors associated with cyclist injury severity in Denmark. *Journal of safety research*, 50, 75-82.
- Kassim, A., Tayyeb, H., Al-Falahi, M. (2020). Critical review of cyclist speed measuring techniques. *Journal of traffic and transportation engineering (English edition)*, 7(1), 98-110.
- Klauer, S. G., Dingus, T. A., Neale, V. L., Sudweeks, J. D., Ramsey, D. J. (2006). The impact of driver inattention on near-crash/crash risk: An analysis using the 100-car naturalistic driving study data, National Highway Traffic Safety Administration, DOT HS 810 594, 2006.
- Kovaceva, J., Bärghman, J., Dozza, M. (2020). A comparison of computational driver models using naturalistic and test-track data from cyclist-overtaking manoeuvres. *Transportation Research Part F: Traffic Psychology and Behaviour*, 75, 87-105.
- Kováčsová, N., de Winter, J. C., Hagenzieker, M. P. (2019). What will the car driver do? A video-based questionnaire study on cyclists' anticipation during safety-critical



- situations. *Journal of Safety Research*, 69, 11-21.
- Kumara, S. S. P., Chin, H. C., Weerakoon, W. M. S. B. (2003). Identification of accident causal factors and prediction of hazardousness of intersection approaches. *Transportation Research Record*, 1840(1), 116-122.
- Lamble, D., Laakso, M., Summala, H. (1999). Detection thresholds in car following situations and peripheral vision: Implications for positioning of visually demanding in-car displays. *Ergonomics*, 42(6), 807-815.
- Larsen, L. (2004). Methods of multidisciplinary in-depth analyses of road traffic accidents. *Journal of Hazardous Materials*, 111(1-3), 115-122.
- Lechner, D., & Malaterre, G. (1991). *Emergency maneuver experimentation using a driving simulator* (No. 910016). SAE Technical Paper.
- Lee, D. N. (1976). A theory of visual control of braking based on information about time-to-collision. *Perception*, 5(4), 437-459.
- Lee, O., Rasch, A., Schwab, A. L., Dozza, M. (2020). Modelling cyclists' comfort zones from obstacle avoidance manoeuvres. *Accident Analysis & Prevention*, 144, 105609.
- Lehtonen, E., Havia, V., Kovanen, A., Leminen, M., Saure, E. (2016). Evaluating bicyclists' risk perception using video clips: Comparison of frequent and infrequent city cyclists. *Transportation Research Part F: Traffic Psychology and Behaviour*, 41, 195-203.
- Lenard, J., Welsh, R., Danton, R. (2018). Time-to-collision analysis of pedestrian and pedal-cycle accidents for the development of autonomous emergency braking systems. *Accident Analysis & Prevention*, 115, 128-136.
- Leo, C., Gruber, M., Feist, F., Sinz, W., Roth, F., & Klug, C. (2020, September). The effect of autonomous emergency braking systems on head impact conditions for pedestrian and cyclists in passenger car collisions. In *Proceedings of the 2020 IRCOBI Conference Proceedings* (pp. 330-357).
- Li, X., Rakotonirainy, A., Yan, X. (2019). How do drivers avoid collisions? A driving simulator-based study. *Journal of Safety Research*, 70, 89-96.
- Lin, Q. F., Cheng, B., Lu, G. Q. (2011). Analysis of characteristics of vehicle-bicycle/pedestrian conflicts using video drive recorder. In *Advanced Materials Research*, 243, 4413-4417. Trans Tech Publications Ltd.
- Lin, Q., Feng, R., Cheng, B., Lai, J., Zhang, H., & Mei, B. (2008). Analysis of causes of rear-end conflicts using naturalistic driving data collected by video drive recorders, SAE Paper

- No. 2008-01-0522, Society of Automotive Engineering.
- Ling, H., & Wu, J. (2004). A study on cyclist behavior at signalized intersections. *IEEE Transactions on Intelligent Transportation Systems*, 5(4), 293-299.
- Loftus, E. F. (1979). *Eyewitness Testimony* Harvard University Press. *Cambridge, Massachusetts*.
- Lubbe, N., & Kullgren, A. (2015, September). Assessment of integrated pedestrian protection systems with forward collision warning and automated emergency braking. In *IRCOBI Conference*.
- Lubbe, N., & Rosén, E. (2014). Pedestrian crossing situations: Quantification of comfort boundaries to guide intervention timing. *Accident Analysis & Prevention*, 71, 261-266.
- Maki, T., Kajzer, J., Mizuno, K., Sekine, Y. (2003). Comparative analysis of vehicle–bicyclist and vehicle-pedestrian accidents in Japan. *Accident Analysis & Prevention*, 35(6), 927-940.
- Malaterre, G., Ferrandez, F., Fleury, D., Lechner, D. (1988). Decision making in emergency situations. *Ergonomics*, 31(4), 643-655.
- Markkula, G., Benderius, O., Wolff, K., Wahde, M. (2012). A review of near-collision driver behavior models. *Human factors*, 54(6), 1117-1143.
- Markkula, G., Engström, J., Lodin, J., Bärgman, J., Victor, T. (2016). A farewell to brake reaction times? Kinematics-dependent brake response in naturalistic rear-end emergencies. *Accident Analysis & Prevention*, 95, 209-226.
- Markkula, G., Romano, R., Waldram, R., Giles, O., Mole, C., Wilkie, R. (2019). Modelling visual-vestibular integration and behavioural adaptation in the driving simulator. *Transportation research part F: traffic psychology and behaviour*, 66, 310-323.
- Matsui, Y., Hitosugi, M., Takahashi, K., Doi, T. (2013). Situations of car-to-pedestrian contact. *Traffic injury prevention*, 14(1), 73-77.
- Matsui, Y., Oikawa, S. (2015). Risks of serious injuries and fatalities of cyclists associated with impact velocities of cars in car-cyclist accidents in Japan. *Stapp car crash journal*, 59, 385.
- Matsui, Y., Oikawa, S., Hitosugi, M. (2016). Analysis of car-to-bicycle approach patterns for developing active safety devices. *Traffic Injury Prevention*, 17(4), 434-439.
- Matsui, Y., Oikawa, S., Takahashi, K., Hitosugi, M. (2015). Features of car–cyclist contact situations in near-miss incidents compared with real-world accidents in Japan. In *24th International Technical Conference on the Enhanced Safety of Vehicles (ESV) National Highway Traffic Safety Administration Paper No. 15-0124*.

- Matsui, Y., Takahashi, K., Imaizumi, R., Ando, K. (2011, June). Car-to-pedestrian contact situations in near-miss incidents and real-world accidents in Japan. In *22nd International Technical Conference on the Enhanced Safety of Vehicles*, Paper No. 110164.
- McGehee, D. V., Mazzae, E. N., & Baldwin, G. S. (2000, July). Driver reaction time in crash avoidance research: Validation of a driving simulator study on a test track. In *Proceedings of the human factors and ergonomics society annual meeting* (Vol. 44, No. 20, pp. 3-320). Sage CA: Los Angeles, CA: Sage Publications.
- McGehee, D. V., Mazzae, E. N., Baldwin, G. H., Grant, P., Simmons, C. J., Hankey, J., Forkenbrock, G. (1999). Examination of drivers' collision avoidance behavior using conventional and antilock brake systems on the iowa driving simulator. *Human Factors & Vehicle Safety Research*, 1.
- McLeod, R. W., Ross, H. E. (1983). Optic-flow and cognitive factors in time-to-collision estimates. *Perception*, 12(4), 417-423.
- Montella, A., Aria, M., D'Ambrosio, A., Galante, F., Mauriello, F., Perneti, M. (2011). Simulator evaluation of drivers' speed, deceleration and lateral position at rural intersections in relation to different perceptual cues. *Accident Analysis & Prevention*, 43(6), 2072-2084.
- Morita, K., Hirose, T., Hatano, T., Kojima, T., & Tanaka, N. (2013). Collision avoidance behavior of drivers when vehicle suddenly appears from side. *Nihon Kikai Gakkai Ronbunshu, C Hen/Transactions of the Japan Society of Mechanical Engineers, Part C*, 79(807), 4311-4320 (in Japanese).
- Muttart, J. W. (2005). *Factors that influence drivers' response choice decisions in video recorded crashes*. SAE Technical Paper 2005-01, 0426, 2005.
- Najm, W. G., Ranganathan, R., Srinivasan, G., Smith, J. D., Toma, S., Swanson, E., Burgett, A. (2013). *Description of light-vehicle pre-crash scenarios for safety applications based on vehicle-to-vehicle communications* (No. DOT-VNTSC-NHTSA-11-11). United States. National Highway Traffic Safety Administration.
- National Police Agency, 2021. Annual Report. Retrieved from. <https://www.e-stat.go.jp/en/statsearch/files?page=1&layout=datalist&toukei=00130002&tstat=000001027457&cycle=7&year=20200&month=0&tclass1val=0>.
- National Police Agency, 2021. Traffic Accidents Situation. Retrieved from. <https://www.e-stat.go.jp/statsearch/files?page=1&layout=datalist&toukei=00130002&tstat=000001027458&cycle=7&year=20200&month=0>.

- Ohlin, M., Strandroth, J., Tingvall, C. (2017). The combined effect of vehicle frontal design, speed reduction, autonomous emergency braking and helmet use in reducing real life bicycle injuries. *Safety Science*, 92, 338-344.
- Papantoniou, P., Yannis, G., Christofa, E. (2019). Which factors lead to driving errors? A structural equation model analysis through a driving simulator experiment. *IATSS Research*, 43(1), 44-50.
- Pein, W. (1997). Bicyclist performance on a multiuse trail. *Transportation Research Record*, 1578(1), 127-131.
- Peng, Y., Chen, Y., Yang, J., Otte, D., Willinger, R. (2012). A study of pedestrian and bicyclist exposure to head injury in passenger car collisions based on accident data and simulations. *Safety Science*, 50(9), 1749-1759.
- Petzoldt, T., Schleinitz, K., Krems, J. F., Gehlert, T. (2017). Drivers' gap acceptance in front of approaching bicycles—Effects of bicycle speed and bicycle type. *Safety Science*, 92, 283-289.
- Poch, M., & Mannering, F. (1996). Negative binomial analysis of intersection-accident frequencies. *Journal of Transportation Engineering*, 122(2), 105-113.
- Pomarjanschi, L., Dorr, M., Barth, E. (2012). Gaze guidance reduces the number of collisions with pedestrians in a driving simulator. *ACM Transactions on Interactive Intelligent Systems (TiS)*, 1(2), 1-14.
- Räsänen, M., & Summala, H. (1998). Attention and expectation problems in bicycle–car collisions: an in-depth study. *Accident Analysis & Prevention*, 30(5), 657-666.
- Rizzi, M., Kullgren, A., Tingvall, C. (2014). Injury crash reduction of low-speed Autonomous Emergency Braking (AEB) on passenger cars. In *Proc. of IRCOBI Conference on Biomechanics of Impacts* (pp. 14-73).
- Rosen, E. (2013, September). Autonomous emergency braking for vulnerable road users. In *Proceedings of IRCOBI conference* (pp. 618-627).
- Rosén, E., Källhammer, J. E., Eriksson, D., Nentwich, M., Fredriksson, R., Smith, K. (2010). Pedestrian injury mitigation by autonomous braking. *Accident Analysis & Prevention*, 42(6), 1949-1957.
- Sander, U. (2017). Opportunities and limitations for intersection collision intervention—A study of real world 'left turn across path' accidents. *Accident Analysis & Prevention*, 99, 342-355.
- Sander, U., & Lubbe, N. (2018). The potential of clustering methods to define intersection test scenarios: Assessing real-life performance of AEB. *Accident Analysis & Prevention*, 113, 1-

11.

- Sarkar, A., Hickman, J. S., McDonald, A. D., Huang, W., Vogelpohl, T., Markkula, G. (2021). Steering or braking avoidance response in SHRP2 rear-end crashes and near-crashes: A decision tree approach. *Accident Analysis & Prevention*, 154, 106055.
- Sharma, A., Zheng, Z., Kim, J., Bhaskar, A., Haque, M. M. (2020). Is an informed driver a better decision maker? A grouped random parameters with heterogeneity-in-means approach to investigate the impact of the connected environment on driving behaviour in safety-critical situations. *Analytic Methods in Accident Research*, 27, 100127.
- Shino, M., Kamata, M., Nagai, M., Michitsuji, Y., Moro, K., 2008. Research on incident analysis using drive recorder part 3: analysis on relationship driving behavior and traffic circumstance based on forward collision near-miss incident data in car following situation. Proceedings of FISITA 2008 World Automotive Congress (No. F2008-08-123).
- Simon, M., Hermitte, T., Page, Y. (2009). Intersection road accident causation: A European view. In *21st International Technical Conference on the Enhanced Safety of Vehicles* (pp. 1-10).
- Stange, M., Grau, M., Osazuwa, S., Graydon, C., Dixon, M. J. (2017). Reinforcing small wins and frustrating near-misses: Further investigation into scratch card gambling. *Journal of Gambling Studies*, 33(1), 47-63.
- Strauss, J., Miranda-Moreno, L. F., Morency, P. (2013). Cyclist activity and injury risk analysis at signalized intersections: A Bayesian modelling approach. *Accident Analysis & Prevention*, 59, 9-17.
- Thompson, D. C., Rebolledo, V., Thompson, R. S., Kaufman, A., & Rivara, F. P. (1997). Bike speed measurements in a recreational population: validity of self reported speed. *Injury Prevention*, 3(1), 43-45.
- Thørrisen, M. M. (2013). *Personality and Driving Behavior. The Role of Extraversion and Neuroticism in Drivers' Behavior Toward Bicyclists* (Master's thesis).
- Uchida, N., Kawakoshi, M., Tagawa, T., Mochida, T. (2010). An investigation of factors contributing to major crash types in Japan based on naturalistic driving data. *IATSS research*, 34(1), 22-30.
- Underwood, G., Crundall, D., Chapman, P. (2011). Driving simulator validation with hazard perception. *Transportation Research Part F: Traffic Psychology and Behaviour*, 14(6), 435-446.
- Wada, T., Doi, S., Imai, K., et al., Analysis of drivers' behaviors in car following based on

- performance index for approach and alienation, SAE Technical Paper 2007-01-0440, 2007.
- Wei, F., Lovegrove, G. (2013). An empirical tool to evaluate the safety of cyclists: Community based, macro-level collision prediction models using negative binomial regression. *Accident Analysis & Prevention*, *61*, 129-137.
- Werneke, J., Dozza, M., & Karlsson, M. (2015). Safety-critical events in everyday cycling—Interviews with bicyclists and video annotation of safety-critical events in a naturalistic cycling study. *Transportation Research Part F: Traffic Psychology and Behaviour*, *35*, 199-212.
- Wu, Y., Abdel-Aty, M., Park, J., Zhu, J. (2018). Effects of crash warning systems on rear-end crash avoidance behavior under fog conditions. *Transportation Research Part C: Emerging Technologies*, *95*, 481-492.

## **Acknowledgements**

This dissertation was carried out at the Department of Mechanical Systems Engineering, Graduate School of Engineering, Nagoya University, Japan. I would like to thank everyone who helped and supported me throughout my study at Nagoya University.

First, I would like to sincerely thank my supervisor Professor Koji Mizuno, who offered me the opportunity to study at Nagoya University and taught me a great deal in my research, as well as a lot of help in adapting to life in Japan. This study would not be completed without him.

I would like to express my heartfelt thanks to Professor Tatsuya Suzuki, Department of Mechanical Systems Engineering, Professor Hiro Aoki, Institutes of Innovation for Future Society, and Professor Eisuke Kita, School of Informatics and Sciences, who reviewed this dissertation and made valuable suggestions.

Particular thanks go to Dr. Joseph N. Kianianthra, previous administrator of U.S. Government's National Highway Traffic Safety Administration, who had discussions with us about the experiments and provided important comments in this study.

Thank to Dr. Makoto Inagami, researcher at Institutes of Innovation for Future Society, who provided technical support and valuable suggestions in the section of gaze analysis.

Thanks go to everyone of Mizuno laboratory, helping me deal with the difficulties I encountered in my life in Japan, and it was a really precious experience to do researches together and discuss with each other.

Thank to my parents for providing help at every moment, and they always encouraged me to bravely pursue my dreams. Thank to all my friends who gave me much comfort and encouragement when I was helpless.

More than a decade ago I never thought I would have the opportunity to learn what I like in another country. In retrospect, the experience studying at Nagoya University was like magic. I have been through many difficulties in the past years, and thus final thanks go to myself for never giving up on finding light even when I was in the dark.